# HARMONIC LOSS CALCULATION OF PWM INVERTER-FED INDUCTION MOTORS USING LOSS FACTOR CHARACTERISTICS

PHOUMY INDARACK



A THESIS SUBMITTED IN PARTIAL FULFILLMENT

OF THE REQUIREMENT FOR THE DEGREE OF

MASTER OF ENGINEERING IN ELECTRICAL ENGINEERING

SCHOOL OF GRADUATE STUDIES

KING MONGKUT'S INSTITUTE OF TECHNOLOGY LADKRABANG

2005

ISBN 974 -5 –1529 -4

| | |
|---|---|
| **หัวข้อวิทยานิพนธ์** | การคำนวณกำลังสูญเสียเนื่องจากฮาร์มอนิกส์ของมอร์เตอร์เหนี่ยวนำที่ถูกขับเคลื่อนด้วยพีดับบลิวเอ็มอินเวอร์เตอร์โดยใช้คุณสมบัติแฟคเตอร์การสูญเสีย |
| **ชื่อนักศึกษา** | นายภูมี อินคารัก |
| **รหัสประจำตัว** | 46060340 |
| **ปริญญา** | วิศวกรรมศาสตรมหาบัณฑิต |
| **สาขาวิชา** | วิศวกรรมไฟฟ้า |
| **พ.ศ.** | 2548 |
| **อาจารย์ผู้ควบคุมวิทยานิพนธ์** | รศ. ดร. วิจิตร กิณเรศ |
| **อาจารย์ผู้ควบคุมวิทยานิพนธ์ร่วม** | ผศ.ดร.สุพัฒน์ กิจติรัตน์สัจจา<br>ศ.ดร. มาซาอากิ คันโดะ |

## บทคัดย่อ

มอร์เตอร์เหนี่ยวนำที่ถูกขับเคลื่อนด้วยพีดับบลิวเอ็มอินเวอร์เตอร์ใช้กันมากในงานอุตสาหกรรม อย่างไรก็ตามกำลังไฟฟ้าสูญเสียที่เพิ่มขึ้นเนื่องจากฮาร์มอนิกส์ อาจเป็นสาเหตุให้พิกัดกำลังของมอร์เตอร์ลดลงและเป็นสิ่งที่เราไม่ต้องการ ทั้งๆที่มีการวิจัยกันอย่างกว้างขวางแต่กลไกการเกิดการสูญเสียเนื่องจากฮาร์มอนิกส์และการเปลี่ยนแปรภายใต้เงื่อนไขการทำงานย่านกว้างยังไม่เป็นที่เข้าใจอย่างถ่องแท้ ดังนั้นวิทยานิพนธ์ฉบับนี้จึงเกี่ยวข้องกับการสูญเสียเนื่องจากฮาร์มอนิกส์ที่ได้จากการคำนวณและการวัด โดยอาศัยแฟคเตอร์การสูญเสียเนื่องจากฮาร์มอนิกส์ภายใต้การเปลี่ยนแปลงโหลดพารามิเตอร์ของพีดับบลิวเอ็มต่างๆ เช่น ดัชนีการมอดูเลตและความถี่สวิตชิ่งเป็นต้น เส้นเคริฟของแฟคเตอร์การสูญเสียนี้จะได้จากการบูรณาการจากวงจรสมมูลมาตรฐานของมอร์เตอร์เหนี่ยวนำได้ทำการตรวจสอบกลไกการสูญเสียเนื่องจากฮาร์มอนิกส์และการเปลี่ยนแปรเนื่องจากพารามิเตอร์ของระบบ เช่น ภาระโหลด ความถี่สวิตชิ่ง ความถี่อินเวอร์เตอร์ ผลการทดลองทำให้เข้าใจกลไกการสูญเสียดังกล่าว โดยเฉพาะค่าการสูญเสียเปลี่ยนตามโหลดและมีขนาดค่อนข้างสูงของการสูญเสียที่ความถี่สูง การคาดคะเนการสูญเสียเนื่องจากฮาร์มอนิกส์ โดยใช้แบบจำลองแฟคเตอร์การสูญเสียที่นำเสนอสอดคล้องอย่างต่อเนื่องกับการวัด ผลการคำนวณสามารถใช้เป็นแนวทางสำหรับการเลือกพารามิเตอร์ของพีดับบลิวเอ็มที่เหมาะสมสำหรับการประยุกต์ใช้งานการขับเคลื่อนและสามารถใช้เป็นคำแนะนำที่เป็นประโยชน์สำหรับผู้ออกแบบมอร์เตอร์เมื่อขับเคลื่อนด้วยพีดับบลิวเอ็มอินเวอร์เตอร์.

| | |
|---|---|
| **Thesis Title** | Harmonic Loss Calculation of PWM Inverter-Fed Induction Motors Using Loss Factor Characteristics |
| **Student** | Mr. Phoumy Indarack |
| **Student ID.** | 46060340 |
| **Degree** | Master of Engineering |
| **Programme** | Electrical Engineering |
| **Year** | 2005 |
| **Thesis Advisor** | Assoc. Prof. Dr. Vijit Kinnares |
| **Co-Thesis Advisor** | Asst. Prof. Dr. Supat Kittiratsatcha |
| | Prof. Dr. Masaaki Kando ( Tokai University of Japan ) |

## ABSTRACT

PWM inverter supplied induction motors are widely used in industrial applications. However, the additional harmonic power loss may cause derating of the motor and this is undesirable. Despite widespread research work in this area, the harmonic loss mechanisms and their variation under a wide range of operating conditions are not well understood. This thesis is concerned with predicted and measured harmonic losses based on harmonic loss factor under load conditions , various PWM parameter such as modulation index and switching frequency .The loss factor curves are derived from the standard equivalent circuit of induction motor. An investigation into harmonic loss mechanisms and their variation with a wide variety of system parameters such as motor load, switching frequency and inverter frequency has been made. The results allow a better understanding of such mechanisms particularly the variation of loss with load and their relatively large magnitude of the high frequency loss. Harmonic loss predictions using the proposed loss factor model are in consistently good agreement with the loss measurements. The calculation results can be guidelines for selection of PWM parameters suitable for drive applications such as switching frequency and can be useful advice for the motor designers and users, when induction motors fed by PWM inverters have to be designed or utilized.

## ACKNOWLEDGEMENTS

I would like to express my special gratitude to my Advisor Assoc. Prof. Dr.Vijit Kinnares, Co-Advisor Assit. Prof. Dr. Supat Kittiratsatcha, Co-Advisor Masaaki Kando (Tokai University) and Asst. Prof. Dr. Anantawat Kunakorn for their guidance, support, patience and encouragement during the course of this project.

I would especially like to thank Department of Electrical Engineering, Faculty of Engineering KMITL for experimental equipment and work place.

I sincerely thank all staffs and my colleagues for their help and good cooperation.

Finally, I would like to thank to AUN/SEED-Net (JICA) for contribution and for giving me the opportunity to carry out this study.

Phoumy Indarack

# TABLE OF CONTENTS

## TABLE OF CONTENTS (Cont.)

## TABLE OF CONTENTS (Cont.)

## LIST OF FIGURES

## LIST OF FIGURES (Cont.)

## LIST OF FIGURES (Cont.)

## LIST OF FIGURES (Cont.)

## LIST OF FIGURES (Cont.)

# CHAPTER 1

# INTRODUCTION

## 1.1 Background

Variable speed drives employing Pulse Width Modulation (PWM) inverter fed induction motors are now in very widespread use throughout industry. Unfortunately, the losses in an inverter fed motors are always greater than those for the same machine operating on a sinusoidal supply and in some cases these require derating of the motor. Despite the numbers of these drives in operation, the harmonic loss mechanisms are not well understood and there is no model available which enable the loss in a particular machine operating with a defined PWM supply to be accurately predicted. In addition, due to the need of energy savings, considerations of the machine design and PWM switching technology for variable speed drives using the more reliable model to meet high efficiency performance are required.

This thesis is concerned with the accurate prediction, measurement and evaluation of harmonic losses. The purposes are to develop prediction techniques and test procedure, to identify shortcomings of a conventional model, to develop a new technique and modeling for determining and predicting additional motor losses, to assess the individual harmonic loss mechanisms, and to improve motor design for variable frequency drives. The prediction has been made under variation of PWM parameters in order to evaluate and specify additional motor losses. The impact of load, influence of flux level, PWM switching frequency, PWM schemes, and machine design on additional losses have been extensively investigated towards developing new techniques for quantifying and modeling loss mechanisms. Some real effects on harmonic loss mechanisms are revealed and analyzed. The predicted and experimental results give fairly good agreement. The contribution of work shows the well understanding of harmonic loss mechanisms on interaction between PWM inverter and induction machines. This new model is capable of considering parameters for machine design to meet improved efficiency requirements. This proposed method to evaluate in induction motor losses in variable speed drives may be useful for manufacturers to specify the harmonic motor loss for design considerations of converters and motors.

It can be concluded that the complicated effect of high frequency harmonic voltages associated with modern PWM inverter drives on motor loss is a challenging subject for further investigation. In particular accurate methods for predicted harmonic losses and their variation with frequency are needed to better understand and verify the mechanisms. This should allow

better models for segregating losses between these mechanisms and provide the means for improved motor design. It is towards this better understanding that the work reported in this thesis is directed.

## 1.2 Objectives and procedure of the research

This research work is concerned with the accurate prediction, analysis and measurement of harmonic losses. A particular focus is the investigation of the harmonic loss mechanisms of PWM inverter fed induction motors using loss model and specially developed PWM techniques. To this end a special purpose PWM inverter system and an induction motor test rig has been developed. A loading system with accurate torque control has been set up using DC motor and taking load by PC via DC Converter SIMOVIS-Board. The load on the motor under test is accurately controlled via load control interface system that acts according to the torque predicted by measured the speed using tachometer. In order to measure and segregate total harmonic power losses among the individual harmonics with acceptable accuracy and repeatability, a dedicated power measurement system has been developed. Motor line voltages and currents are monitored using Power Analyzer (PZ 4000).

The technique also enables multiple harmonics to be injected to check for interactions between harmonics. The influences of harmonic frequency, PWM switching frequency, PWM strategy and motor design on harmonic losses have been investigated using the test rig. These loss measurements have been interpreted in terms of loss mechanisms in the motor. A harmonic loss factor relating loss to harmonic frequency is proposed and is determined by calculations. This provides the basis for identifying the dependence of harmonic losses on motor design as a step towards improved efficiency design.

## 1.3 Structure of the Thesis

CHAPTER 2 the harmonic losses in motors are discussed. The expected influence of motor parameters in terms of the traditional equivalent circuit is discussed.

CHAPTER 3 discusses the modeling and prediction of power losses by empirical formulae. The choice of a suitable empirical function for the harmonic loss factor curve is described. This harmonic loss characteristic is analyzed in terms of the loss mechanisms and motor parameters

which influence it. Finally the benefits of using an harmonic loss factor curve fitting approach for loss prediction are discussed.

CHAPTER 5 describes the hardware and software for the SVPWM generation. Test results are provided to confirm the correct operation of the system and discuss the prediction of harmonic voltage spectra and harmonic loss using equivalent circuit. The harmonic loss factor curve predicted using standard equivalent circuit. The harmonic circuit impedance is also determined. The methods for determining the stray core loss parameters are discussed. The total harmonic power loss predictions using this model for SVPWM operating conditions are in good agreement with the measurements.

CHAPTER 5 discusses the comparison between the predicted and measured harmonic losses under variation of load torque, inverter frequency and switching frequency.

## 1.4 Benefits and Contributions

By using the special loss factor method proposed, the harmonic loss mechanisms for a wide range of operating conditions can be evaluated and analyzed. This technique offers a means for accurate measurement of loss variation with frequency. Subsequently, the predicted loss characteristic curve allows harmonic loss on SVPWM supply to be predicted with better accuracy than the existing motor equivalent circuit models. The sensitivity of harmonic loss due to harmonic frequency has been found due to the inherent copper, core and stray load loss components. Particularly interesting features of the predictions are the variation of loss with load and the relatively large magnitude of the high frequency loss. The important effect of load on harmonic losses which has generally been neglected previously can be found with the proposed measurement technique. Also, the influence of motor aspects can be interpreted which will support the understanding of loss mechanisms. The standard motor equivalent circuit models give improved loss prediction and confirm the significance of harmonic stray load. This model and the proposed loss factor model allow the breakdown of loss components and the influence of motor parameters to be determined which is important for optimized design and the choice of a suitable power derating coefficient. The proposed loss prediction technique can be applied to the any type of AC motor in which the individual and total harmonic losses are to be determined particularly for the purpose of motor design.

# CHAPTER 2

# LOSSES IN INDUCTION MOTORS

## 2.1 Introduction

Induction motors can be supplied from various types of solid-state adjustable frequency controllers. In all cases, however, the inverter and motor combination result in the necessity to derate the motor to some degree relative to its single frequency, sinusoidal rating. With PWM inverter fed induction motors, the stator and rotor currents as well as the air-gap flux in motor are inherently non-sinusoidal. Harmonics contribute negligible useful torque. As a result, the losses in the machines are always greater than in the traditional sinusoidal excitation case. The magnitude and distribution within the motor of the additional losses and the related motor derating depend both on the harmonic content of the applied voltage and on the machine designs.

The thesis restricts itself to considering harmonic power loss in induction motors in the steady states. In this chapter, the motor model to be employed is derived based on improvements to the work of previous authors [3] [4] [5] . The loss components associated with operation from PWM voltages are discussed. The essential factors influencing motor losses are pointed out.

## 2.2 Induction Motor Power Flow

The losses associated with induction motor operating at no-load condition can be given as show in the following relation.

$$P_{no-load} = P_{core} + P_{cu-s} + P_{cu-r} + P_{rot} \qquad (2.1)$$

where

$P_{no\text{-}load}$ is the total no-load input power.

$P_{core}$ is core losses.

$P_{cu\text{-}s}$ is stator copper losses.

$P_{cu\text{-}r}$ is rotor copper losses.

$P_{rot}$ is rotational losses.

The power flow in induction machines fed from a non-sinusoidal supply is shown in Figure 2.1. The induction machine operated from a non-sinusoidal supply has the usual motor losses and

some additional losses due to the time harmonics. The loss components and their causes for fundamental and time harmonics can be summarized as follows:

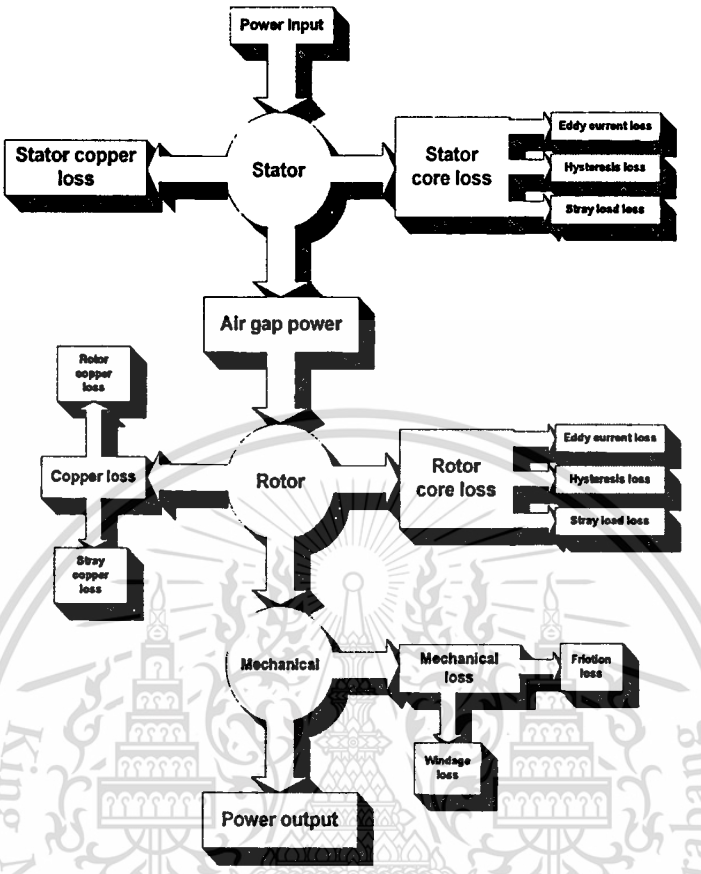


**Figure 2.1** Induction Motor Power Flow

## 2.3 Conductors Losses

### 2.3.1 Stator Winding Copper Loss

The non-sinusoidal supply results in an increased rms current which causes additional stator winding copper loss. Moreover, significance is the additional loss arising from frequency dependent skin effect increasing winding resistance due to current redistribution. However, normally this may be neglected in random wire-wound stator machines. It should be taken into consideration when the conductor size is appreciable compared to the skin depth.The stator winding copper loss can be computed by:

$$P_{cu-stat} = 3R_s I_s^2 \quad (2.2)$$

where

$R_S$ is stator phase dc resistance;

$I_S$ is rms value of the input no-load phase current

### 2.3.2 Rotor winding copper loss

The current in the rotor winding comprises the slip frequency currents induced by the fundamental flux and high frequency current arising from the fluxes set up by the applied time harmonic voltages resulting in increased rotor winding copper loss. Skin effect causes significant increase in rotor resistance and decrease in rotor leakage inductance at high frequency for the deep bar and double cage rotor. Most low voltage induction machines up to 200 to 300 KW have random wire wound stators but they have bar type rotor windings so skin effect is of most significance in the rotor.

The rotor winding copper loss can be computed by:

$$P_{cu-rot} = 3R_r I_r^2 \quad (2.3)$$

where

$R_r$ is rotor phase resistance.

$I_r$ is rms value of the rotor phase current.

### 2.3.3 Influence of Harmonic Frequency upon Conductor Resistance and Loss

The winding resistance and leakage inductance are functions of harmonic frequencies. For slot imbedded conductors, the inductance of an element of conductor's increases towards the bottom of the slot. The impedance of conductor elements at the bottom of the slot is increasingly greater than those at the top of the slot as the frequency of conductor currents increase. This forces the majority of current to the top of the conductor increasing resistance and decreasing inductance with increasing frequency of current. The link between conductor resistance and inductance is therefore unavoidable. The standard formulae for parallel sided slots relating to the increase of resistance and decrease in inductance relative to the dc value.

$$\frac{R_{ac}}{R_{dc}} = \alpha h\left[\frac{\sinh\ (2\alpha h)+ \sin\ (2\alpha h)}{\cosh\ (2\alpha h)- \cos\ (2\alpha h)}\right] \tag{2.4}$$

$$\frac{L_{ac}}{L_{dc}} = \frac{3}{2\alpha h}\left[\frac{\sinh\ (2\alpha h)- \sin\ (2\alpha h)}{\cosh\ (2\alpha h)- \cos\ (2\alpha h)}\right] \tag{2.5}$$

$$\alpha = \sqrt{\frac{\mu_0 \omega}{2\rho}} \tag{2.6}$$

where $h$ is the depth of the conductor and slot, $\omega$ is the angular frequency of the bar currents, $\rho$ is the resistively of the conductor and the subscripts ac and dc refer respectively to the values at the frequency of the bar currents and dc value.

**2.3.4 Assessment of Simplifications Sometimes Used to Provide First Order Analysis**

Some authors have used the following simplifications of these expressions to estimate the effect of frequency upon total conductor loss. When skin depth and conductor size are of the same order of magnitude, the rate of change of resistance and leakage inductance is approximately dependent on $f_n^2$ [6]. As the frequency continues to increase, the rate of change decreases and the variation ultimately becomes proportional to $f_n^{0.5}$ as the skin depth becomes small compared to conductor size.

Assuming the harmonic frequency is much larger than the fundamental frequency, the harmonic slip will be close to unity and the reactive terms (leakage and magnetizing reactance) will be much larger than the resistive terms in the harmonic circuit. The harmonic magnetizing current is therefore negligible. At the harmonic frequencies, stator resistance and rotor resistance are usually negligible compared with the leakage reactance of the motor. Therefore, the $n^{th}$ harmonic current is given by:

$$I_n \approx \frac{V_n}{2\pi f_n L_\sigma} \tag{2.7}$$

where

$I_n$ is $n^{th}$ harmonic current

$V_n$ is per unit (pu) $n^{th}$ harmonic voltage

$L_\sigma$ is leakage inductance

$f_n$ is per unit (pu) fundamental frequency

The $n^{th}$ harmonic conductor loss is then given to a good approximation by

$$P_{cn} \approx I_n^2(R_s + R_r) \approx (\frac{V_n}{2\pi f_n L_\sigma})^2(R_s + R_r) \quad (2.8)$$

Assuming that all of the stator resistance and rotor resistance have skin effect and that skin depth is relatively small compared to conductor size, and then total resistance becomes:

$$(R_s + R_r) = k\sqrt{f_n} \quad (2.9)$$

For the time being we assuming that $L_{ls}$ and $L_{lr}$ are not influenced substantially by skin effect. It is also assumed that iron losses and magnetizing current are neglected and the motor impedance is effectively $j\omega(L_{ls} + L_{lr})$.

Then, from equation (2.7) and (2.8), total harmonic copper loss is:

$$p_c = \sum_{n \neq 1} \frac{kV_n^2}{f_n^{1.5}} \quad (2.10)$$

However, the frequency exponent of 1.5 is only a first approximate value. This value and that of constant k are normally dependent on the following factors:

(i) The assumption that only slot leakage inductance accounts for the variation of $L_{ls}$ and $L_{lr}$ with frequency.

(ii) The shape of rotor bar, bar depth, material, temperature and open or closed slot character.

(iii) The ratio of skin depth compared to conductor sizes.

(iv) The ratio of coil end resistance to slot resistance is negligible.

(v) The number of conductor layers.

(vi) The conductor cross sectional shape, material and temperature.

(vii) The equality between useful stator and rotor slot depth.

It will be apparent from the above that such simplifications are purely first order estimates and that a much more effective approach is required to study conductor loss in detail.

## 2.4 Iron Losses

### 2.4.1 Stator Core Loss

The stator iron loss is the function of frequency and flux density in the core. In theoretical and experimental investigations have confirmed that the increase in core loss due to time harmonic main fluxes is negligible [6]. It is significantly influenced by machine construction, magnetic material used, and thickness of laminations.

### 2.4.2 Rotor Core Loss

The nature of the rotor core loss mechanism is not still fully explained. Many publications assume that the time fundamental as well as time harmonics of rotor flux gives negligible extra loss. However, more investigation is needed to verify this assumption. High frequency rotor flux is more likely to produce additional rotor iron loss since the flux wave will not rotate almost synchronously with the rotor as for the fundamental.

### 2.4.3 Effect of Flux Level and Frequency on Iron Losses

The accurate prediction of core losses requires a detailed knowledge of flux distributions resulting from the effects of the various harmonics. The high frequency effect is the most important factor for core losses. Owing to the presence of harmonic current, there is a higher peak flux density in the iron in conjunction with the increased magnetizing current.

The iron loss is generally accepted as being the sum of the hysteresis loss and the eddy current loss in the stator and rotor. The hysteresis losses are proportional to the frequency and the eddy current losses to the square of frequency. The iron losses in stator can be described by the following expression:

$$P_{fe,s} = \beta_h f \phi^2 + \beta_e f^2 \phi^2 \tag{2.11}$$

or

$$P_{fe,s} = \left(\frac{\beta_h}{f} + \beta_e\right) f^2 \phi^2 \tag{2.12}$$

These basic formulae have been used by almost all of the authors analyzing the effect of PWM harmonics upon iron loss. There is however in the literature [7] a statement that high

frequency eddy current loss should include an additional loss term to cover domain realignment or excess loss. When this is included the formula becomes

$$P_{fe,s} = \beta_h f\phi^2 + \beta_e f^2\phi^2 + \beta_d \phi^{1.5} f^{1.5} \tag{2.13}$$

The results obtained by [8] show that at 50 Hz hysterisis loss, eddy current loss and the domain loss from respectively 52.73%, 28.57% and 17.70% of the total loss for typical magnetic steel used for motor laminations. In fact few authors [9] and 10] have considered this effect at all from the point of view of analyzing high frequency iron loss associated with machines operating from inverters. The analysis will continue at this point assuming that the traditional formula holds but the additional loss term will be reintroduced later.

### 2.4.4 Simplifications to Provide First Order Analysis

Assuming that the rotor or laminations are made of the same material as that of the stator and that stator and rotor cores are subjected to the same level of flux density, core loss is then found by substituting sf for f in equation (2.12).

$$P_{fe,r} = (\frac{\beta_h s}{f} + \beta_e s^2) f^2\phi^2 \tag{2.14}$$

The total core loss of the fundamental (assuming similar volumes for stator and rotor) is:

$$P_{fe} = P_{fe,s} + P_{fe,r} \tag{2.15}$$

$$P_{fe} = [\frac{\beta_h (1+s)}{f} + \beta_e (1+s^2)] f^2\phi^2 \tag{2.16}$$

The part $f\phi$ is proportional to the air-gap voltage $V_m$. Hence (2.16) can be written as :

$$P_{fe} = V_m^2 [\beta_c [\frac{\beta_h (1+s)}{f} + \beta_e (1+s^2)]] \tag{2.17}$$

Assuming that $\beta_c$, $\beta_h$ and $\beta_e$ are properties of the material and machine configuration and thereby do not change with frequency. Core loss can then be modeled by a resistance $R_m$ in

parallel with the magnetizing path of the equivalent circuit with loss equal to $V_m^2 / R_m$. If we let $K_1 = \beta_e / \beta_h$ (the ratio of eddy current to hysterisis loss coefficient) then :

$$R_m = \frac{f}{\beta_c \beta_h [(1+s) + K_1 (1+s^2) f]} \tag{2.18}$$

At harmonic frequencies, the value of the core loss resistance is determined by substitution of the appropriate values of harmonic frequency and harmonic slip in equation (2.18). Usually, only the sum of $\beta_h$ and $\beta_e$ is known; $K_1$ is difficult to measure.

Note that due to the complicated nature of core losses, several authors have suggested different empirical formulae for hysterisis loss per unit volume such as [1] and [11]:

$$P_{hys} = k_h f B^X \; ; \; 1.5 \le X \le 2.3 \; ; \tag{2.19}$$

$$P_{hys} = k_h \frac{V^2}{f} \tag{2.20}$$

$$P_{hys} = k_h f^{1.1} B^2 \tag{2.21}$$

Some of the most commonly used empirical formulae for the eddy current loss given in [1] [11] are:

$$P_{edd} = k_e f^2 B^2 \tag{2.22}$$

$$\begin{aligned} P_{edd} &= k_{e1} V^2 && \text{at low frequency} \\ &= k_{e2} \frac{V^2}{f^{0.5}} && \text{at high frequency} \end{aligned} \tag{2.23}$$

$$P_{edd} = k_e f^{1.9} B^2 \tag{2.24}$$

Some have considered the iron losses as a whole, including eddy-current and hysterisis losses for example the work reported in [12] gives:

$$P_{fe} = a f^b \left(\frac{V}{f}\right)^c \tag{2.25}$$

Where b and c depend on the motor configuration and material; b is found empirically to lay in the range from 1.26 to 1.35 and c in the range from 1.77 to 1.84. If b=1.3 and c=1.8, this gives:

$$P_{fe} = \frac{aV^{1.8}}{f^{0.5}} \tag{2.26}$$

The analysis in [13], also gives time-harmonic iron losses as compared to the time-fundamental iron losses at nominal frequency $f_{1,nom.}$ :

$$\frac{P_{fe}(f_n)}{P_{fe,nom}} = \left(\frac{f_n}{f_{1,nom.}}\right)^{1.5}\left(\frac{B_n}{B_{1,nom}}\right)^2 = \left(\frac{f_n}{f_{1,nom}}\right)^{0.5}\left(\frac{V_n}{V_{1,nom}}\right)^2 \tag{2.27}$$

Which means that $P_{fe}$ is proportional to $f^{1.5}B^2$ or $V^2/f^{0.5}$.

Although many authors suggest different formulae for core losses, these formulae are common in many cases in that they state that core losses are proportional to the square of voltage or flux density. They are also independent of the load applied to the machine other than by variation of slip which generally has negligible effect for changes from no load to full load conditions. The various attempts that have been made to fit a single formula to model the core loss, and the different formulae which results highlight the complexity of the phenomena involved. It is clearly not possible to obtain exact, general expressions for iron losses in induction machines operated with PWM inverters since these losses depend on the core material used and on the machine construction and condition of operation.

## 2.5 Stray Losses

### 2.5.1 Stray Load Losses

Stray losses are the excess of the total measured losses above the sum of the segregated copper, iron and friction and windage loss. The nature of stray losses occurring in induction machines operating on sinusoidal supplies has been well defined in the literature over many years[14]. The prediction of these losses is however still not fully understood to the extent that they may be accurately determined from design data. The reason is the fact that the stray loss mechanism involves several kinds of losses, some of which are not precisely iron losses. For

example, inter bar currents which flow in skewed motors are effectively conductor loss. Additionally, parasitic currents induced in rotor conductors due to space harmonic mmfs with magnitude dependent upon the chain harmonic equivalent circuit for its variation with frequency and flux level. In particular, end-leakage and skew leakage fluxes can cause appreciable losses which are considered as iron stray load loss. Motor slot skewing is common practice for reduction of parasitic torques and noise. The effects of skewing can cause axial field distortion leading to increased iron losses. Skewing dependent iron losses are harmonic current dependent and inversely proportional to leakage reactance. The end-leakage flux may produce an appreciable core loss due to eddy currents set up in the end structure of the machine by harmonic leakage fluxes.

### 2.5.2 Simplifications to Provide First Order Analysis

The objective of this thesis is to predict the motor losses associated with PWM harmonics. Therefore, only that component of stray loss which is due to the harmonic content of inverter waveforms has been considered and the traditional sources of stray load loss for operation from sinusoidal supplies have been neglected. The approximation of end-leakage loss can be found in[2]. Total harmonic end-losses can be given as:

$$P_{end-loss} \approx \sum_{n \neq 1} k_1 (I_n)^2 f_n \tag{2.28}$$

Also, it can be defined as:

$$P_{end-loss} \approx \sum_{n \neq 1} \frac{k_2 V_n^2}{f_n} \tag{2.29}$$

The total stray load losses are given more generally by:

$$P_{SL-Loss} \approx \sum_{n \neq 1} k_{s1} (I_n)^x (f_n)^y \tag{2.30}$$

Where the x and y coefficients depend on the machine construction. It has been determined experimentally that the total stray load losses due to harmonics are obtained with reasonable

accuracy putting x=2 and y=1.5 [2]. This gives total stray load losses (assuming purely inductive impedance) of:

$$P_{SL-Loss} \approx \sum_{n\neq 1} \frac{k_{s2} V_n^{\,2}}{f_n^{\,0.5}} \tag{2.31}$$

Separation of stray loss from iron loss is impossible with these simplified formulae as it has same dependence on voltage and frequency as the simplified equation (2.27) for iron loss.

Separation of end loss and stray loss experimentally is very difficult since they are the same function of voltage and different only in their frequency variation.

## 2.6 Friction and Windage Loss

The friction and windage loss are usually dependent only upon shaft speed and temperature. The friction will be relatively constant once the bearings are warmed up. The windage loss will generally vary with cube of speed. However, it is likely to be assumed constant over a wide range of operating conditions for calculating motor performance when operation is from a fixed frequency supply.

## 2.7 Conclusion

The assessment of the harmonic loss components associated with PWM voltages has been given. Also the essential factors influencing motor losses have been discussed. The review of induction motor modeling techniques is given to justify choices in harmonic loss analysis. The traditional time harmonic equivalent circuits and parameters are explained.

# CHAPTER 3

# HARMONIC LOSS MODEL

## 3.1 Introduction

Generally loss calculation is challenging and complicated particularly for harmonic core losses. Suitable techniques should enable prediction of harmonic loss without neglecting realistic factors such as magnetic saturation, load conditions and high frequency effects.

This chapter deals with the analysis of harmonic loss mechanisms and modelling of harmonic power loss through the predicted results for particular machines and for various operating conditions. The method used is to evaluate the coefficients of a formula for the variation of the loss function with the frequency and load. A comparison of predicted results with the model prediction is given. Also, the evaluation of model accuracy and validity is made. Actually , this chapter provides prediction of harmonic loss using standard equivalent circuits. The harmonic loss mechanisms can be examined using a loss factor of standard machine equivalent circuits and predicted results. Also, the PWM harmonic voltage model is determined. Correct evaluation of leakage inductance is shown to be particularly important. With the identification of shortcomings of the conventional circuit model, the improved harmonic stray loss equivalent circuit is applied as below.

## 3.2 Harmonic Loss Equivalent Circuit

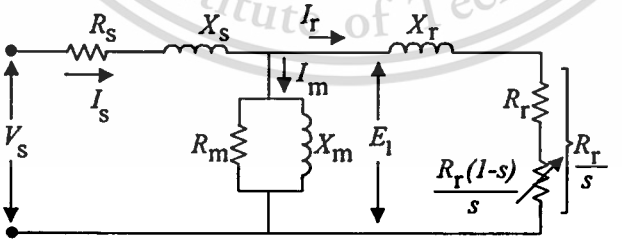


**Figure 3.1** Per phase equivalent circuit of induction motor

where

$R_s$ is stator resistance

$X_s$ is stator leakage reactance

$X_m$ is magnetizing reactance

$R_r$ is rotor resistance

$X_r$ is rotor leakage reactance

S is slip

$E_1$ is Air-gap voltage

From Figure 3. 1 the harmonic power losses can be computed by:

$$P_{cu1} = \sum I_{sn}^2 R_{sn} \tag{3.1}$$

$$P_{cu2} = \sum I_{rn}^2 R_{rn} \tag{3.2}$$

$$P_c = \sum I_{mn}^2 R_{mn} \tag{3.3}$$

where

$P_{cu1}$ is stator copper losses

$P_{cu2}$ is rotor copper losses

$P_c$ is core losses

The input power of induction motor can be computed by:

$$P_{in} = P_{Fund.} + P_h \tag{3.4}$$

and

$$P_h = P_{in} + P_{Fund.} \tag{3.5}$$

or

$$P_h = P_{cu1} + P_{cu2} + P_c + P_{stray-loss} \tag{3.6}$$

The total of harmonic power copper loss excluding skin effect of induction motors can be expressed by:

$$P_{h(ex)} = \sum_{n \neq 1} I_n^2 R_n \tag{3.7}$$

and

$$I_n = \frac{V_n}{nf_1 X} \tag{3.8}$$

then

$$P_{h(ex)} = \frac{1}{X^2} \sum_{n \neq 1} \left( \frac{V_n}{nf_1} \right)^2 R_n \tag{3.9}$$

where

$P_{h(ex)}$ is harmonic power loss excluding skin effect

$I_n$ is n$^{th}$ harmonic current

$V_n$ is per unit (pu) n$^{th}$ harmonic voltage

$f_1$ is per unit (pu) fundamental frequency

X is per unit (pu) leakage reactance at base frequency

$R_n$ is resistance of motor to the n$^{th}$ harmonic

The total harmonic power copper loss including skin effect of induction motors can be expressed by:

$$P_{h(in)} \approx I_n^2 (R_{s+} R_r) \tag{3.10}$$

with

$$I_n \approx \frac{V_n}{2\pi f_n L_\sigma} \tag{3.11}$$

then

$$P_{h(in)} \approx \left( \frac{V_n}{2\pi f_n L_\sigma} \right)^2 (R_s + R_r) \tag{3.12}$$

where

$P_{h(in)}$ is total harmonic power loss including skin effect

$L_\varsigma$ is leakage inductance

$R_s$ is stator resistance

$R_r$ is rotor resistance

$f_n$ is per unit (pu) fundamental frequency

$k$ is constant

Assumed that all of the stator resistance and rotor resistance have skin effect and that skin depth is relatively small compared to conductor size, then total resistance become:

$$R_s + R_r \approx k\sqrt{f_n} \tag{3.13}$$

therefore

$$P_{h(in)} = \sum_{n\neq 1} \frac{kV_n^2}{f_n^{1.5}} \tag{3.14}$$

## 3.3 Harmonic Loss Factor

To use the loss factor for predicting harmonic losses when operating with SVPWM regimes, it is necessary to interpolate between the experimental data using a curve fitting method. Then, the loss characteristic curve can be represented by functions. The solution is based on the minimising function method using nonlinear least squares. This method allows solution with considerable accuracy within a relative error of 0.001 or better. However, a "guess" function is needed for this method. The choices of a suitable function will be discussed in the next section.

### 3.3.1 Harmonic Loss Factor Derived from Standard Equivalent Circuit

The selection of a suitable function requires preliminary knowledge of loss behaviour in order to fit a curve through the predicted points as closely as possible. Basically, using a simplified loss model, the two main components are conductor loss and core loss (plus stray loss). Several attempts have been made at searching for the appropriate function. Initially, possible "guess" functions are assumed as follows equation

$$K_{hn} = \frac{P_{mn} + P_{sn} + P_{rn}}{V_n^2} \tag{3.15}$$

or

$$K_h = \frac{A}{f^{\alpha}} + \frac{B}{f^{\beta}} \tag{3.16}$$

Figure 3.2 shows that the functions can fit the predicted data and the Equation (3.16) gives coefficients A, B, and frequency exponents $\alpha, \beta$ of 0.55, 0.79 (Load 10%), 1.5, 0.3-0.56 respectively.

This Equation (3.16) suggests a reduction in loss with increasing harmonic frequency to zero at infinite frequency. This Equation seems more reasonable compared to others considering actual machine equivalent circuit models. However, at relatively high frequencies, it is considerably difficult to extrapolate due to the lack of measured data. Improvements to overcome this problem could be the subject of further work. Since there are many solutions with equally accurate predictions, there is difficulty in selecting that which is the most appropriate.

### 3.3.2 Harmonic Loss Characteristics Curves.

Using the data of standard equivalent circuit from Figure 3.1, the harmonic loss factor can be shown as below:

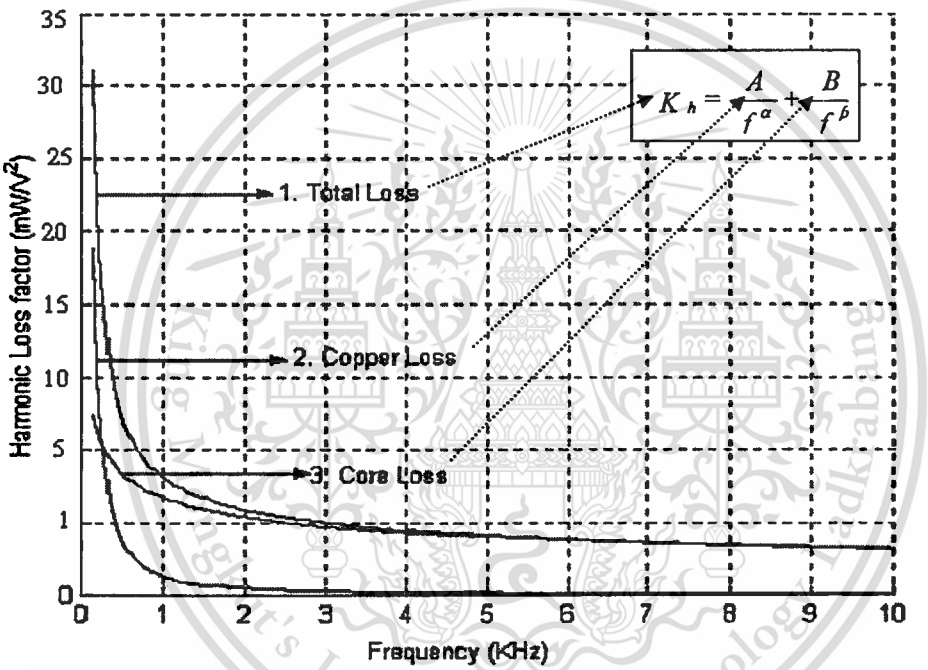


**Figure 3.2** Harmonic loss factor curves for each loss component using standard equivalent circuit for a given load and fundamental frequency of 50 Hz.

The calculation of loss factor based on the standard motor equivalent circuits of Figure 3.1 for this motor load are separated into copper and iron loss component as in Figure 3.2. These results can be evaluated, that the copper loss decreases rapidly as frequency increases and the iron loss decrease very slowly as frequency increases.

Frequency dependent loss characteristics under various operating conditions are shown in Figure 3.2. Then, the total harmonic power loss can be expressed by:

$$P_h = \sum_{n\neq 1} \left(\frac{A}{f_n^{\alpha}} + \frac{B}{f_n^{\beta}}\right) V_n^2 \qquad (3.17)$$

where

$V_n$ is the $n^{th}$ harmonic voltage influenced by modulation depth

$f_n$ is harmonic frequency.

### 3.3.3 Loss Factor Curves for Variation of Load Conditions

#### 3.3.3.1 Motor parameters which influence harmonic loss curve

Obviously, copper losses in the motor winding need to be controlled. The mechanisms of harmonic copper loss and core (plus stray loss) are different in that the harmonic copper loss is dependent on harmonic currents while the high frequency harmonic core (stray) is dependent on harmonic voltages. The required parameter changes to reduce harmonic loss should not adversely affect the fundamental frequency loss.

Essential factors influencing core losses are types of magnetic material and the thickness of laminations. These are not considered here since costs and mechanical constraints are external factors which limit what can be done in this respect.

These were investigated by adjusting independently the motor parameter values in the equivalent circuit assuming no effects on other elements. Adjusting stator leakage inductance ($L_{ls}$), rotor leakage inductance ($L_{lr}$) and bar depth ($h_b$) between - 50 % to + 50 % of normal values.

At harmonic frequencies skin and proximity effects become significant factors in determining conductor losses. For slot imbedded conductors, the variation of the conductor resistance and inductance with frequency follows the general pattern illustrated in Figure 5.5. The initial change in R and L as frequency increases is rapid, being approximately dependent on $f^2$. This region occurs where the skin depth and conductor size are of the same order of magnitude.

As the frequency continues to increase, the rate of change decreases and the variation ultimately becomes proportional to $f^{1/2}$ as the skin depth become small compared to conductor size. While these results apply in general, the portion of the conductors in the slots are affected to a much greater degree since the slot (leakage) fluxes are much large than the fluxes surrounding conductors in air, such as the end turn conductors. Proximity effects are thus larger for the slot imbedded conductors.

Assuming the harmonic frequency is much larger than the fundamental frequency, the harmonic slip will be close to unity and the reactive terms (leakage and magnetizing reactance) will be much

large than the resistive terms in the harmonic equivalent circuit. The harmonic magnetizing current is therefore negligible and the harmonic motor current is determined almost entirely by the applied harmonic voltage and the harmonic leakage reactance. The conductor losses are then given to a good approximation.

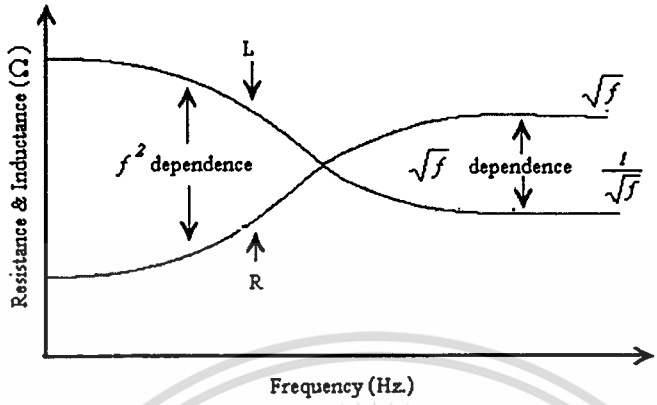


**Figure 3.3** Skin Effect R and L Variation for Conductors in Slots

**3.3.3.2 Equivalent Circuit Parameter**

The basic parameters of the harmonic equivalent circuits defined in Figure 3.1 are evaluated in different ways by different authors. The parameters are functions of fundamental current, and frequency . The majority of the frequency and harmonic effects have been considered at figure.

- **Magnetizing Inductance $L_r$**

The magnetizing reactance $X_r$ ($\omega L_r$) at base frequency is influenced by saturation of the main magnetic circuit. The greater the flux levels the lower the value $L_r$. The value of $X_r$ may be measured using a standard no-load test with sinusoidal excitation. For this loss calculation, Lr is assumed constant at full flux level and was provided by the motor manufacturer. The value of $X_m$ used in the higher time-harmonic equivalent circuit is obtained by simple frequency scaling of base value $X_r$.

- **Core Loss Resistance $R_m$ ($R_c$)**

The resistance $R_m$ ($R_c$) represents the no-load or voltage (flux)-dependent core loss. It is nonlinear function of frequency and is significantly dependent of saturation. The evaluation of this value is discussed in Section 2.4.4 equation 2.18.

## 3.4 Prediction of Harmonic Loss Model Using Data of Standard Equivalent Circuit of Induction Motors

This section provided the prediction of harmonic loss factor using standard equivalent circuit of induction motor. The harmonic loss mechanisms can be examined using a comparison of harmonic loss factor between the traditional equivalent circuit and measured results. Also, the PWM harmonic voltage model is determined. Correct evaluation of leakage inductance is shown to be particularly important. With the identification of shortcomings of the conventional circuit model, the improved harmonic stray loss equivalent circuit is applied. The curve of difference load conditions derived from the rotor inductance including skin effect by motor operated a 10%, 50% and 90% load. This parameter can be adjusted between 50% of the total rotor leakage inductance and the predicted results shown at the Equations (3.18),(3.19) and (3.20).

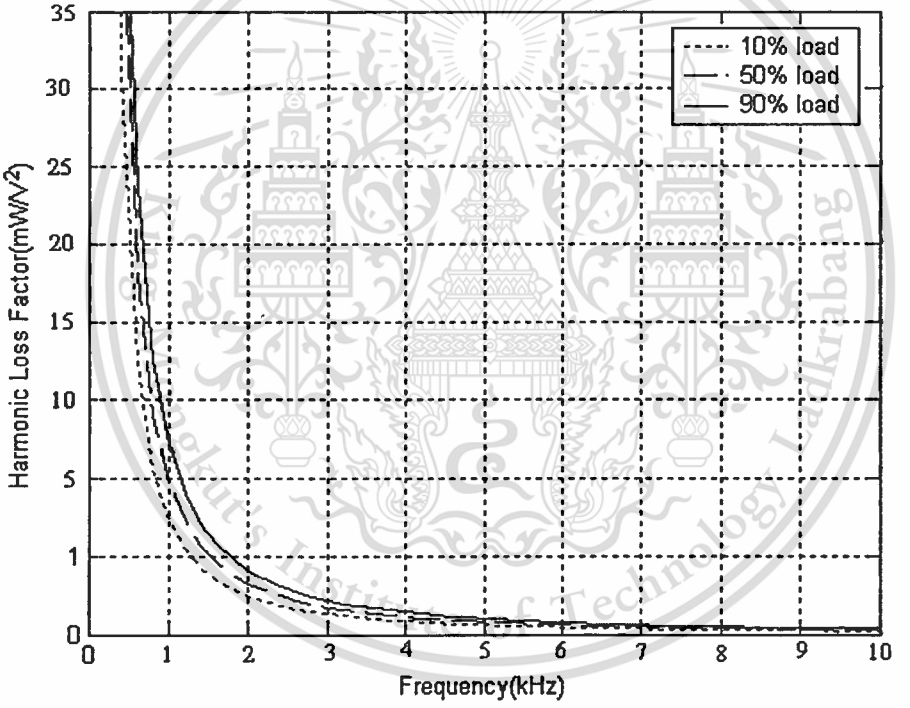


**Figure 3.4** Loss factor curve of standard equivalent circuit with variation of load conditions

Figure 3.4 shows curve fitting of typical results for the test induction motor for different loading conditions.

To test induction motor, the functions at a given load and rated flux are as follows:

$$K_{h(10\%)} = \frac{0.55}{f_n^{1.5}} + \frac{0.70}{f_n^{0.3}} \tag{3.18}$$

$$K_{h(50\%)} = \frac{0.63}{f_n^{1.5}} + \frac{0.89}{f_n^{0.3}} \tag{3.19}$$

$$K_{h(90\%)} = \frac{0.98}{f_n^{1.5}} + \frac{0.93}{f_n^{0.3}} \tag{3.20}$$

The data of parameters *A*, *B*, $\alpha, \beta$ from Equations(3.18-3.20) in above derived from the standard equivalent circuit, while the motor is operated under load 10%, 50% and 90% respectively. This loss model (loss factor) will be used for the prediction of harmonic voltage spectra, loss spectra and total harmonic loss in next chapter.

# CHAPTER 4

# PREDICTION OF HARMONIC LOSS USING LOSS FACTOR CHARACTERISTICS

## 4.1 Introduction

In previous chapter proposed the loss factor curves derived from equivalent circuit of induction motor with different load condition. This chapter provides the prediction of harmonic voltage spectra, harmonic loss spectra and total harmonic loss of induction motor using loss factor characteristics under variation of modulation index, inverter frequency and switching frequency. The predicted results of them shown as below sections:

## 4.2 Harmonic Voltage Spectra

This section mainly deals with the hardware and software for generating the SVPWM schemes employed in this work for determining harmonic losses in induction machines. SVPWM schemes has been implemented which encompass most of the important types for this work. The particular implementation technique allows switching between various PWM strategies while the motor is running which is important for comparative tests. In addition to standard PWM methods, a special PWM technique for determining individual harmonic losses has also been developed and implemented. Simulation results are presented and are compared with the theory to confirm the accuracy of the PWM generation system.

### 4.2.1 Space Vector PWM Technique

In the SVPWM strategy, the required output voltage is represented as a vector in polar coordinates with respect to a stationary reference frame based on the park transformation. The vector space is divided into six sectors by the voltage vectors representing the six active switching states of the inverter ($V_1$ and $V_6$) as shown in Figure 4.1. The two zero switching states ($V_0$ to $V_7$) correspond to the origin.

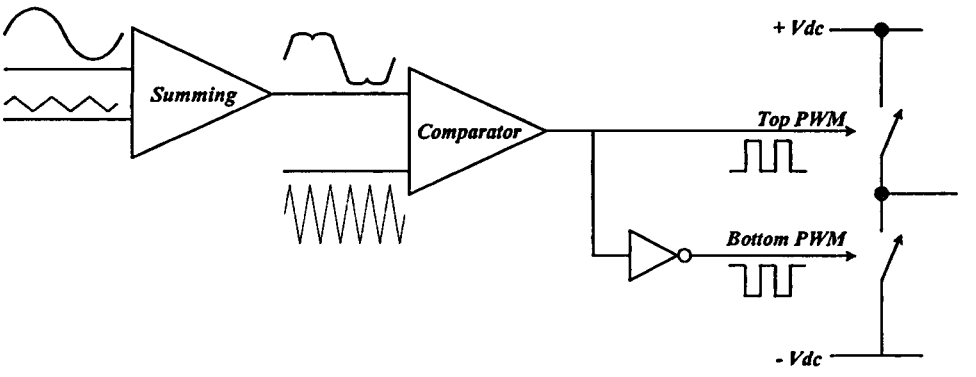


**Figure 4.1** Space Vector PWM techniques

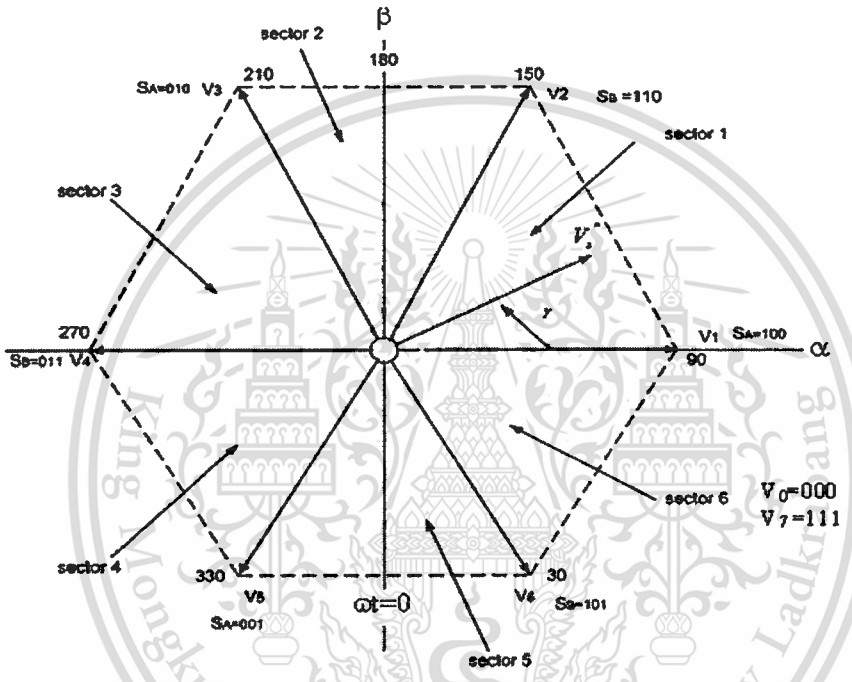


**Figure** 4.2 Inverter output voltage space with desired output voltage vector $V_s$. Inverter leg switching states are designated 1(high) and 0(low).

The typical pulse pattern of SVPWM corresponding to sector 1 as shown in Figure 4.2. It is assumed that during each switching period (T), the desired output voltage space vector ($V_s$) is constant. For any sector, equating the volt second integral of vector (Vs) with the inverter output voltage vectors over one switching period gives:

$$V_s T = V_0 t_0 + V_a t_a + V_b t_b + V_7 t_7 \tag{4.1}$$

where

$V_a, V_b$ are the adjacent active voltage vector components allocated to the switching states (100), (101) or (001) and (110), (011), or (101)

$V_0, V_7$ are null voltage vector components corresponding to switching states (000) and (111), Respectively.

$$T = t_a + t_b + t_7 + t_0 \tag{4.2}$$

where

$t_a, t_b$ is active pulse times

$t_7, t_0$ is null pulse times

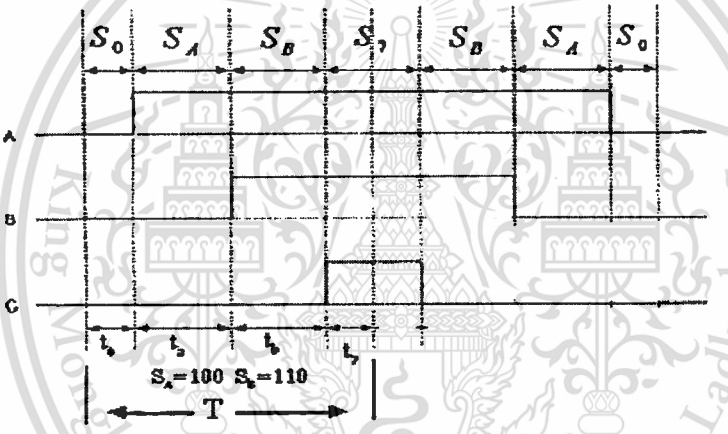


Figure 4.3 Pulse pattern of SVPWM in sector 1

Taking into account that $V_a$ and $V_b$ are constant and $V_0$, $V_7 = 0$ and resolving the above equation into orthogonal components gives:

$$t_a = \frac{\sqrt{2}|v_s|}{V_{dc}} T \sin(60 - \gamma) \tag{4.3}$$

$$t_b = \frac{\sqrt{2}|v_s|}{V_{dc}} T \sin\gamma \tag{4.4}$$

$0 \le \gamma \le 60°$

Corresponding expressions can be derived for the remaining sectors; more comprehensive details can be found in [15].

Generally, $t_7, t_0$ are chosen to be equal and then the space vector phase switching sequences can be exactly represented as an asymmetric regular sampled PWM waveform using a modified modulation waveform (SVPWM) under steady state conditions as shown in Figure 4.4. In this figure, curve ***b*** is the modulating waveform equivalent to space vector and curve ***a*** is the fundamental component. The equivalent modulating waveform is given by:

$$\begin{aligned} V_{SVM} &= \frac{3}{2}\sin(\omega t) && 0 \le \omega t \le \frac{\pi}{6} \\ V_{SVM} &= \frac{3}{2}\sin(\omega t + \frac{\pi}{6}) && \frac{\pi}{6} \le \omega t \le \frac{\pi}{2} \end{aligned} \tag{4.5}$$

With quarter wave symmetry defining the rest of the waveform.

The space vector modulation wave can be regarded as a sum of the desired fundamental sine wave component and a third harmonic triangular distortion waveform as shown in Figure 4.4.

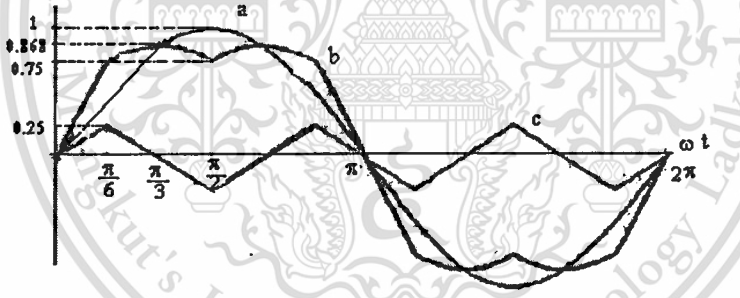


**Figure 4.4** Space vector phase voltage components

(a) Fundamental sinusoidal

(b) Space vector phase voltage (b = a+c )

(c) Third harmonic triangle wave distortion

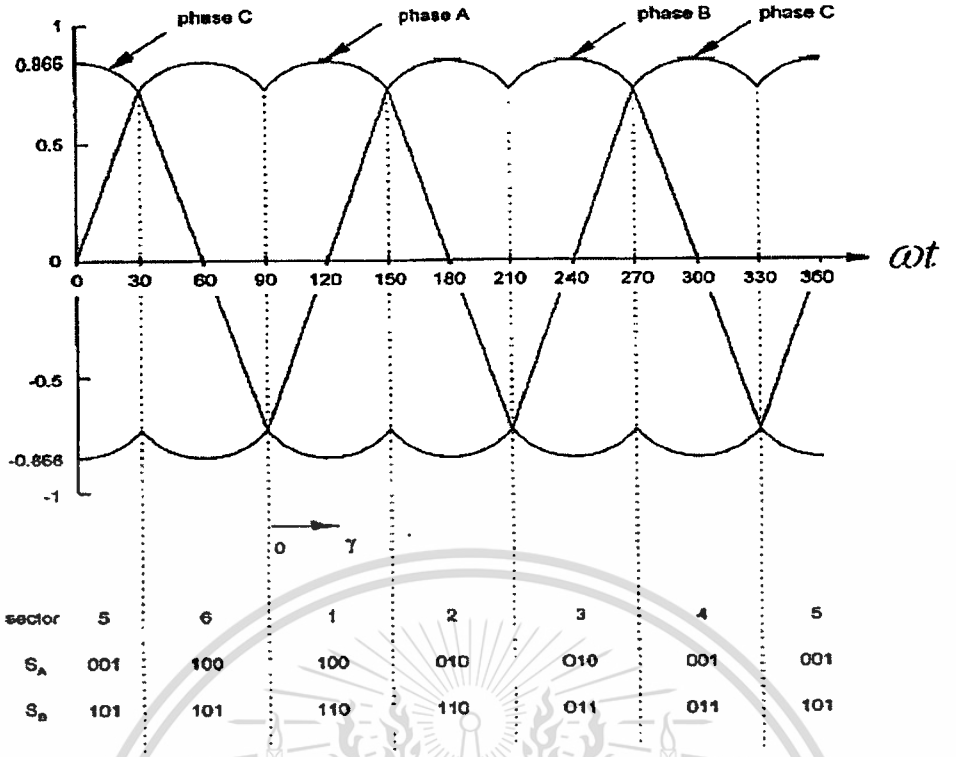


**Figure 4.5** Typical three phase waveform showing the presence of common third harmonic (Sine wave amplitude = 1)

Figure 4.4 shows the three equivalent modulating waveforms for the space vector method. Since the peak amplitude for unity fundamental is $\sqrt{3}/2$ this allows a modulation index of $2/\sqrt{3}$ (=1.15) before over-modulation occurs and is one of the advantages of the SVPWM of the original regular sampling method. The regular sampling method with triple harmonic addition however has the same advantage.

In a high performance drive system the SVPWM calculations are generally updated at each sampling period due to the need to continuously vary the output voltage frequency and amplitude. In this project which is concerned with steady state losses it is possible to implement both regular sampling and space vector modulation with the same control program by interchanging the modulation waveform

### 4.2.2 Prediction of Harmonic Voltage Spectra under Various of Modulation Index and with V/f in Constant

Due to the frequency and voltage dependence of core losses, the PWM voltage spectra need to be determined at various modulation depths (ma) under inverter frequency50Hz. The simulated results showed the PWM voltage spectra with a variation of modulation depth (ma) and by keeping V/f in constant. The predicted or simulation results will be evaluated as below:

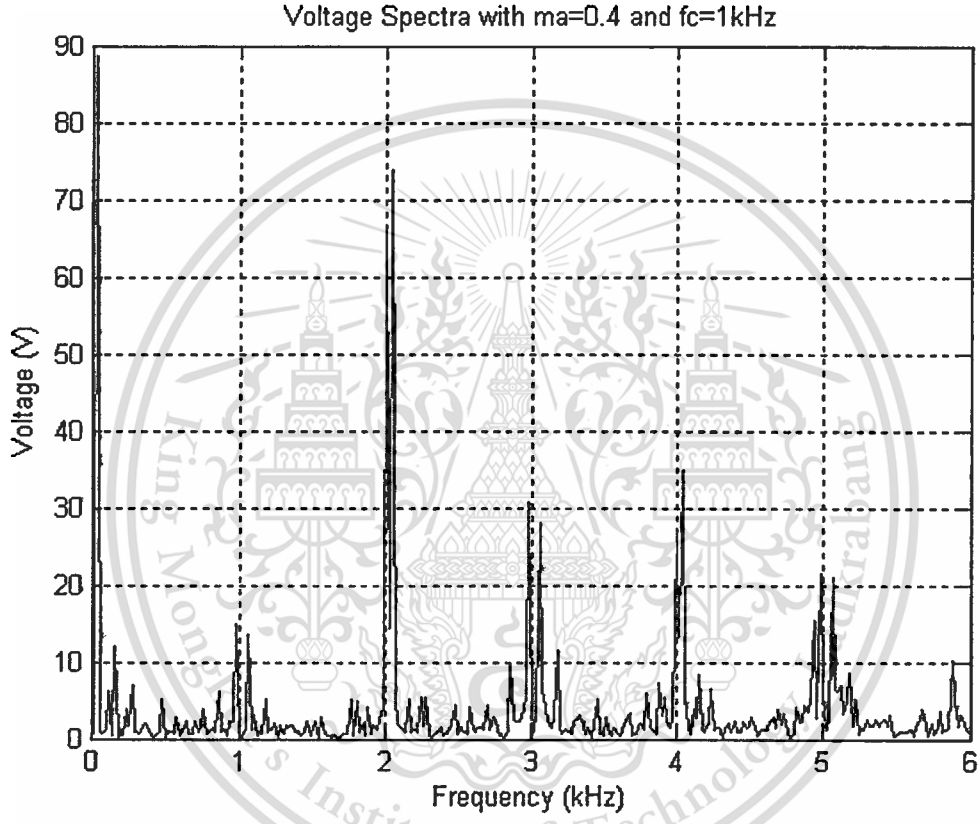


**Figure 4.6** Predicted results of fundamental voltage with ma=0.4 and $f_c$=1 kHz

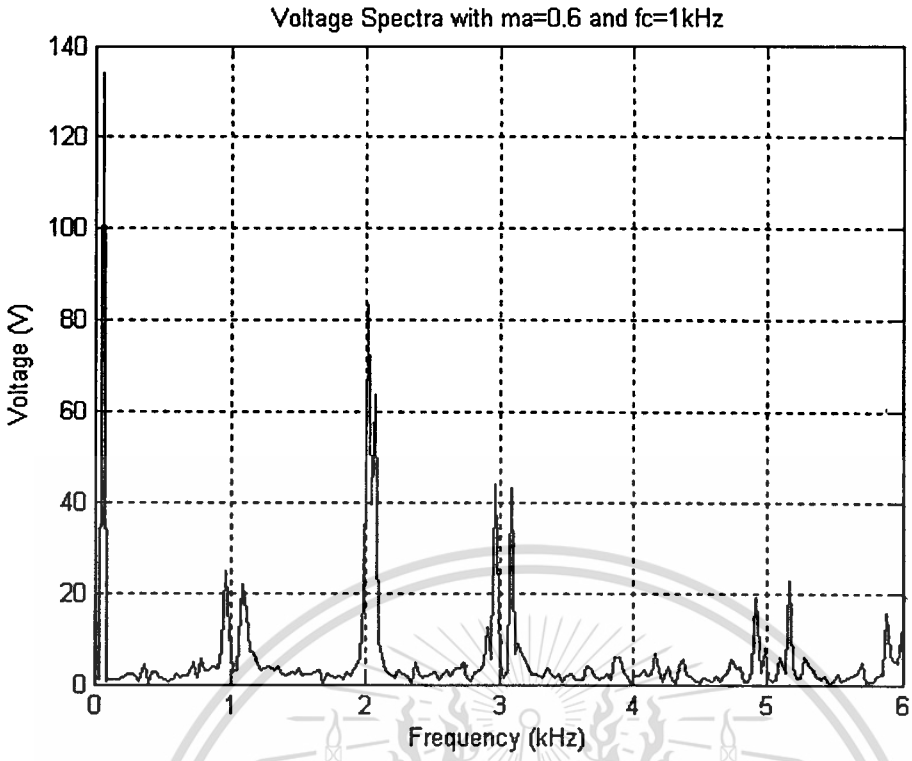


**Figure 4.7** Predicted results of fundamental voltage with ma=0.6 and $f_c$=1 kHz

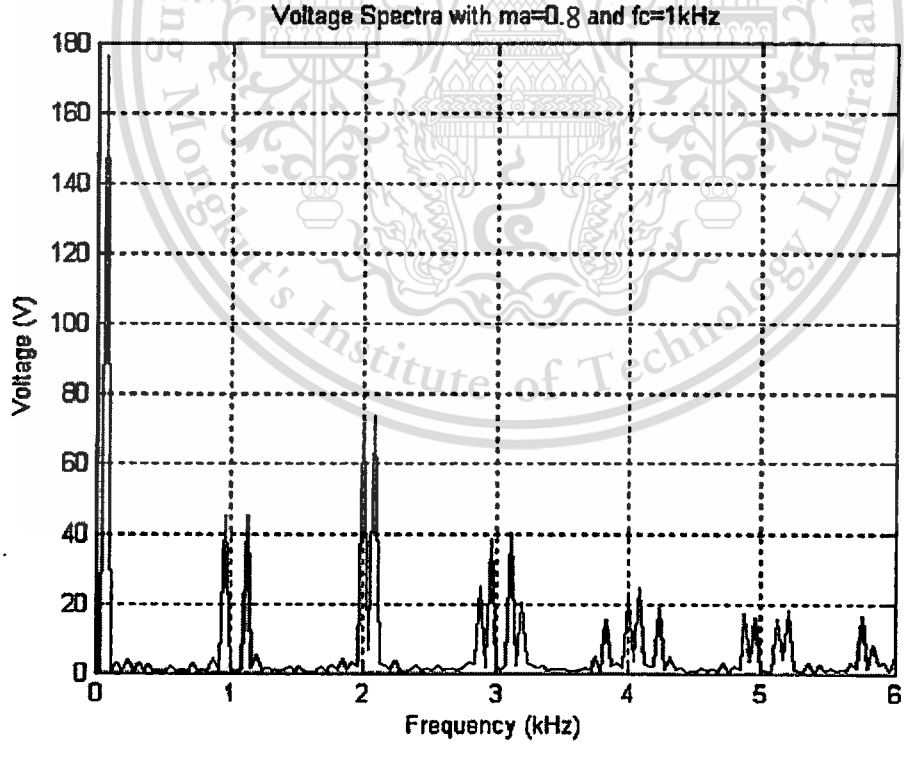


**Figure 4.8** Predicted results of fundamental voltage with ma=0.8 and $f_c$=1 kHz

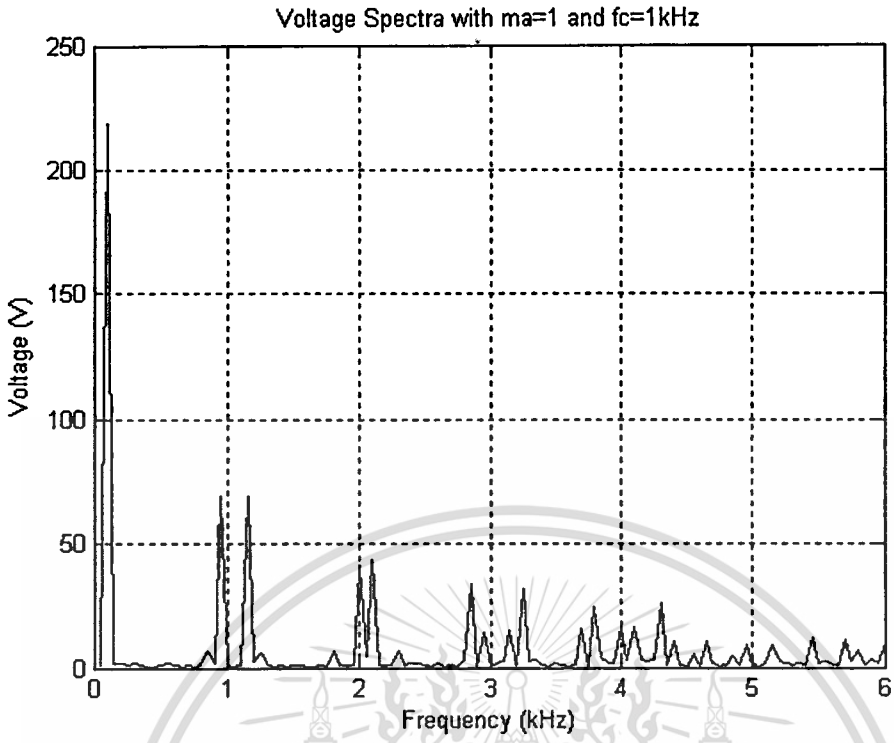


**Figure 4.9** Predicted results of fundamental voltage with ma=1and $f_c$=1 kHz.

The predicted results shows in Figure 4.6 up to 4.9, when increasing modulation depth(ma) then, the harmonic voltage decreases and the same time the fundamental voltage will be increased. Therefore the harmonics voltage should be minimized by keeping modulation depth (ma) as high as possible.

### 4.2.3 Prediction of Harmonic Voltage Spectra under Variation of Modulation Index and by Keeping of Fundamental Voltage (220V)

The effect of modulation index to harmonic voltage is played very important role in harmonic loss calculation. The purpose of this title is in order to meet the effect of modulation index (ma) to the harmonic voltage spectra and harmonic loss spectra. The predicted results will be shown at the figures below:

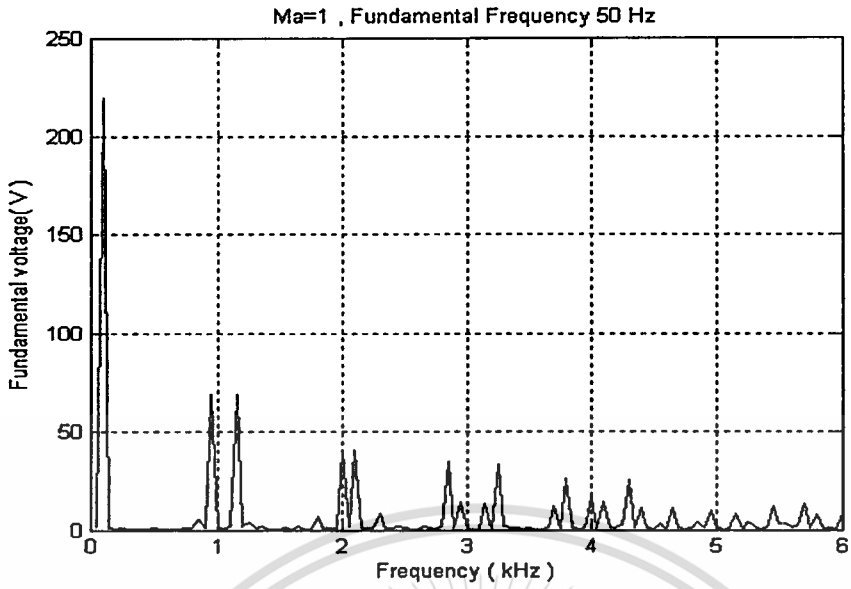


**Figure 4.10** Predicted results of voltage spectra with ma = 1, fundamental frequency 50 Hz, switching frequency of 1 kHz and $V_{Fund.}$ = 220 V.

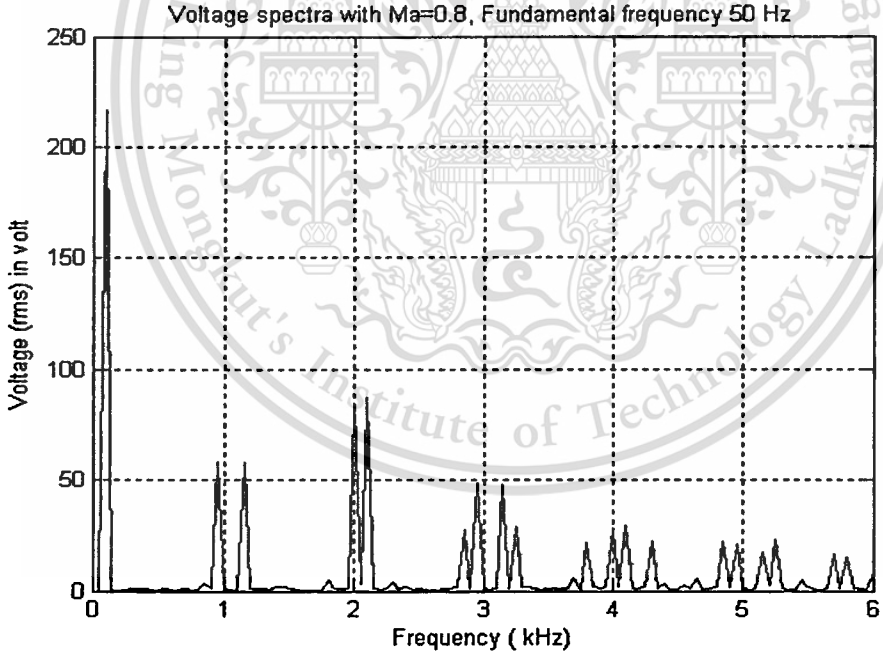


**Figure 4.11** Predicted results of voltage spectra with the effect of modulation index ma=0.8, $f_s$=50Hz, switching frequency of 1 kHz and with constant voltage (rms)=220V

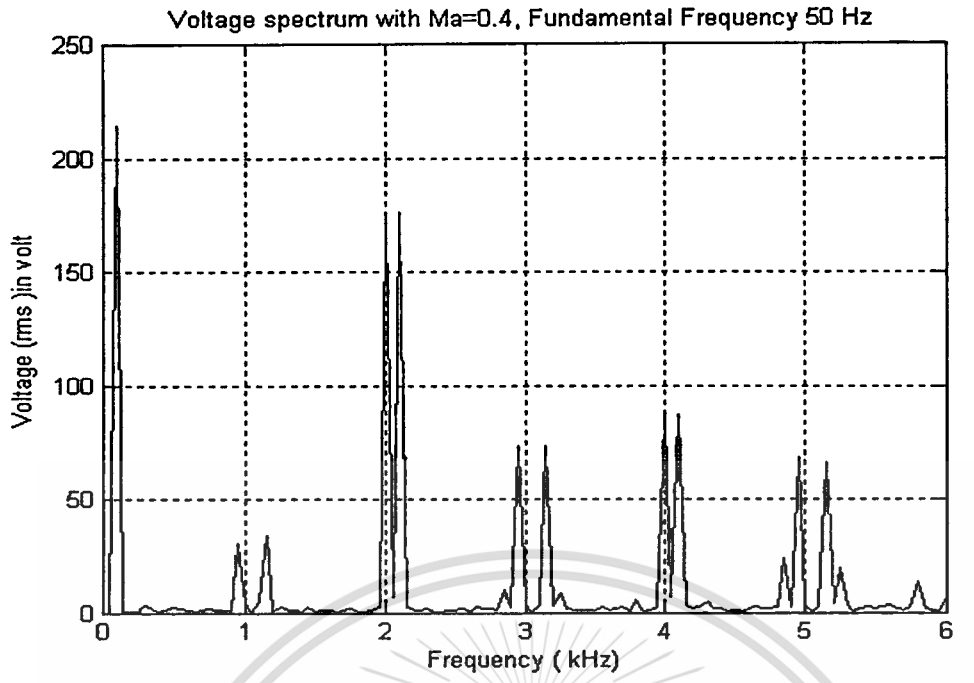


**Figure 4.12** Predicted results of voltage spectra with the effect of modulation index ma=0.4, $f_s$ =50Hz switching frequency of 2 kHz and with constant voltage ( rms )220V

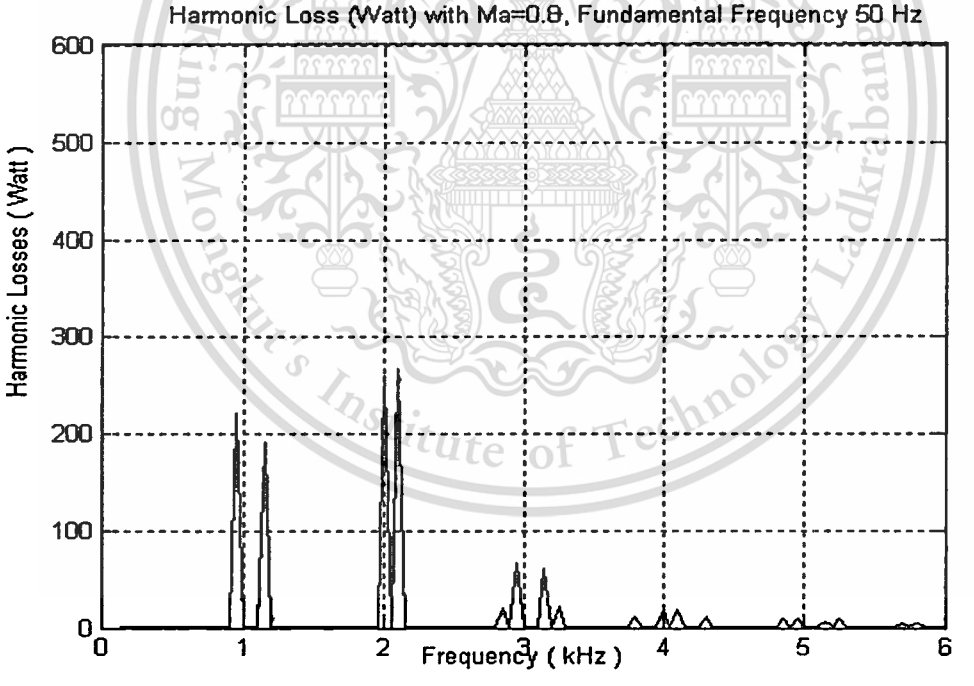


**Figure 4.13** The Effects of Voltage Spectra and Modulation Index into Harmonic Losses Corresponding to Figure 4.11

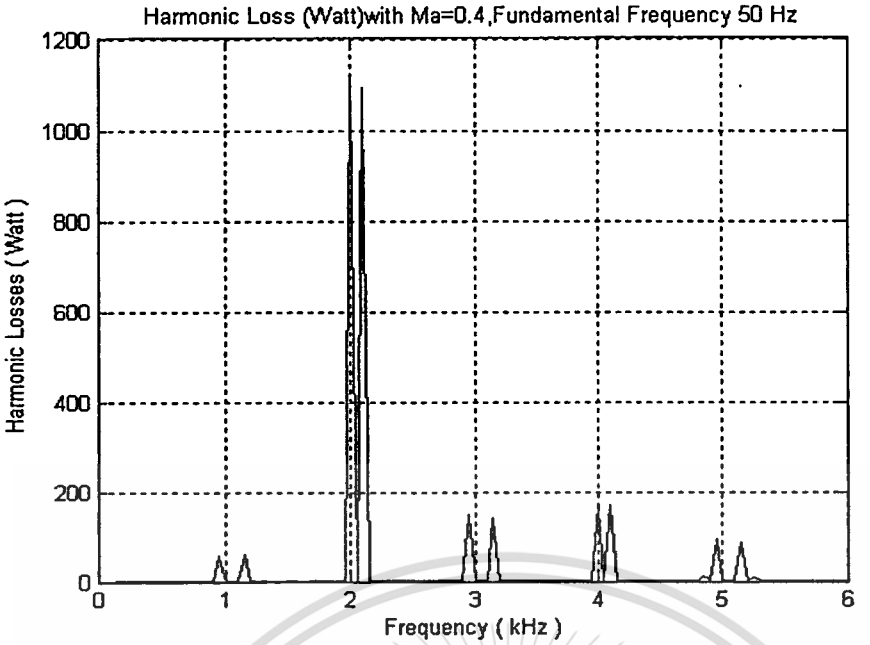


**Figure 4.14** The Effects of Voltage Spectra and Modulation Index into Harmonic Losses Corresponding to Figure 4.12

The predicted results shown in above Figures are the effect of modulation index into harmonic voltage spectra and harmonic loss spectra. Figures 4.10 to 4.12 can be evaluated, that when modulation index is decreased, then the harmonic loss spectra will be increased and Figures 4.13 and 4.14 shown the effect of modulation index in to harmonic loss spectra, that when ma is decreased, then the harmonic loss spectra will be increase. Therefore the modulation index should be kept as equal or less than 1.

### 4.2.4 Prediction of Harmonic Voltage Spectra and Loss Spectra under Variation of Inverter Frequency and Switching Frequency

The harmonic voltage and loss spectra are related together. For the prediction of harmonic losses, the harmonic voltage and loss spectra need to be determined. This purpose of this title is the simulation of harmonic voltage and loss spectra under several of switching frequency and variation of inverter frequency. The simulation results are the comparative between harmonic spectra and harmonic loss spectra and shows as followings Figures:

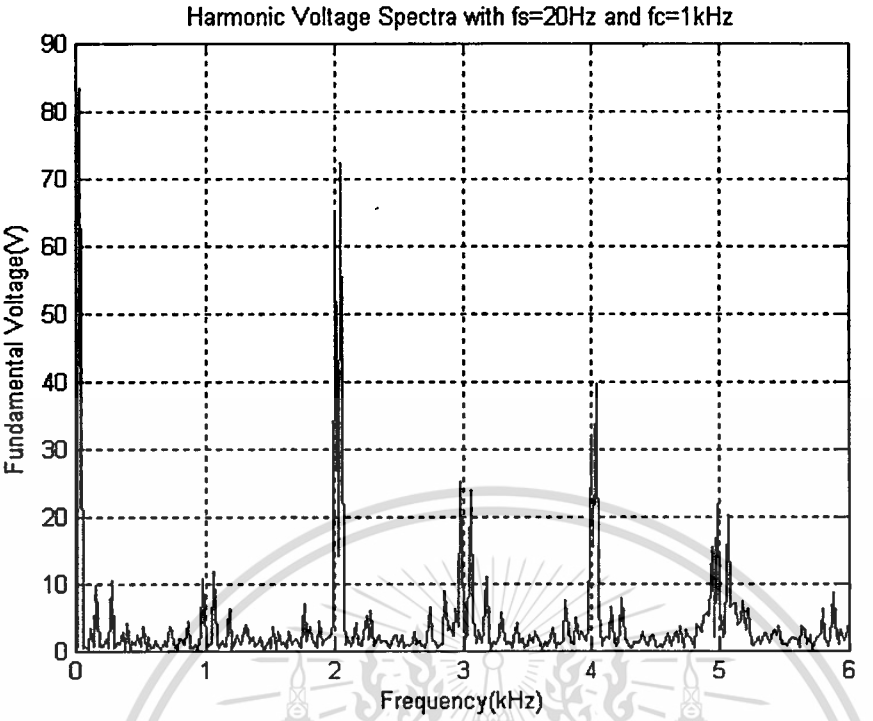


(a) Harmonic voltage spectra

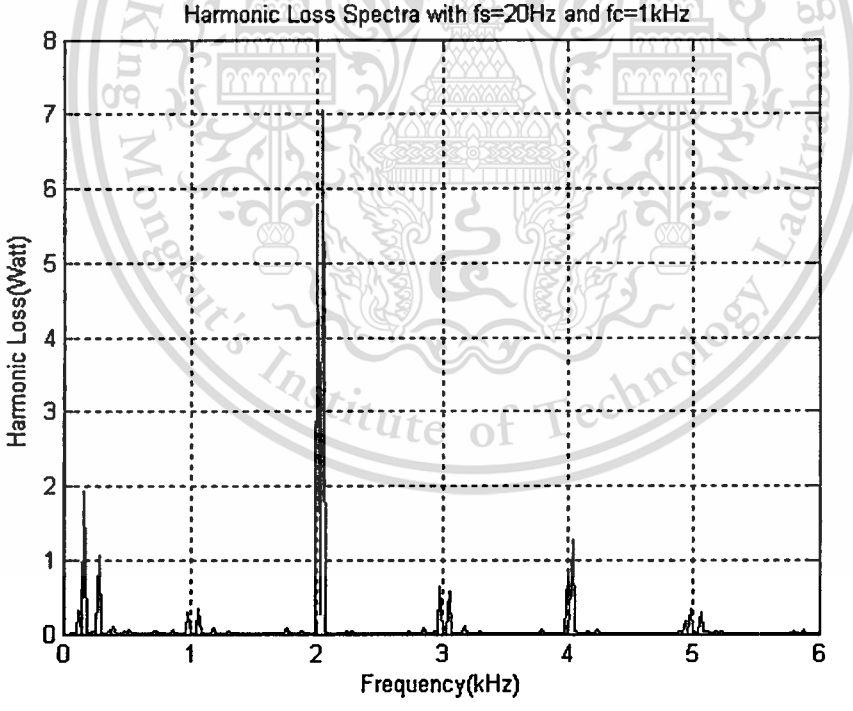


(b) Harmonic loss spectra

**Figure 4.15** The predicted results of (a) harmonic voltage spectra and (b) harmonic loss spectra with fundamental frequency of 20 Hz and 1 kHz switching frequency.

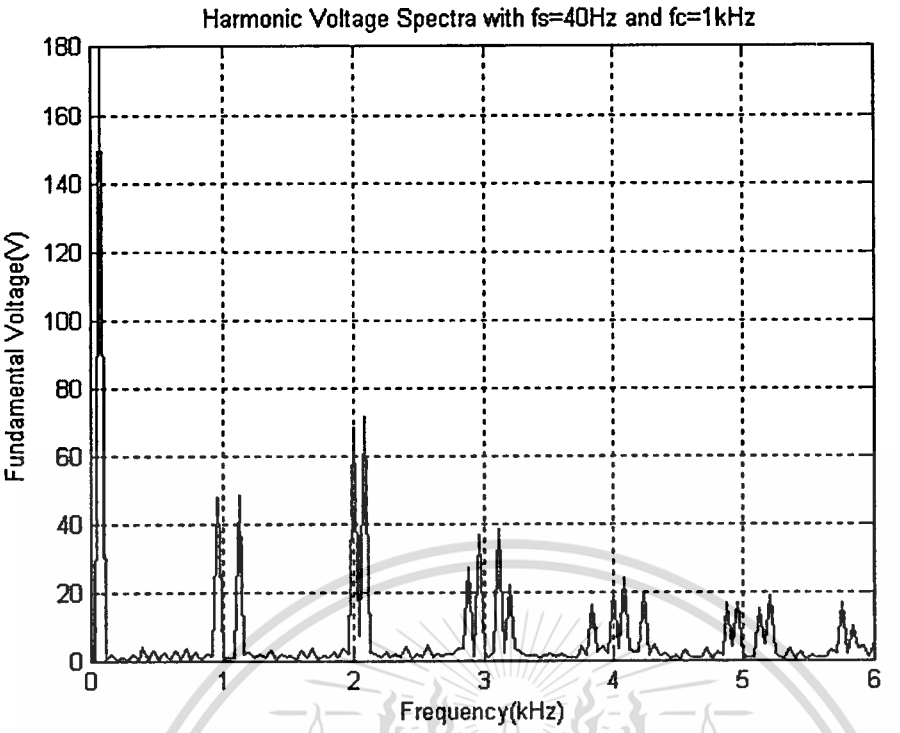


(a) Harmonic voltage spectra

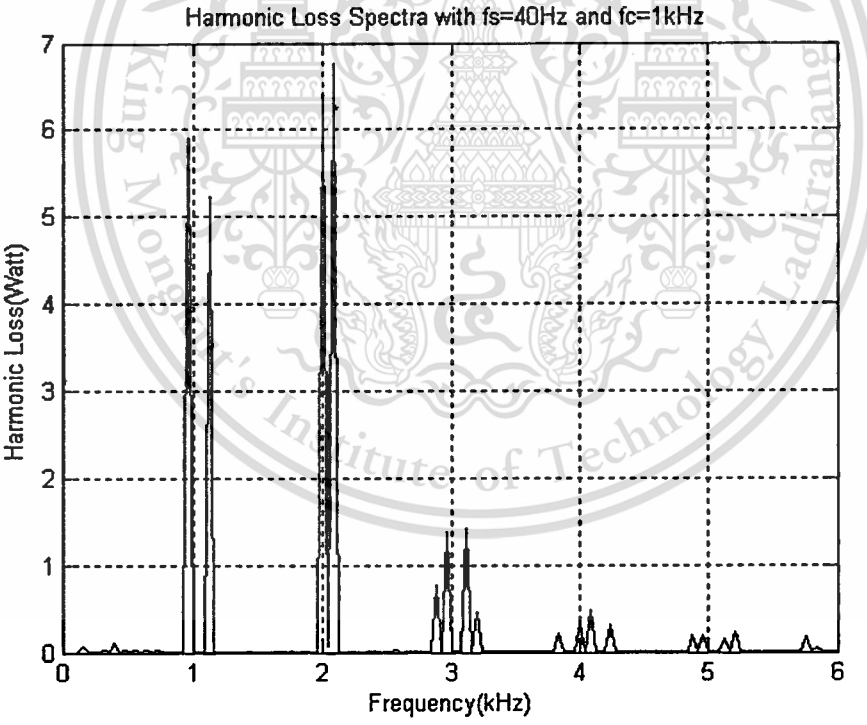


(b) Harmonic loss spectra

**Figure 4.16** The predicted results of (a) harmonic voltage spectra and (b) harmonic loss spectra with fundamental frequency of 40 Hz and 1 kHz switching frequency.

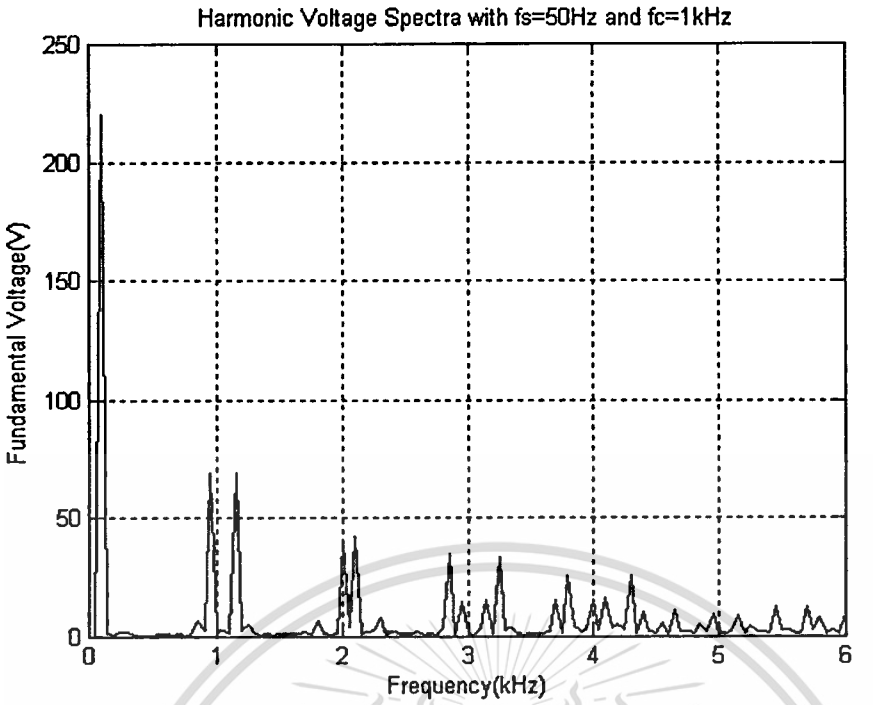


(a) Harmonic voltage spectra

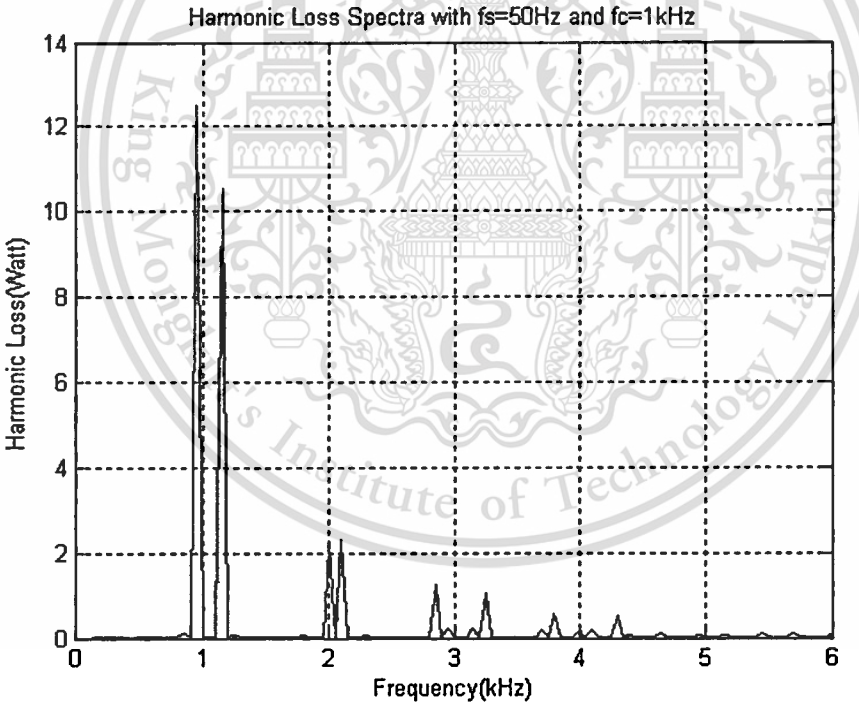


(b) Harmonic loss spectra

**Figure 4.17** The predicted results of (a) harmonic voltage spectra and (b) harmonic loss spectra with fundamental frequency of 50 Hz and 1 kHz switching frequency.

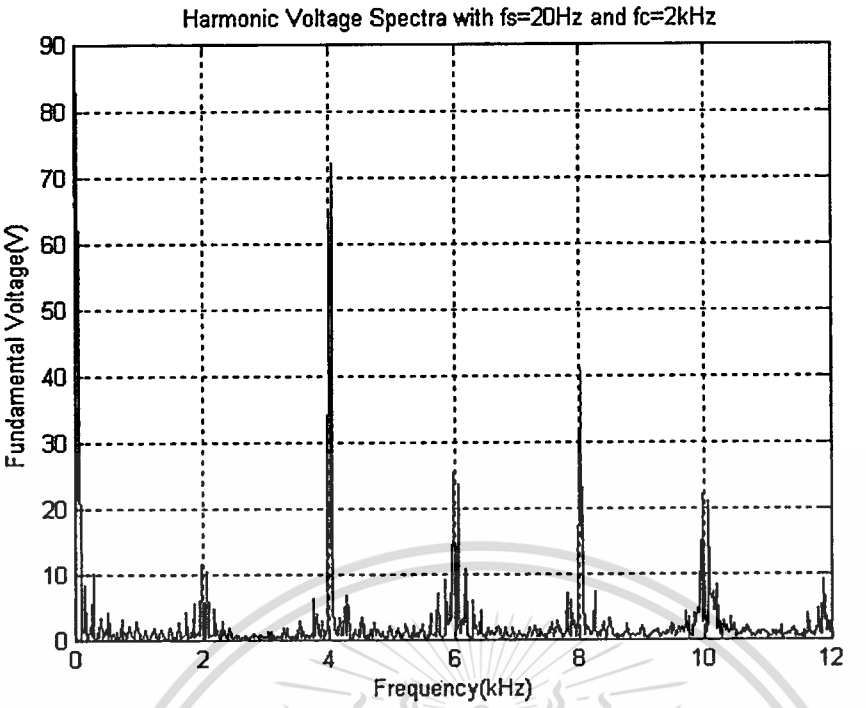


(a) Harmonic voltage spectra

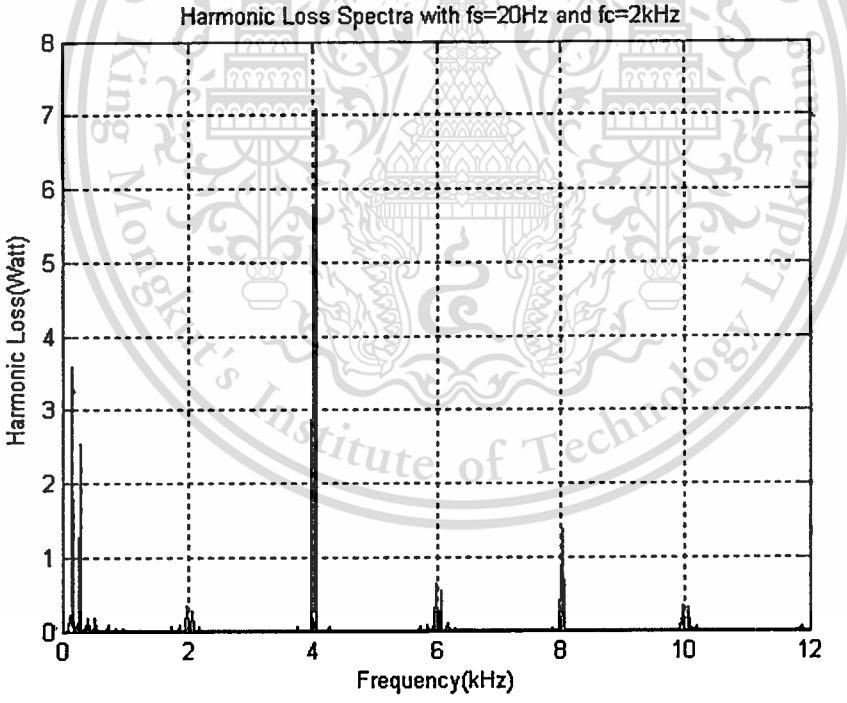


(b) Harmonic loss spectra

**Figure 4.18** The predicted results of (a) harmonic voltage spectra and (b) harmonic loss spectra with fundamental frequency of 20 Hz and 2 kHz switching frequency.

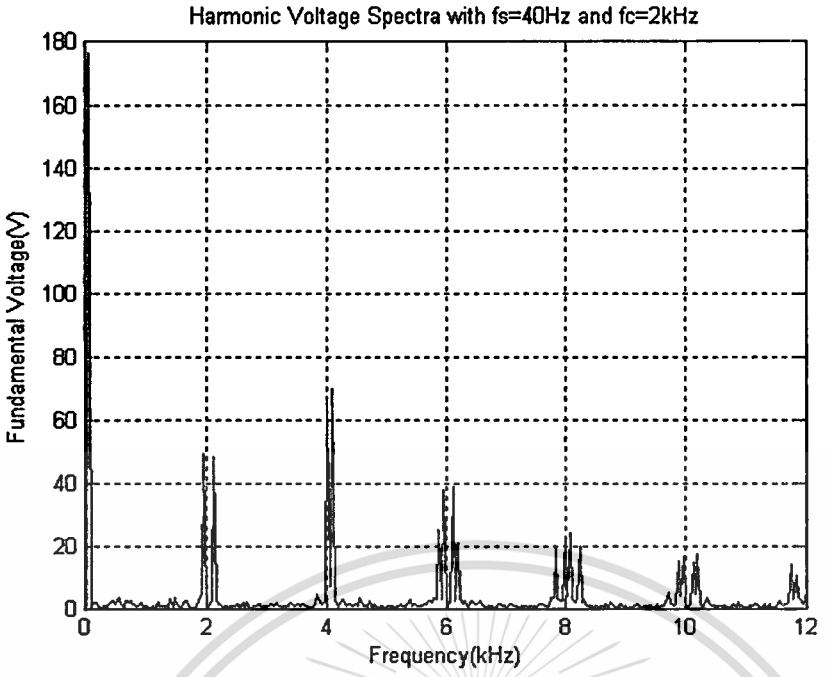


(a) Harmonic voltage spectra

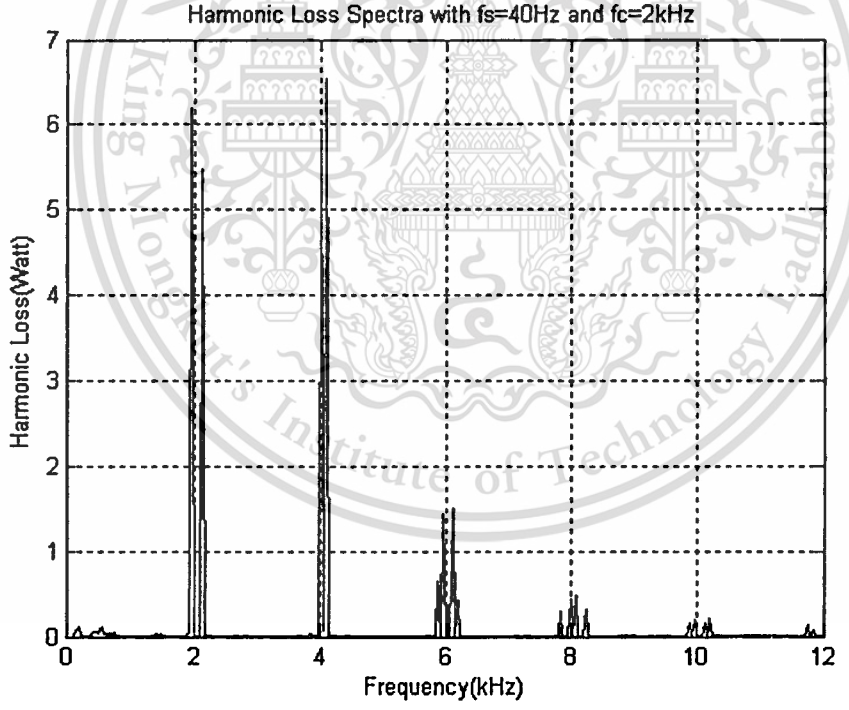


(b) Harmonic loss spectra

**Figure 4.19** The predicted results of (a) harmonic voltage spectra and (b) harmonic loss spectra with fundamental frequency of 40 Hz and 2 kHz switching frequency.

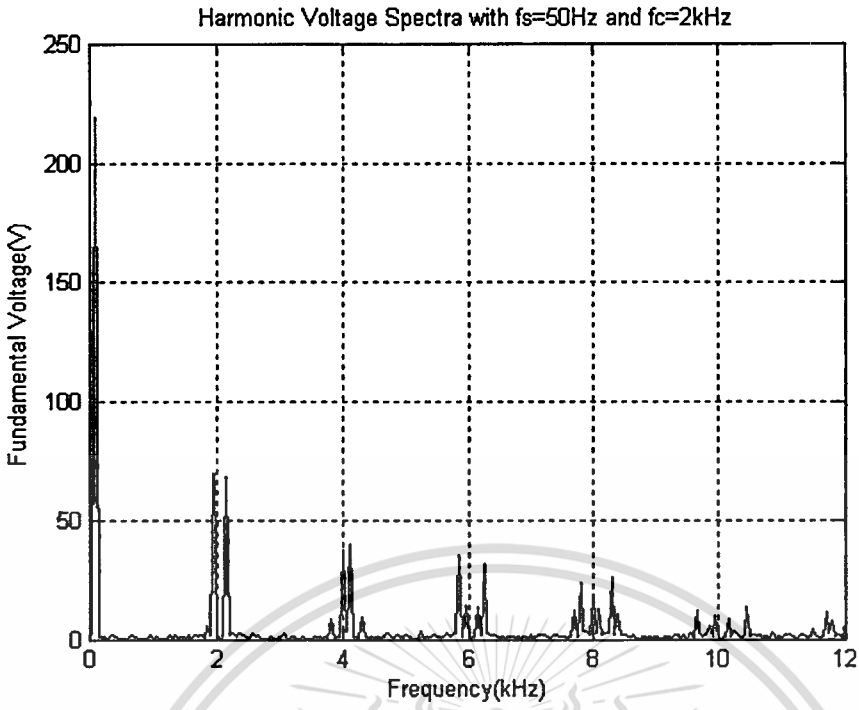


(a) Harmonic voltage spectra

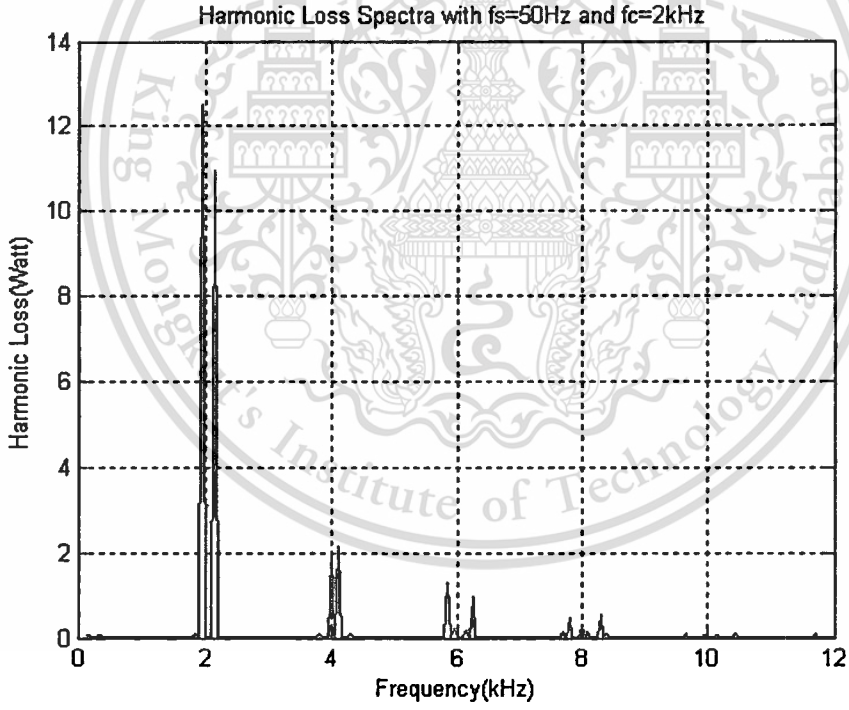


(b) Harmonic loss spectra

**Figure 4.20** The predicted results of (a) harmonic voltage spectra and (b) harmonic loss spectra with fundamental frequency of 50 Hz and 2 kHz switching frequency.

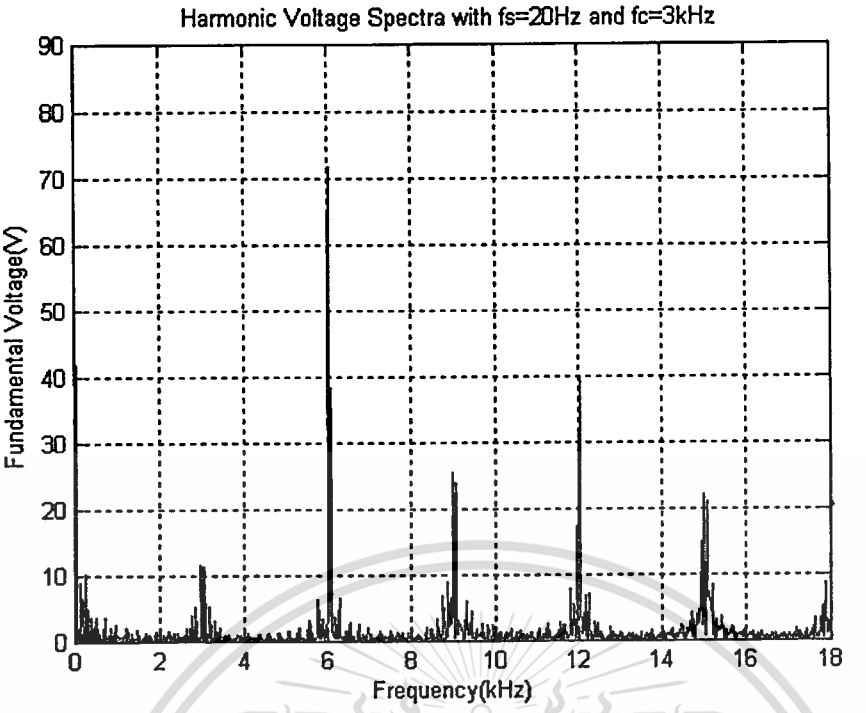


(a) Harmonic voltage spectra

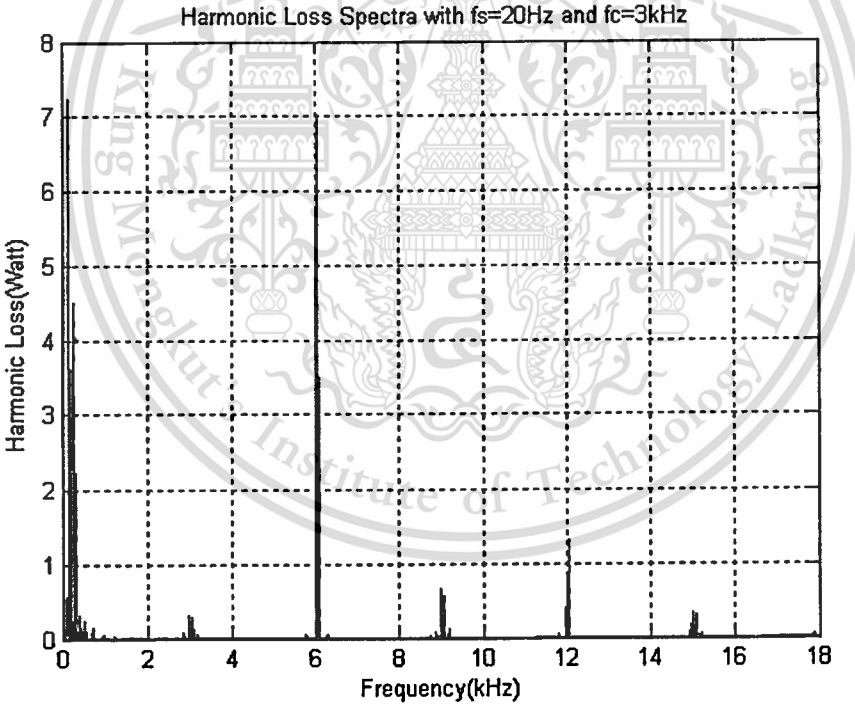


(b) Harmonic loss spectra

**Figure 4.21** The predicted results of (a) harmonic voltage spectra and (b) harmonic loss spectra with fundamental frequency of 20 Hz and 3 kHz switching frequency.

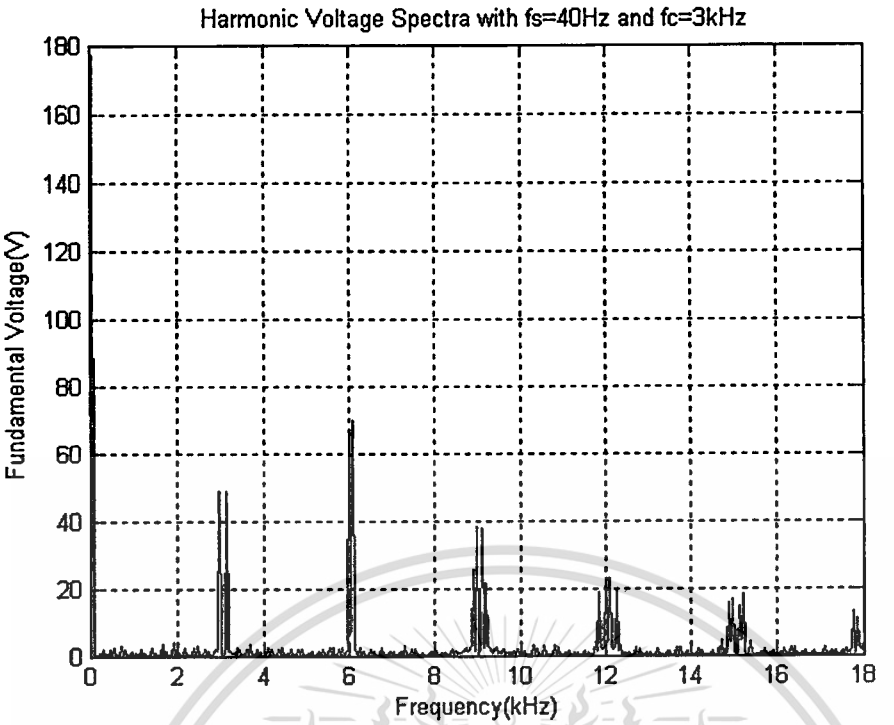


(a) Harmonic voltage spectra

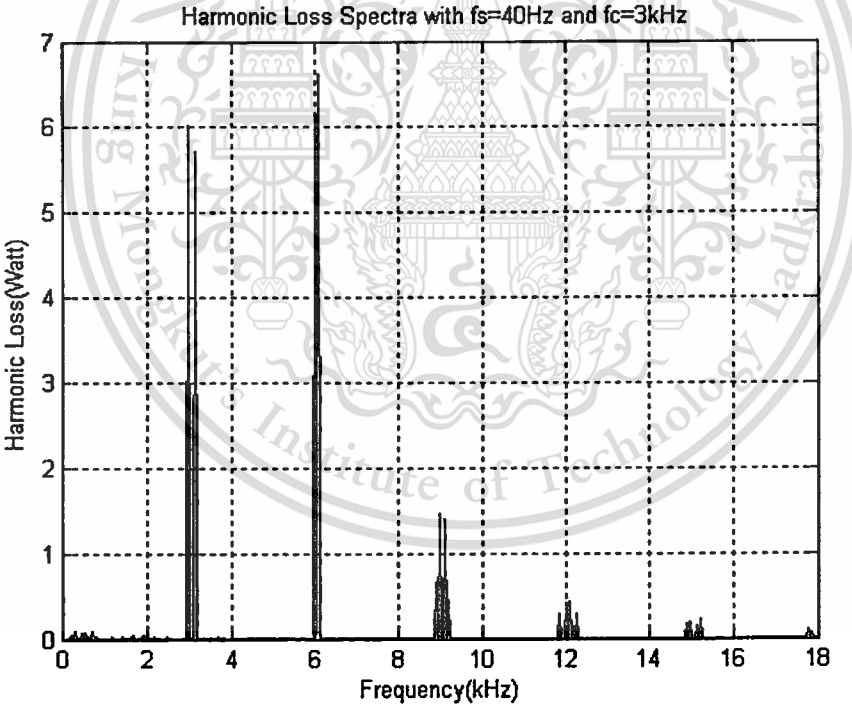


(b) Harmonic loss spectra

**Figure 4.22** The predicted results of (a) harmonic voltage spectra and (b) harmonic loss spectra with fundamental frequency of 40 Hz and 3 kHz switching frequency.

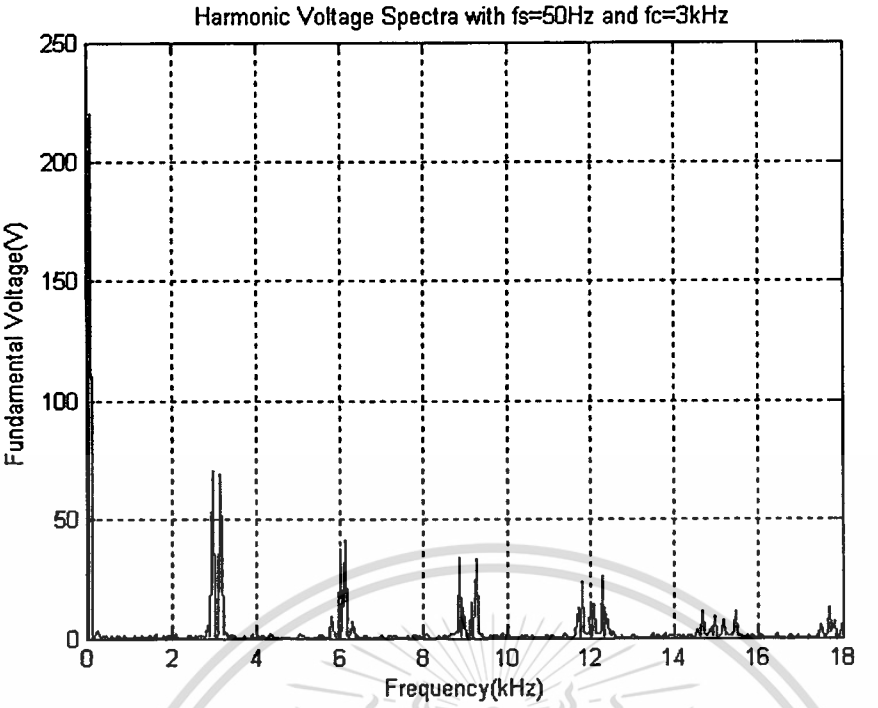


(a) Harmonic voltage spectra

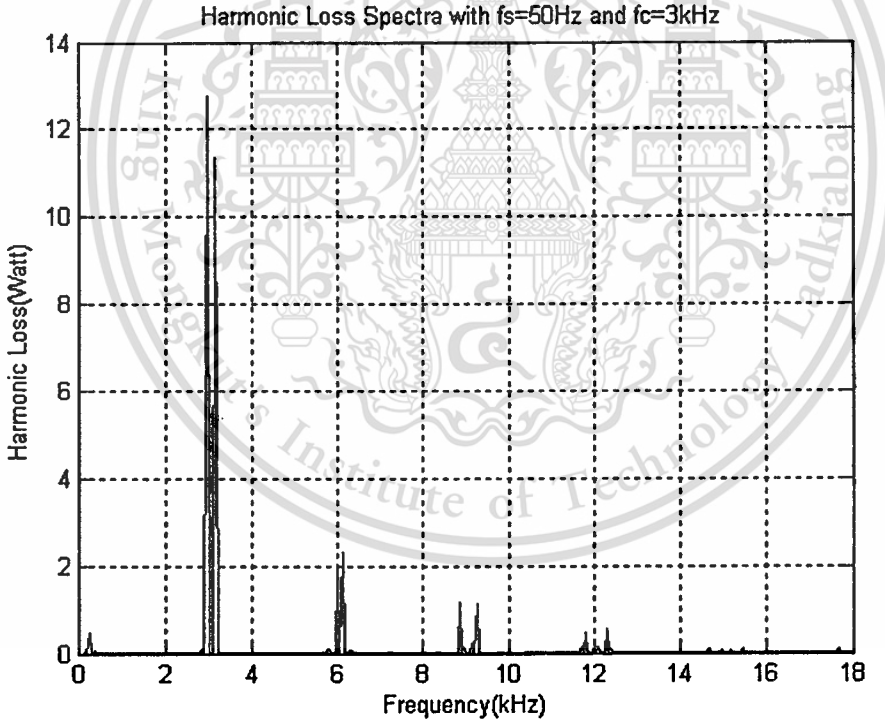


(b) Harmonic loss spectra

**Figure 4.23** The predicted results of (a) harmonic voltage spectra and (b) harmonic loss spectra with fundamental frequency of 50 Hz and 3 kHz switching frequency.

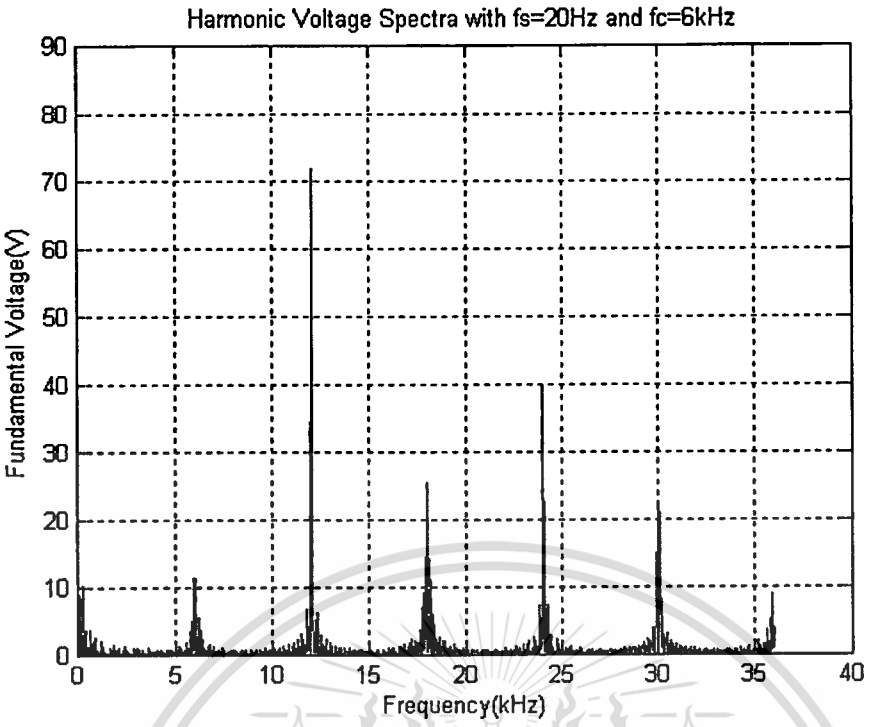


(a) Harmonic voltage spectra

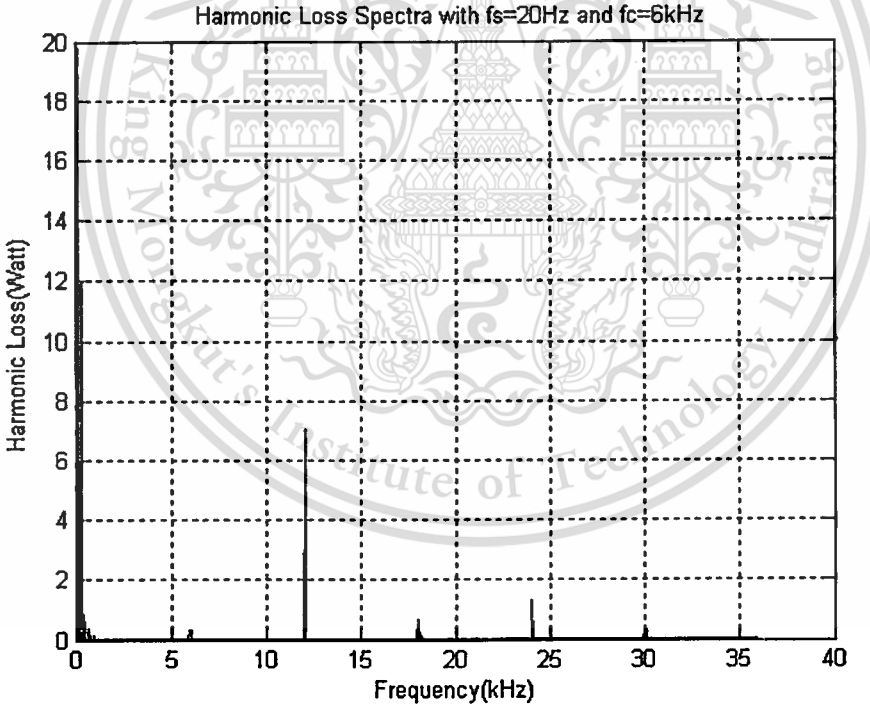


(b) Harmonic loss spectra

**Figure 4.24** The predicted results of (a) harmonic voltage spectra and (b) harmonic loss spectra with fundamental frequency of 20 Hz and 6 kHz switching frequency.

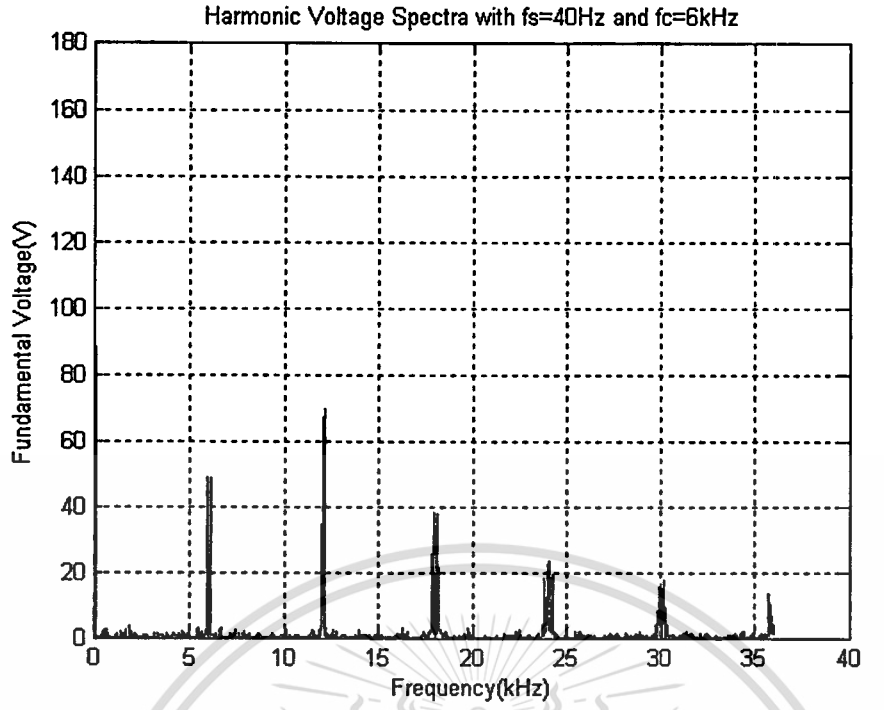


(a) Harmonic voltage spectra

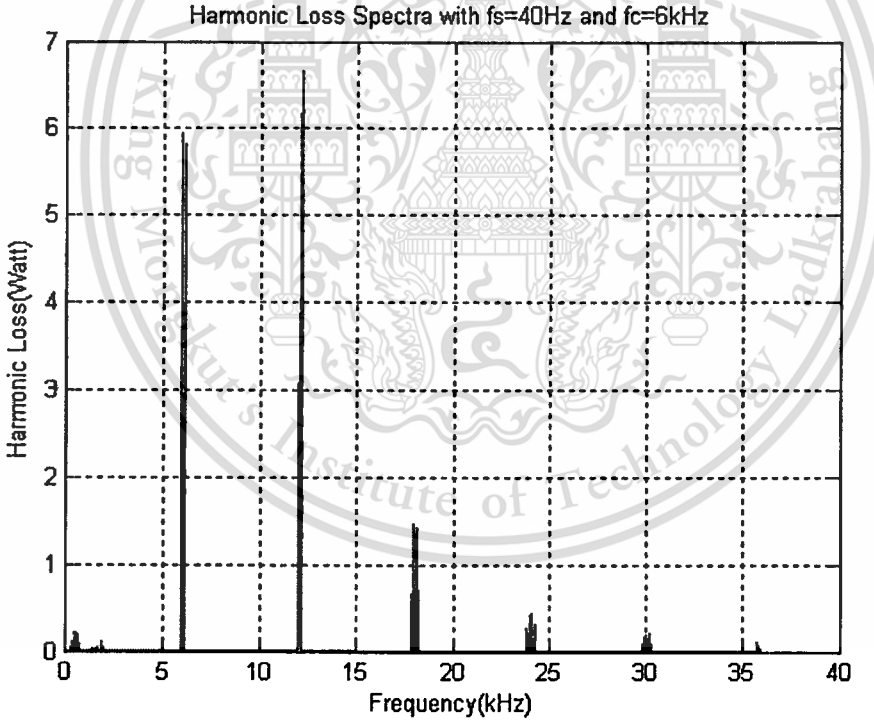


(b) Harmonic loss spectra

**Figure 4.25** The predicted results of (a) harmonic voltage spectra and (b) harmonic loss spectra with fundamental frequency of 40 Hz and 6 kHz switching frequency.

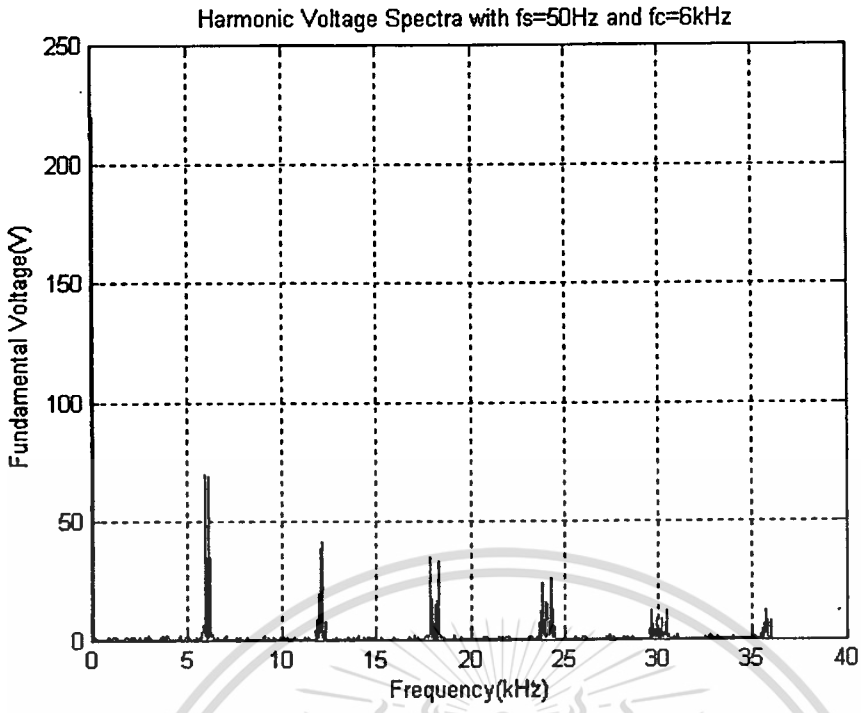


(a) Harmonic voltage spectra

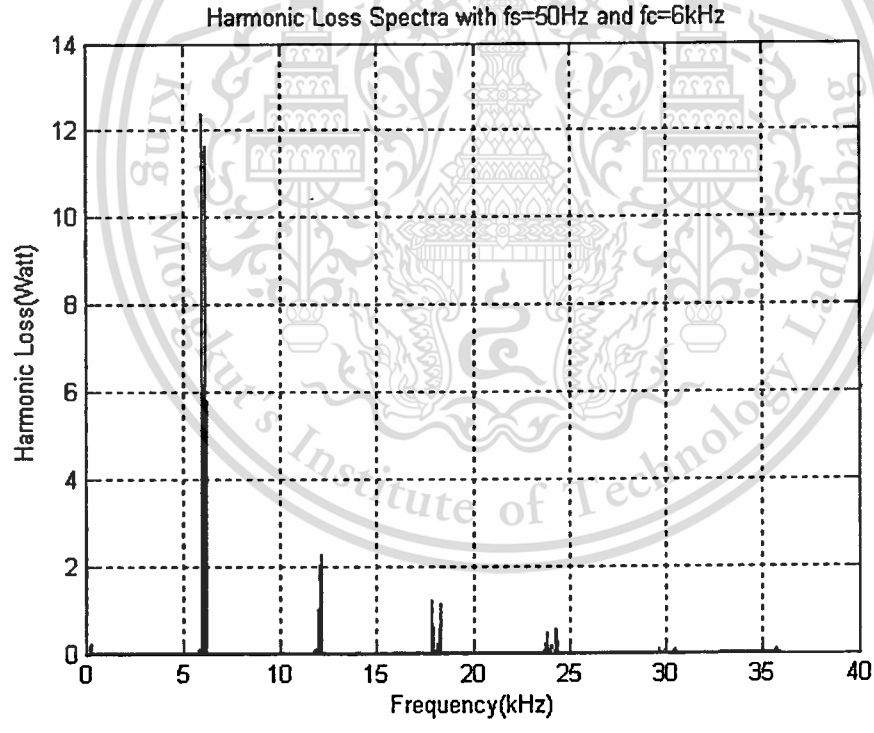


(b) Harmonic loss spectra

**Figure 4.26** The calculation results of (a) harmonic voltage spectra and (b) harmonic loss spectra with fundamental frequency of 50 Hz and 6 kHz switching frequency.

The accuracy of the SVPWM system has been proved by comparing the voltage spectra and harmonic loss spectra with those expected from an ideal PWM generation process and with variations of fundamental frequency (V/f). Detailed investigation of the low frequency spectrum has confirmed that the effects of inverter interlock delay are negligible for the switching frequencies considered. The simulation results the harmonic voltage and loss spectra with the effect of inverter frequency and switching frequency. From Figure 4.15 to 4.26 shows the comparison of voltage spectra and loss spectra. It is insight that, when switching frequency increases, then the spectra of harmonic voltage and loss decrease. In contrary, when the inverter frequency increases, then the spectra of harmonic voltage and loss increases.

## 4.3 Prediction of Total Harmonic Loss under Various Operation Conditions (Inverter Frequency, Load Conditions and Switching Frequency)

This title proposed the prediction of harmonic loss of induction motor using loss factor characteristics from Figure 4.10 and under variation of inverter frequency, load condition and switching frequency

### 4.3.1 Prediction of Total Harmonic Loss under Variation of Switching Frequency and with Various of Inverter Frequency and Load Torque .

Figure 4.27 to 4.41 results the prediction of total harmonic losses under variation of switching frequency and several of load condition and inverter frequency. The results can be concluded, when increases switching frequency, harmonic loss decreases and in contrary when increases inverter frequency and load torque, then the harmonic loss increases.

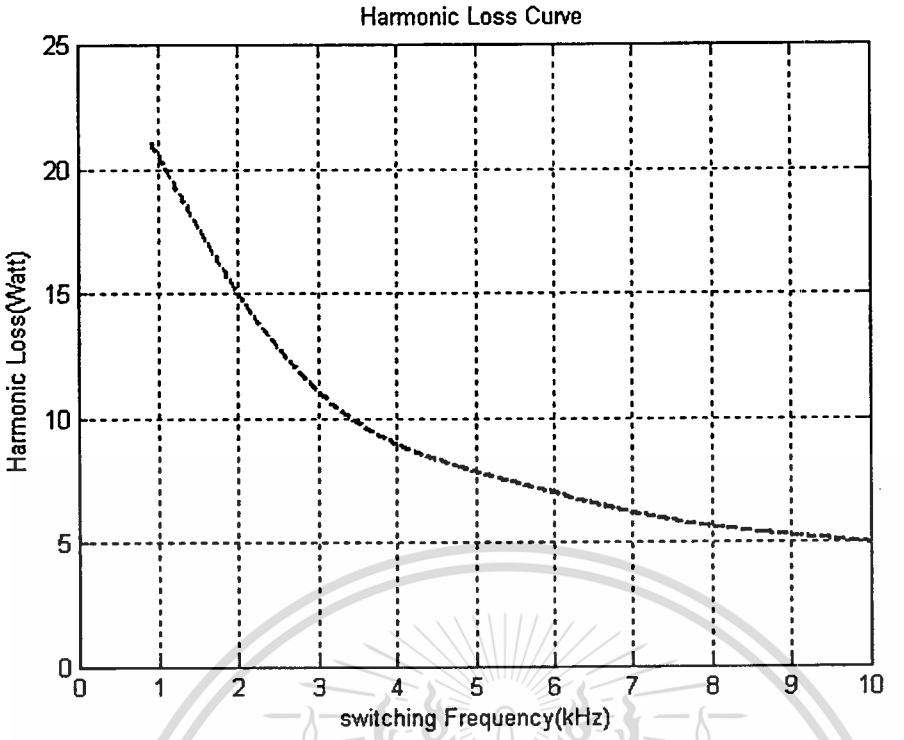


**Figure 4.27** Predicted results of total harmonic loss with 10Hz inverter frequency and 10% load torque.

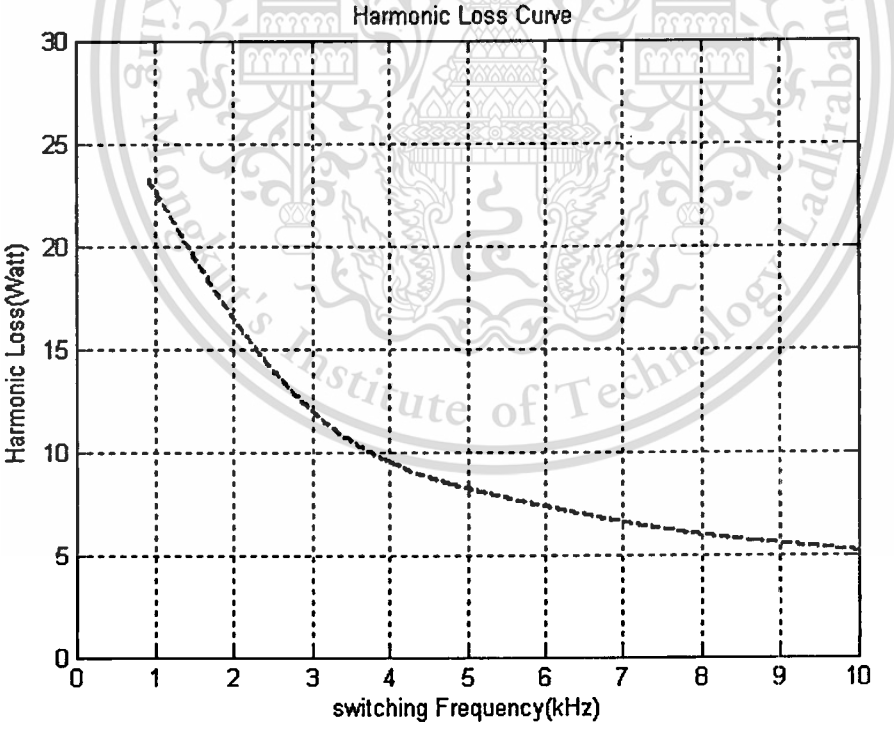


**Figure 4.28** Predicted results of total harmonic loss with 20Hz inverter frequency and 10% load torque

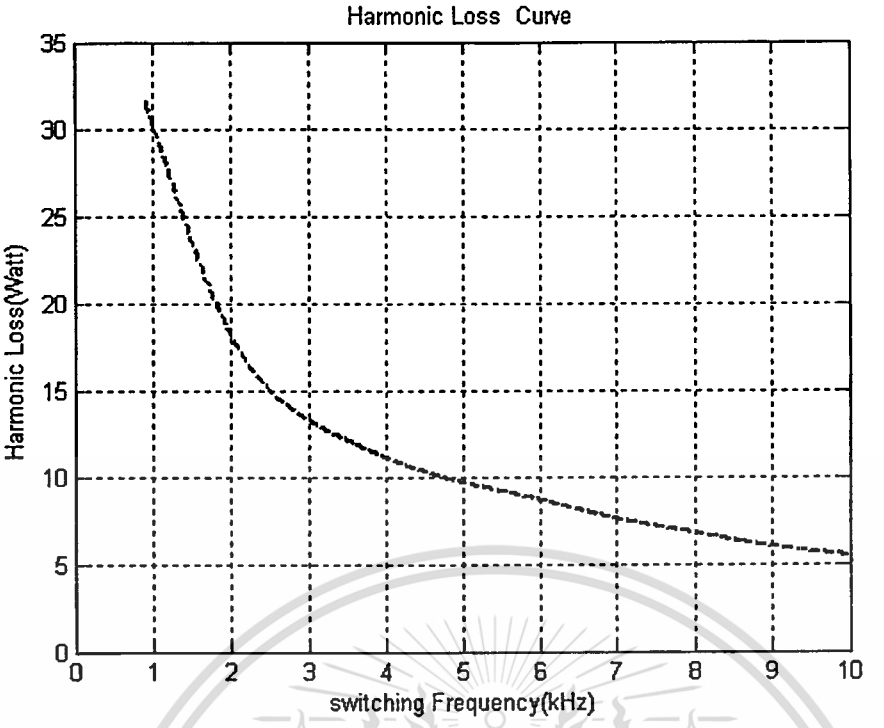


**Figure 4.29** Predicted results of total harmonic loss with 30Hz inverter frequency and 10% load torque

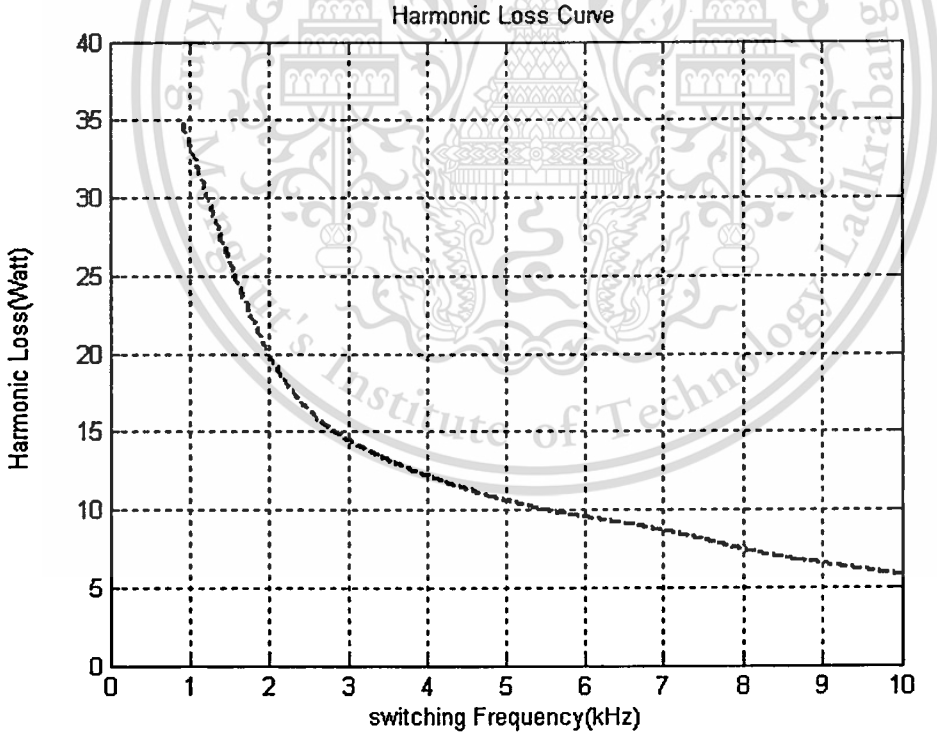


**Figure 4.30** Predicted results of total harmonic loss with 40Hz inverter frequency and 10% load torque

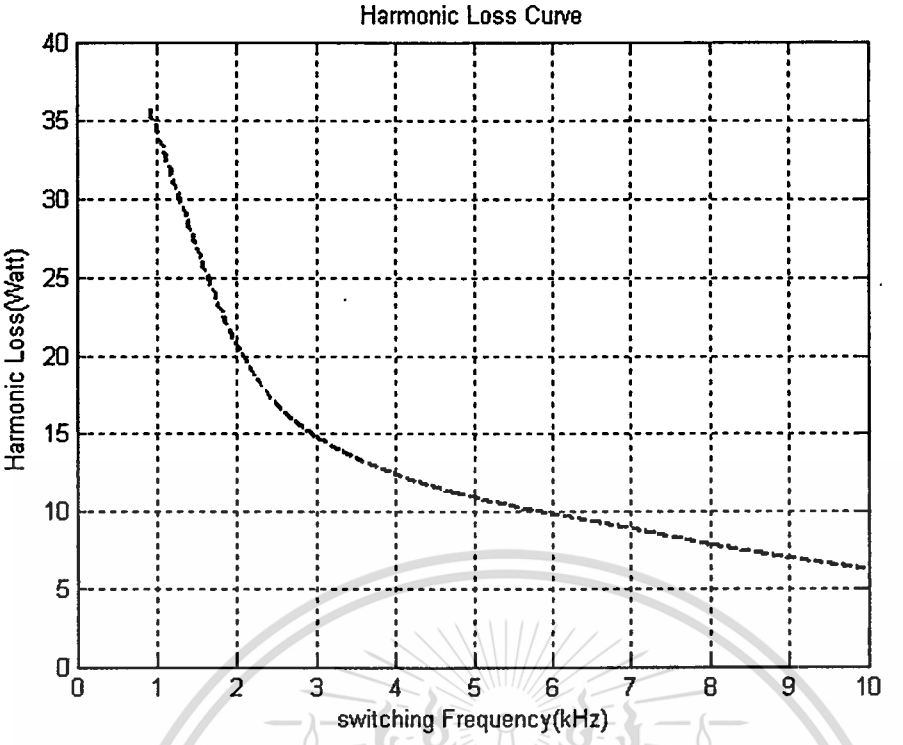


**Figure 4.31** Predicted results of total harmonic loss with 50Hz inverter frequency and 10% load torque

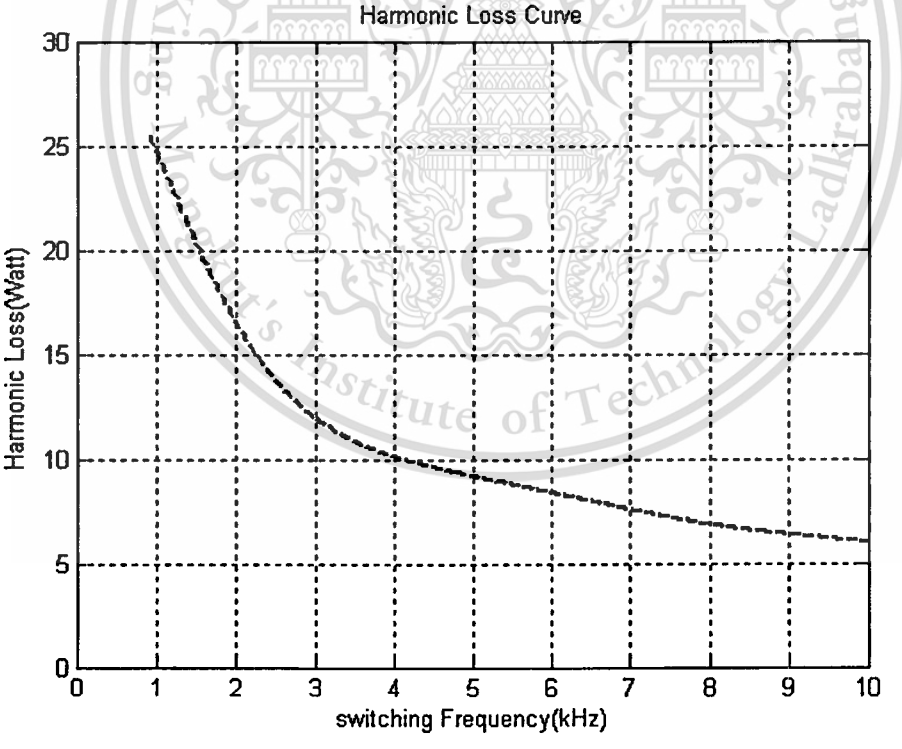


**Figure 4.32** Predicted results of total harmonic loss with 10Hz inverter frequency and 50% load torque

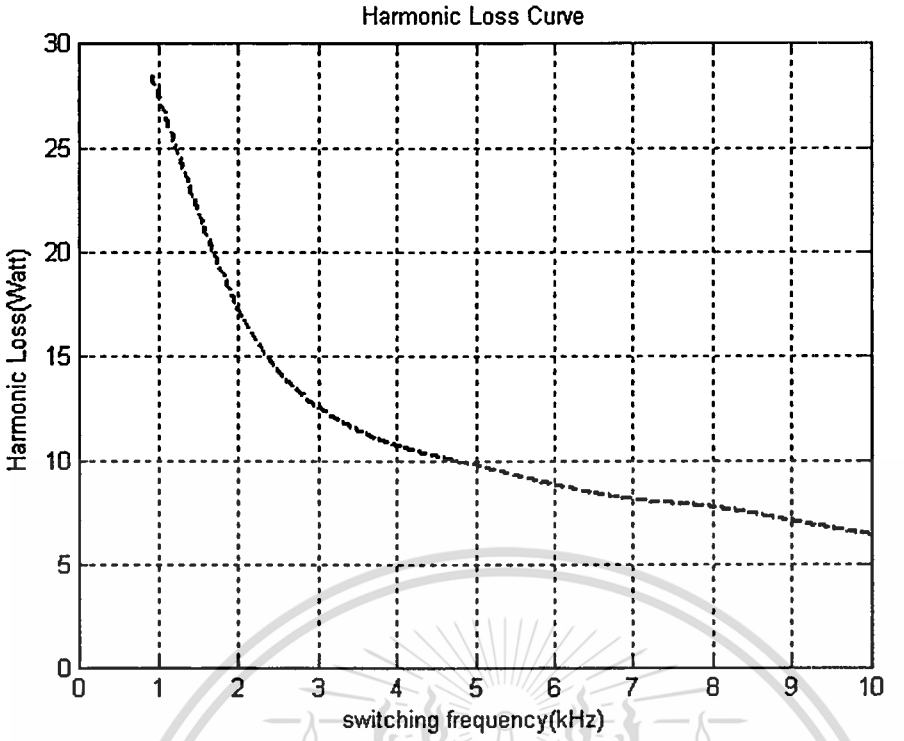


**Figure 4.33** Predicted results of total harmonic loss with 20Hz inverter frequency and 50% load torque

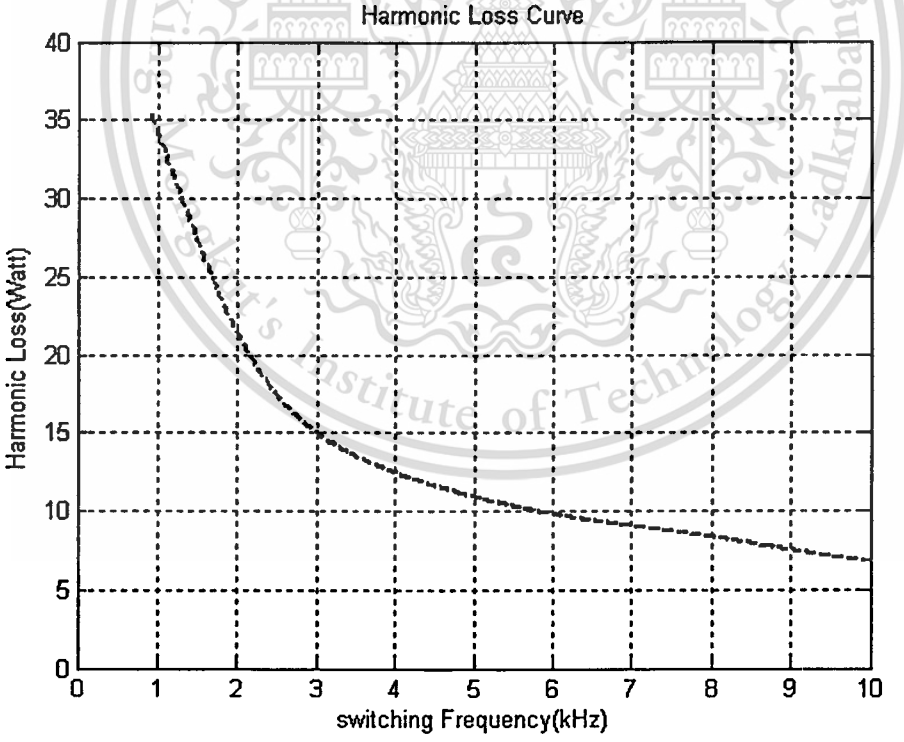


**Figure 4.34** Predicted results of total harmonic loss with 30Hz inverter frequency and 50% load torque

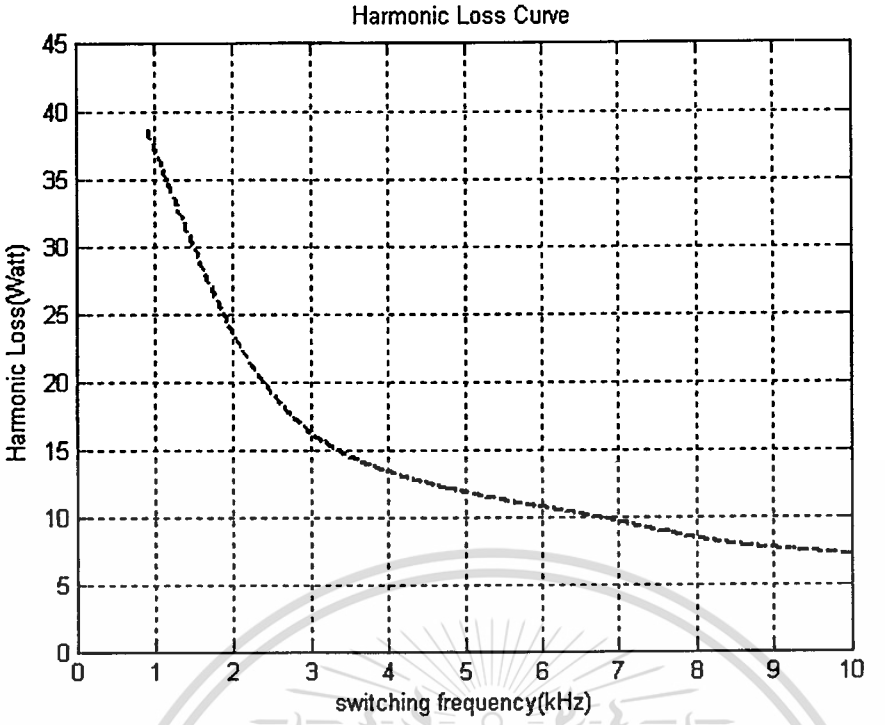


**Figure 4.35** Predicted results of total harmonic loss with 40Hz inverter frequency and 50% load torque

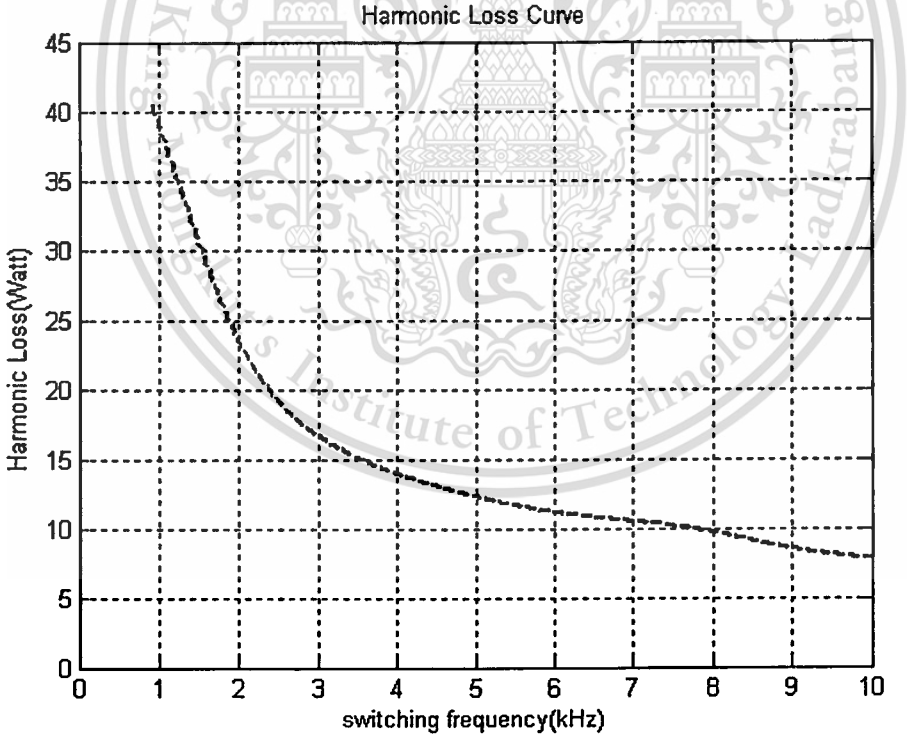


**Figure 4.36** Predicted results of total harmonic loss with 50Hz inverter frequency and 50% load torque

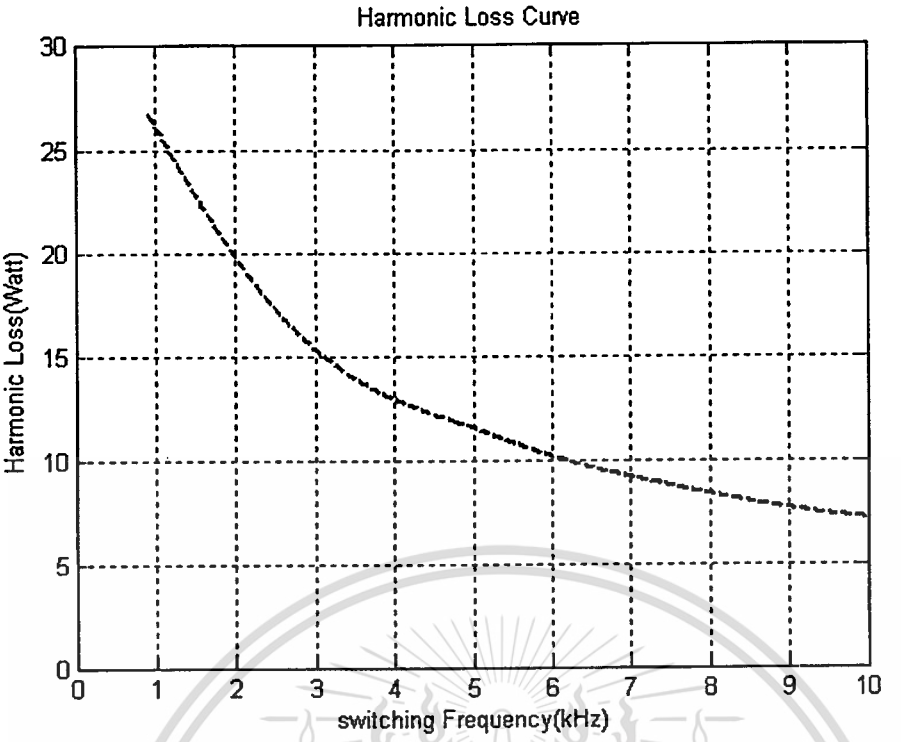


**Figure 4.37** Predicted results of total harmonic loss with 10Hz inverter frequency and 90% load torque

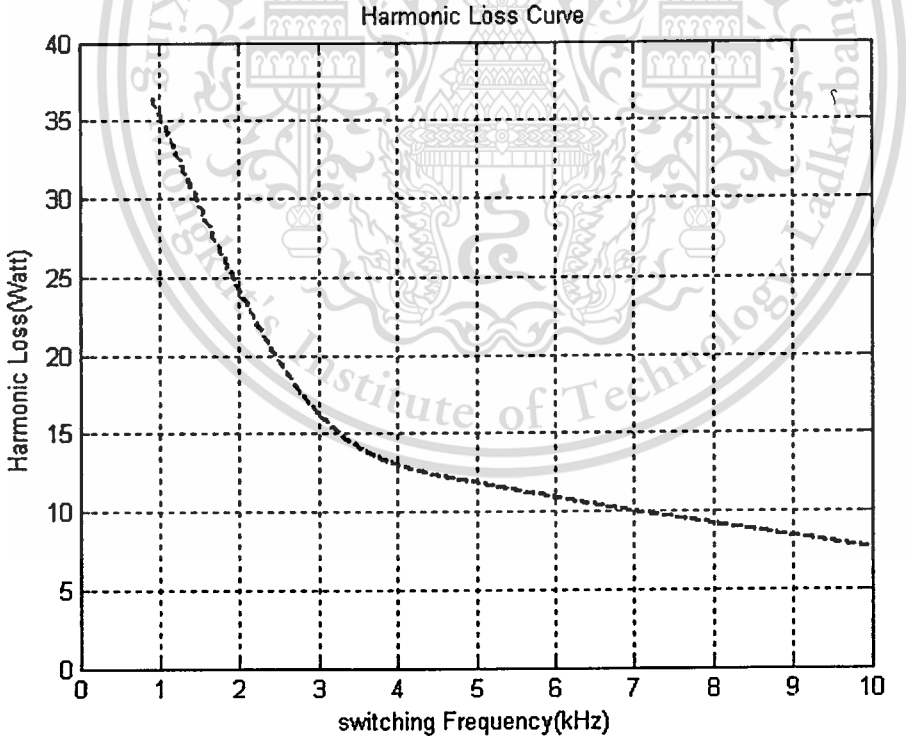


**Figure 4.38** Predicted results of total harmonic loss with 20Hz inverter frequency and 90% load torque

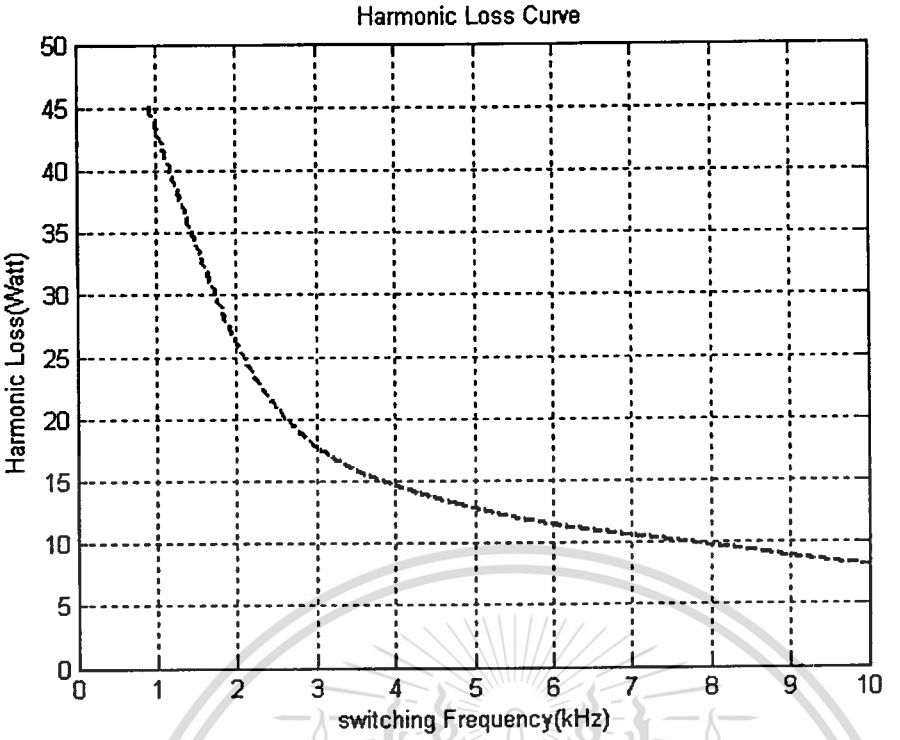


**Figure 4.39** Predicted results of total harmonic loss with 30Hz inverter frequency and 90% load torque

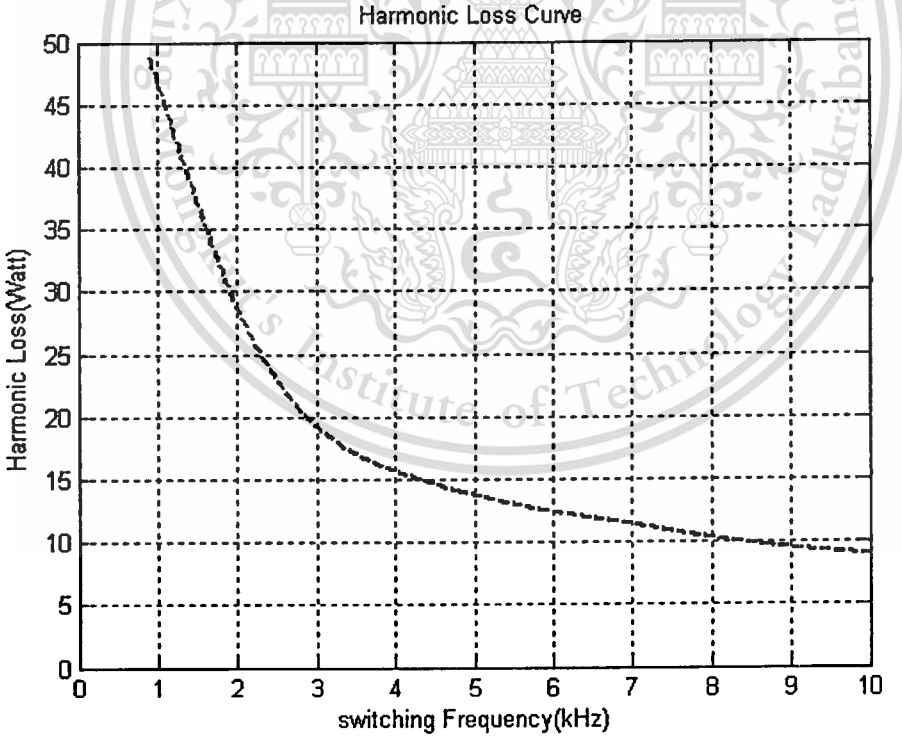


**Figure 4.40** Predicted results of total harmonic loss with 40Hz inverter frequency and 90% load torque

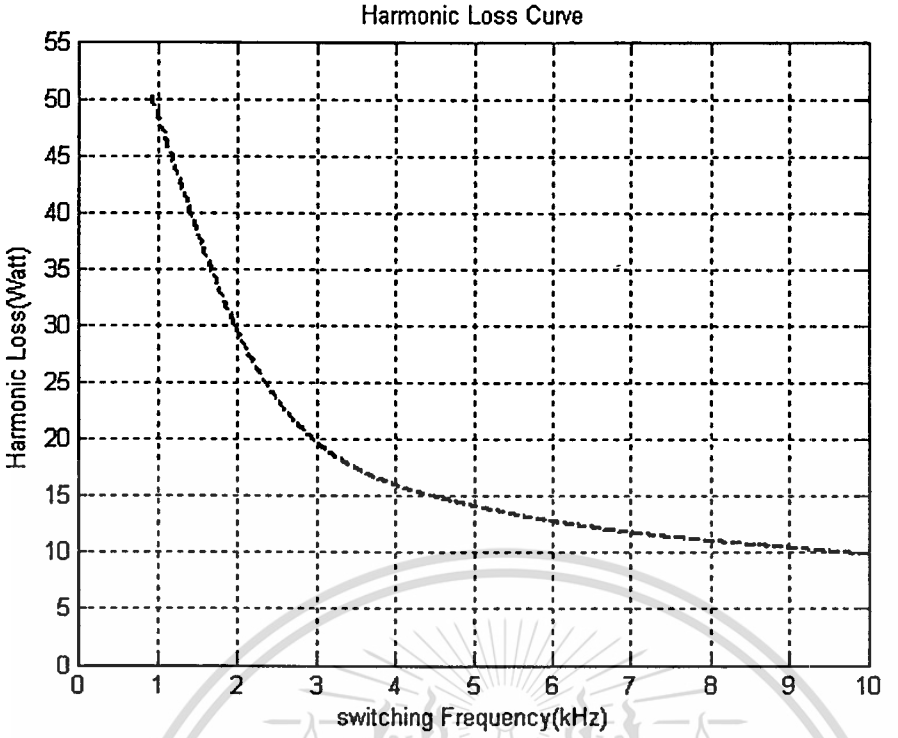


**Figure 4.41** Predicted results of total harmonic loss with 50Hz inverter frequency and 90% load torque

### 4.3.2 Prediction of Total Harmonic Loss under Variation of Load Torque and Various of Inverter Frequency and Switching Frequency

Figure 4.42 to 4.56 results the prediction of total harmonic losses under variation of load torque and several of inverter frequency and switching frequency. The results can be concluded, when increases load torque, harmonic loss increases and in contrary when increases switching frequency, then the harmonic loss decreases.

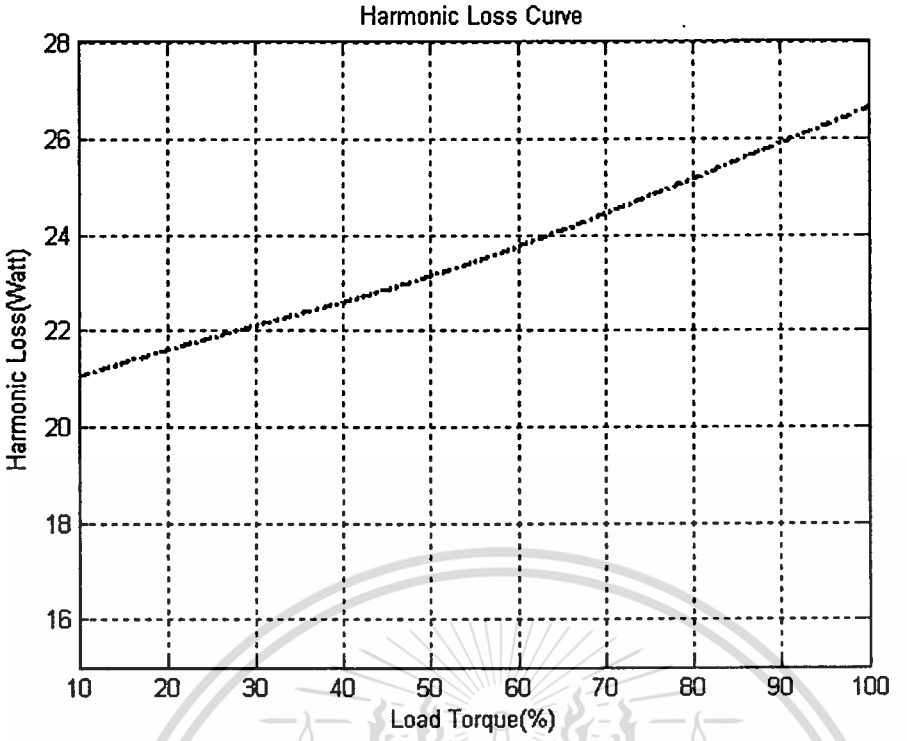


**Figure 4.42** Predicted results of total harmonic loss with 10 Hz inverter frequency and 1 kHz switching frequency

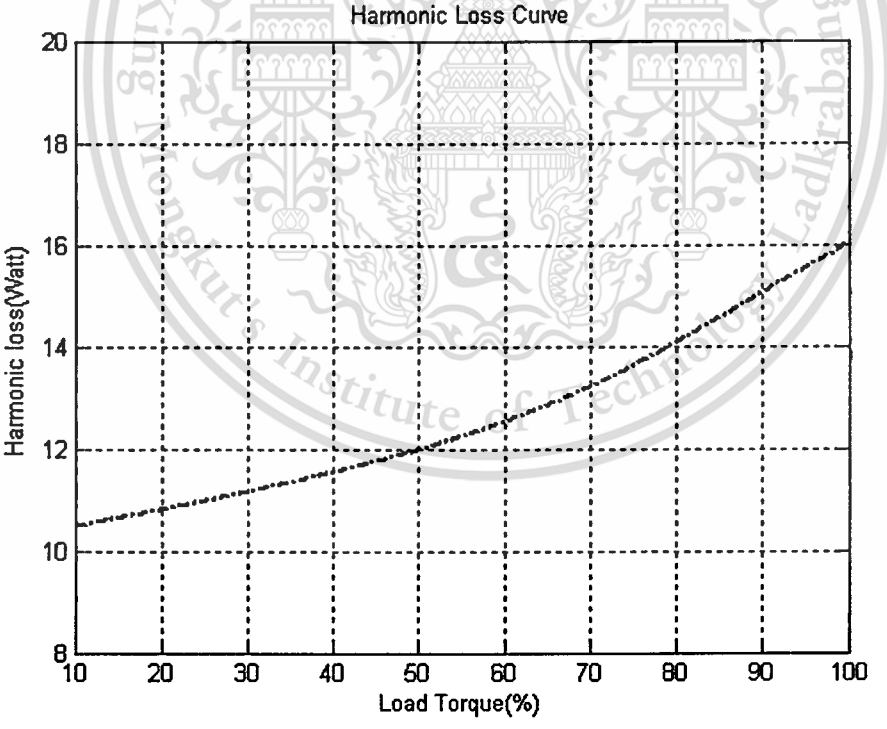


**Figure 4.43** Predicted results of total harmonic loss with10 Hz inverter frequency and 3 kHz switching frequency .

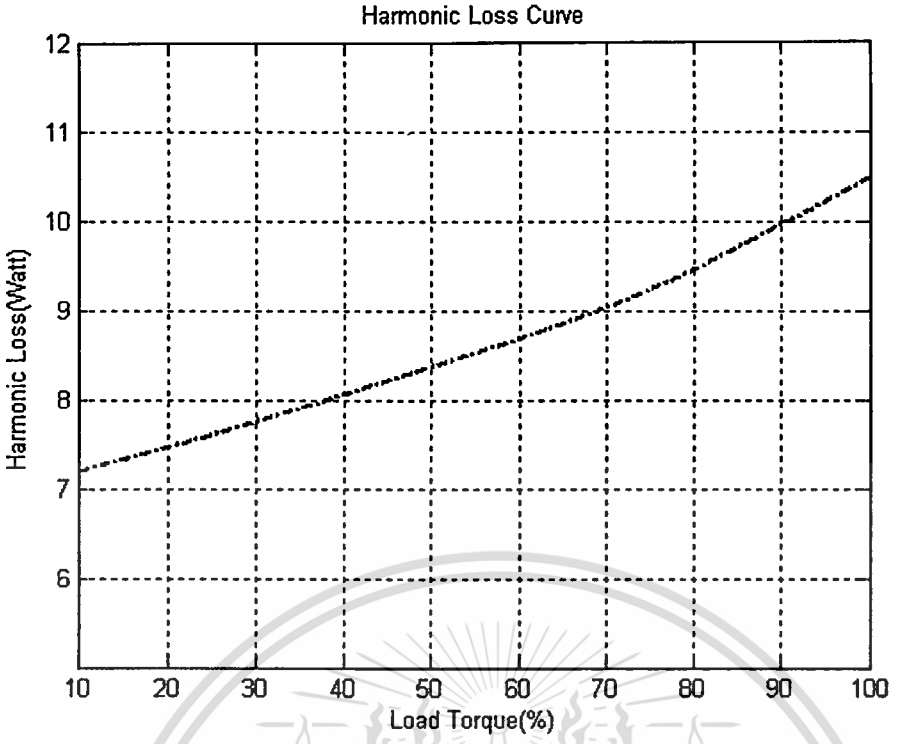


**Figure 4.44** Predicted results of total harmonic loss with 10 Hz inverter frequency and 6 kHz switching frequency.

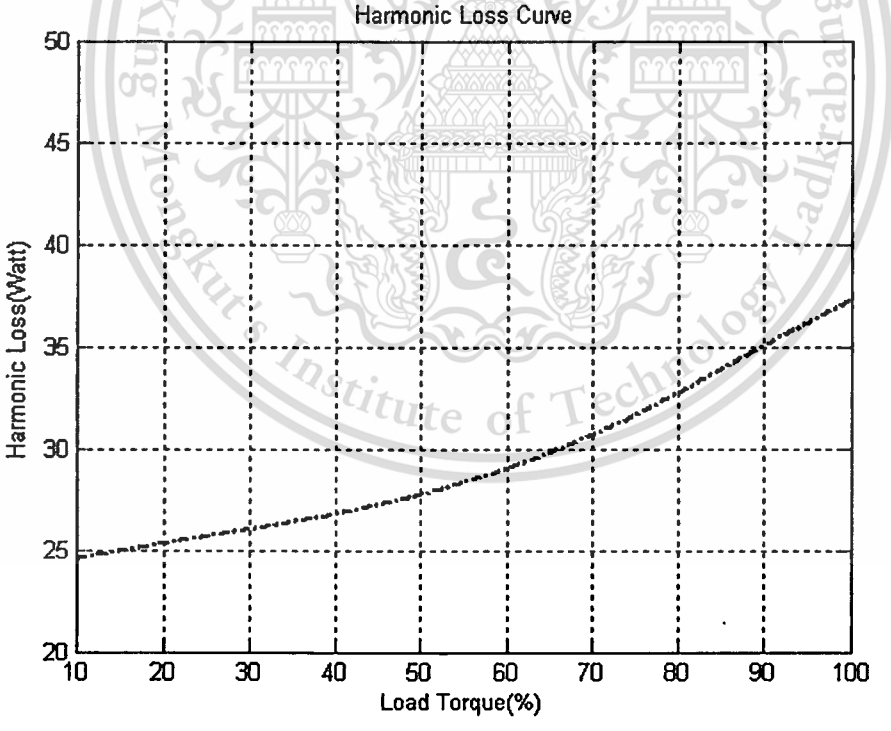


**Figure 4.45** Predicted results of total harmonic loss with 20 Hz inverter frequency and 1 kHz switching frequency.

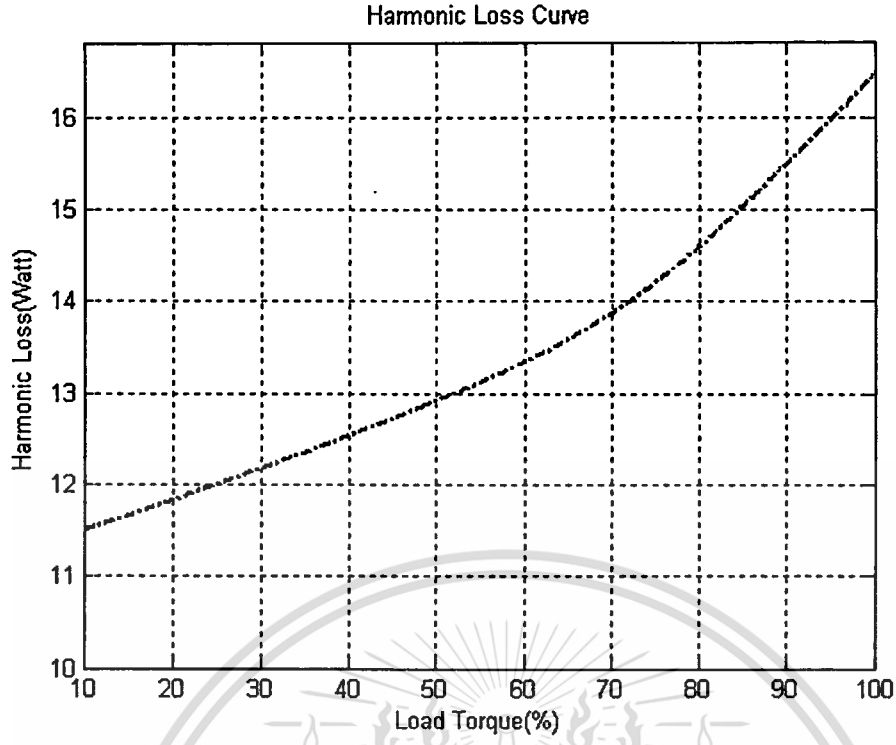


**Figure 4.46** Predicted results of total harmonic loss with 20 Hz inverter frequency and 3 kHz switching frequency.

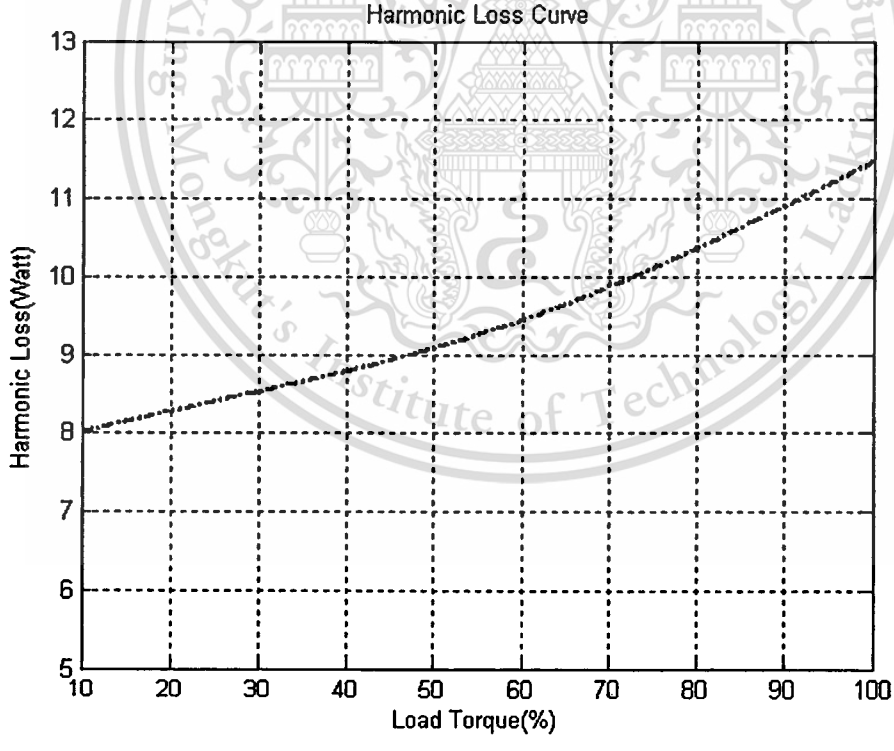


**Figure 4.47** Predicted results of total harmonic loss with 20 Hz inverter frequency and 6 kHz switching frequency

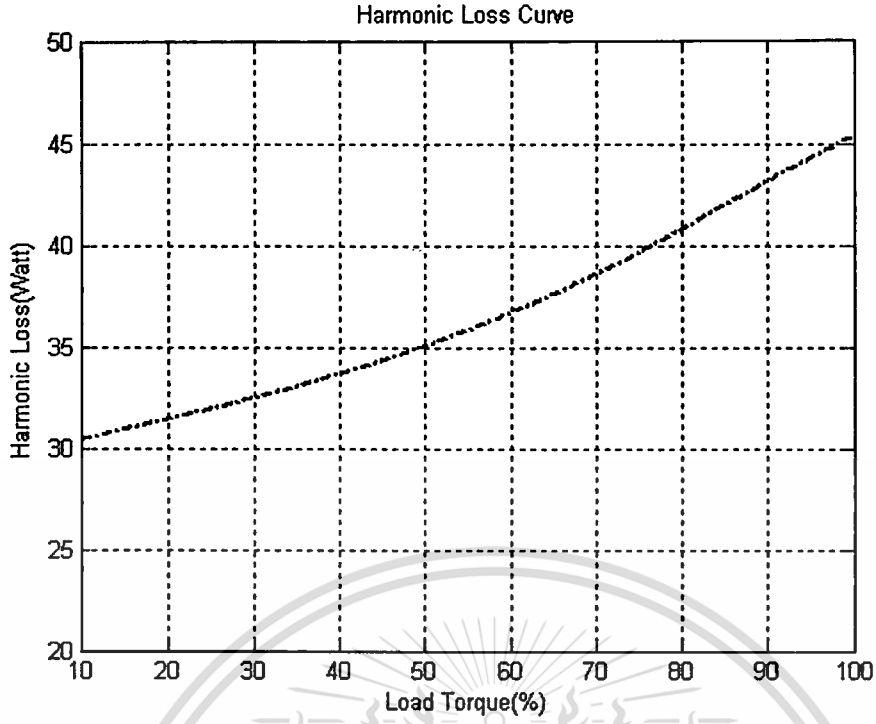


**Figure 4.48** Predicted results of total harmonic loss with 30 Hz inverter frequency and 1 kHz switching frequency

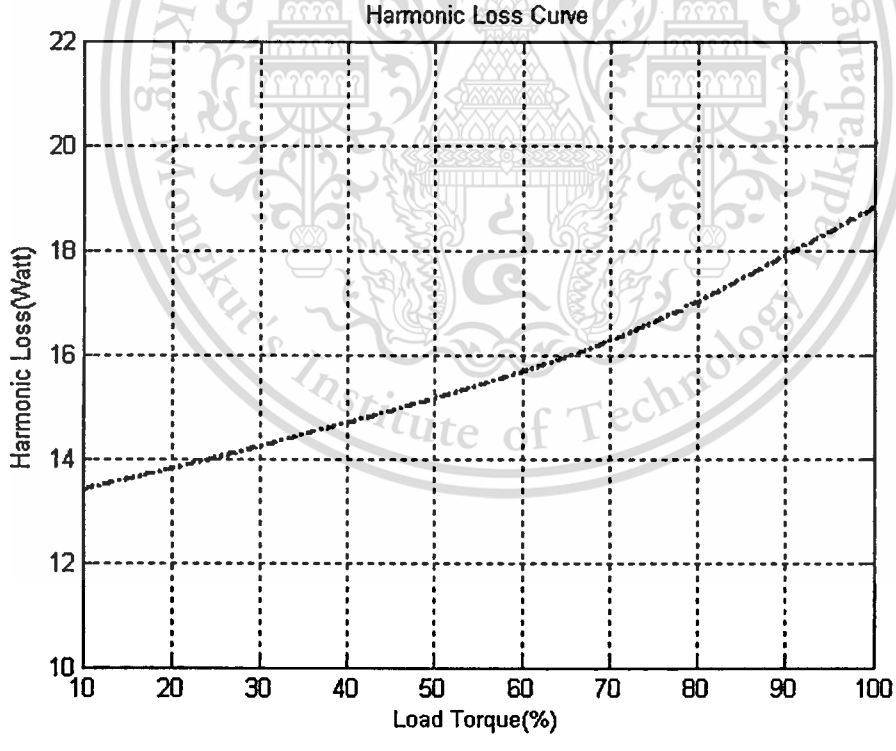


**Figure 4.49** Predicted results of total harmonic loss with 30 Hz inverter frequency and 3 kHz switching frequency

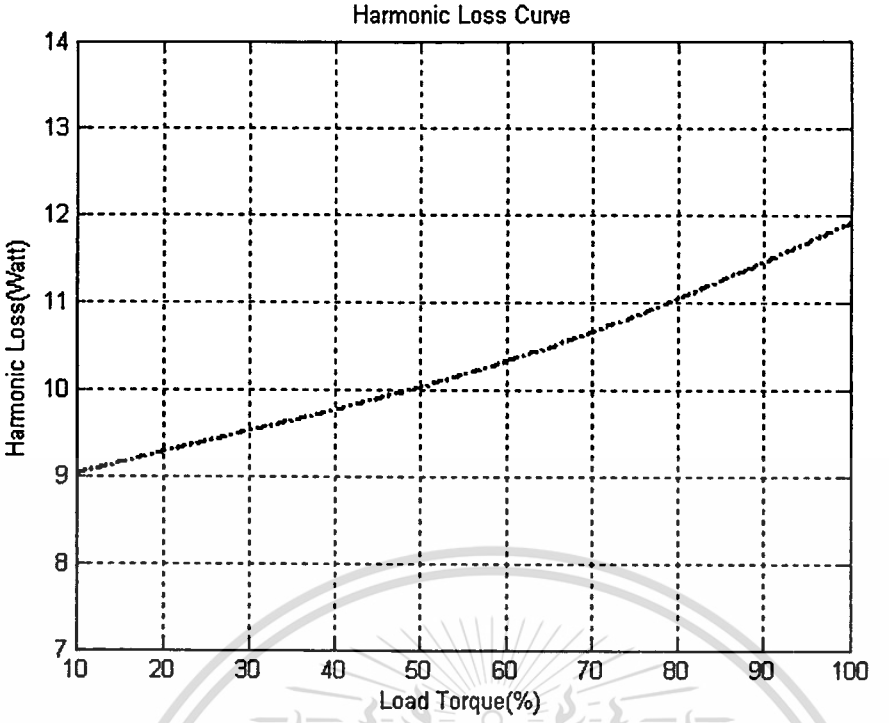


**Figure 4.50** Predicted results of total harmonic loss with 30 Hz inverter frequency and 6 kHz switching frequency

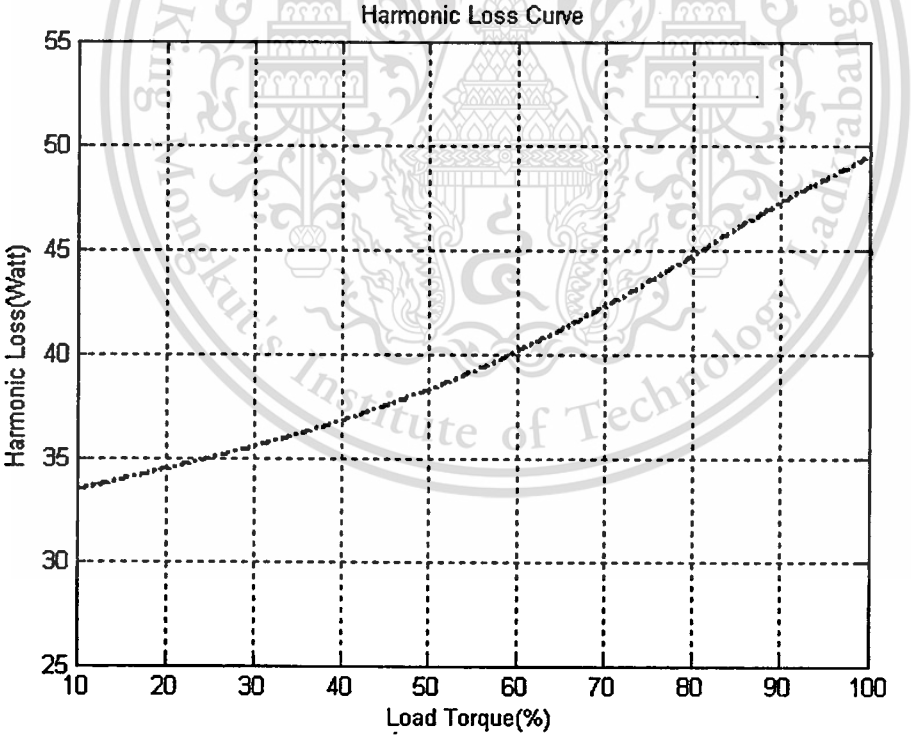


**Figure 4.51** Predicted results of total harmonic loss with 40 Hz inverter frequency and 1 kHz switching frequency

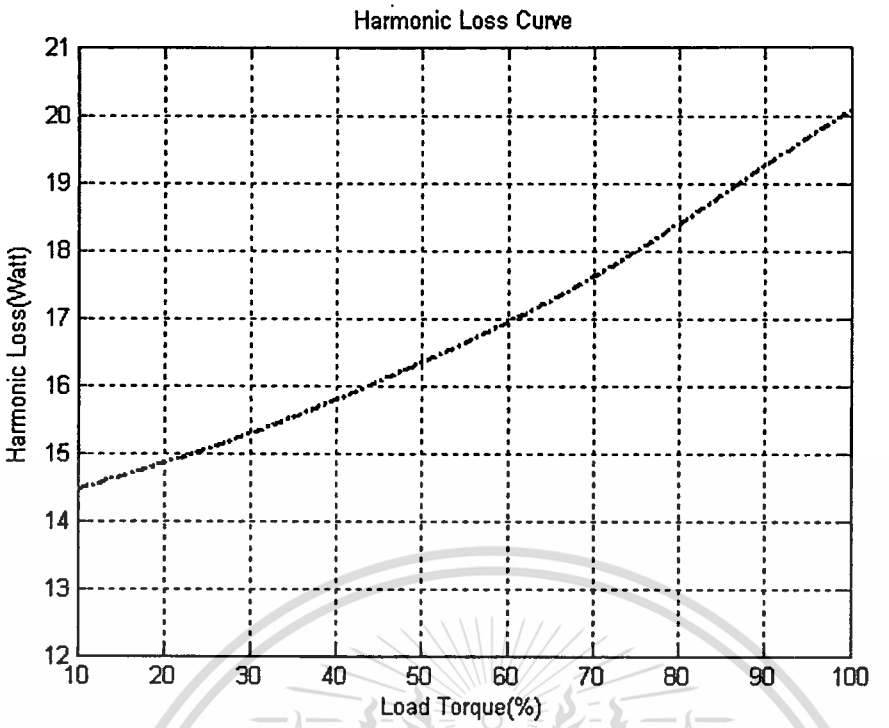


**Figure 4.52** Predicted results of total harmonic loss with 40 Hz inverter frequency and 3 kHz switching frequency

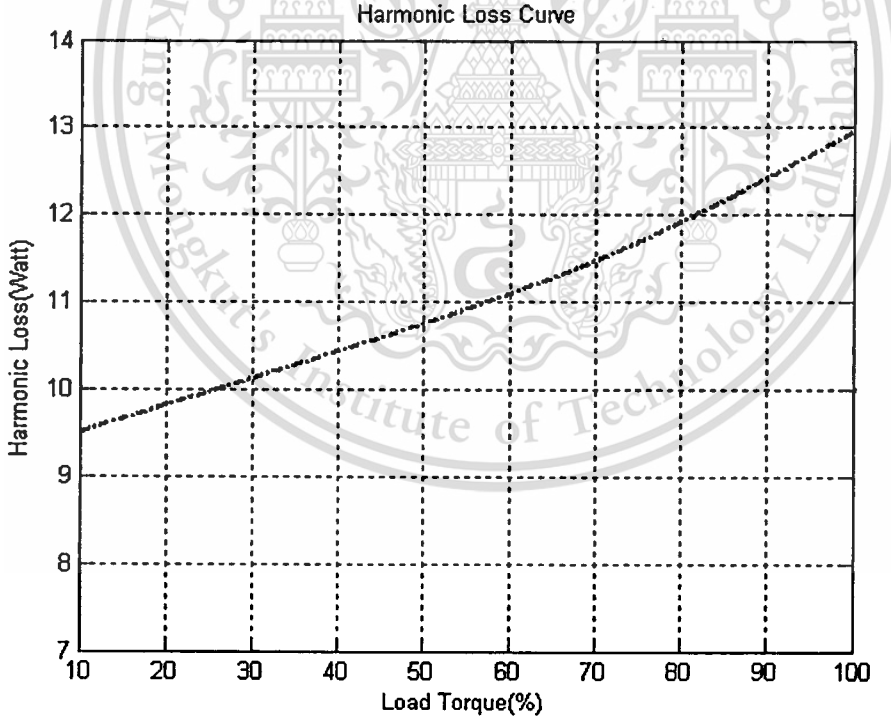


**Figure 4.53** Predicted results of total harmonic loss with 40 Hz inverter frequency and 6 kHz switching frequency

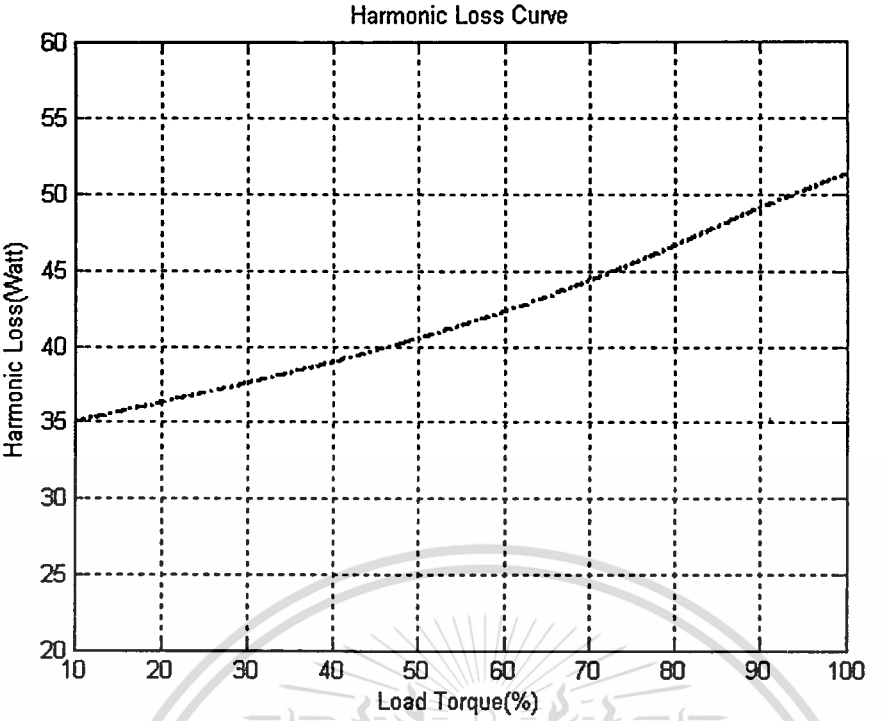


**Figure 4.54** Predicted results of total harmonic loss with 50 Hz inverter frequency and 1 kHz switching frequency

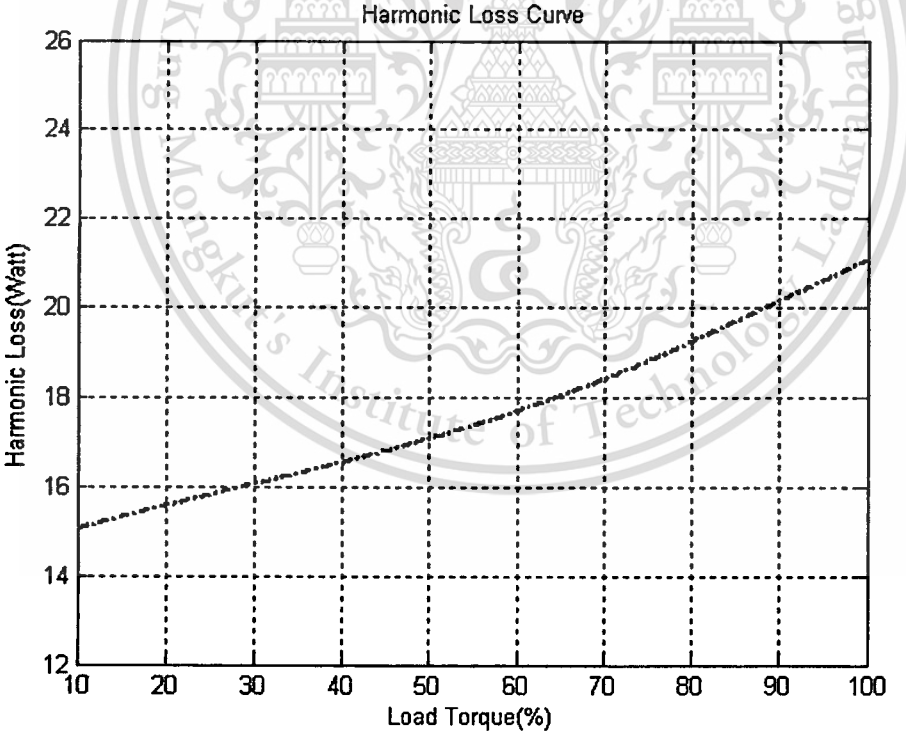


**Figure 4.55** Predicted results of total harmonic loss with 50 Hz inverter frequency and 3 kHz switching frequency

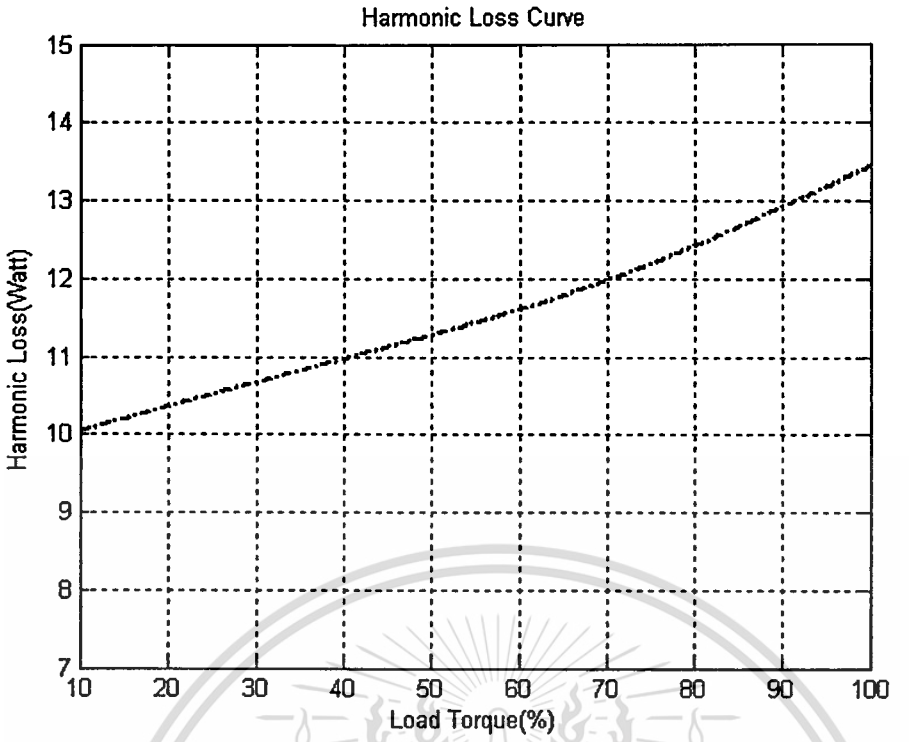


**Figure 4.56** Predicted results of total harmonic loss with 50 Hz inverter frequency and 6 kHz switching frequency

## 4.4 Conclusion

This chapter has simulated and predicted harmonic voltage spectra, harmonic loss spectra and total harmonic power losses based on the loss factor characteristic. The simulated and predicted results are used the parameters of standard equivalent circuit of induction motors. With the aid of the loss factor model it is possible to deduce how the conventional equivalent circuit model should be extended to give improved harmonic loss prediction. This results is concluded that the switching frequency is very important by induction motor operation .It is insight that when increases switching frequency the harmonic losses increases at shown in Figures 4.27 to 4.56.

# CHAPTER 5

# COMPARISON BETWEEN PREDICTED AND MEASURED HARMONIC LOSSES UNDER VARIOUS OPERATING CONDITIONS

## 5.1 Introduction

This chapter demonstrates the results of the loss prediction method compared to practical results for both individual and overall harmonic losses under various operating conditions.

## 5.2 Comparison Between Predicted and Measured Harmonic Losses under Various Load Conditions

Figure 5.1 to 5.9 show the comparison between predicted and measured harmonic losses with variation of inverter frequency and load conditions. For this results implemented with switching frequency 1 kHz, 3 kHz and 6 kHz and for a range of load conditions and inverter frequency. It is very clearly, that PWM switching frequency increases for both the total harmonic loss decreases.

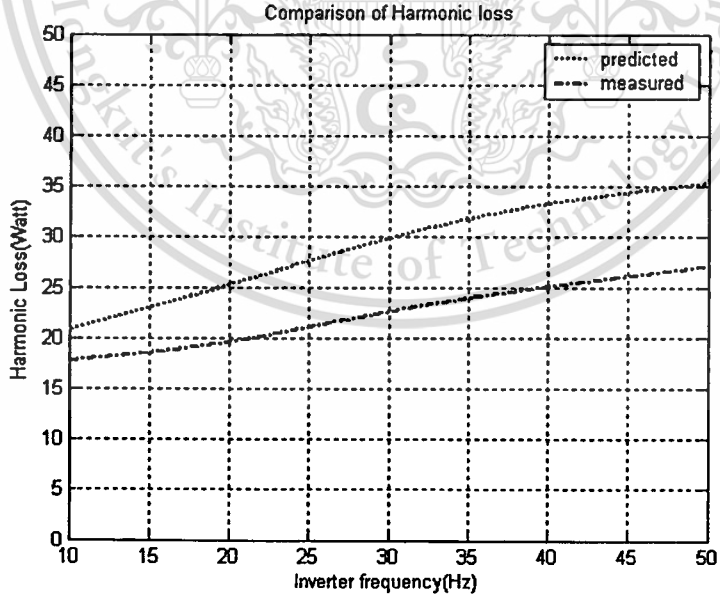


**Figure 5.1** Comparison between predicted and measured harmonic loss with variation of inverter frequency , 10% load torque and 1kHz switching frequency

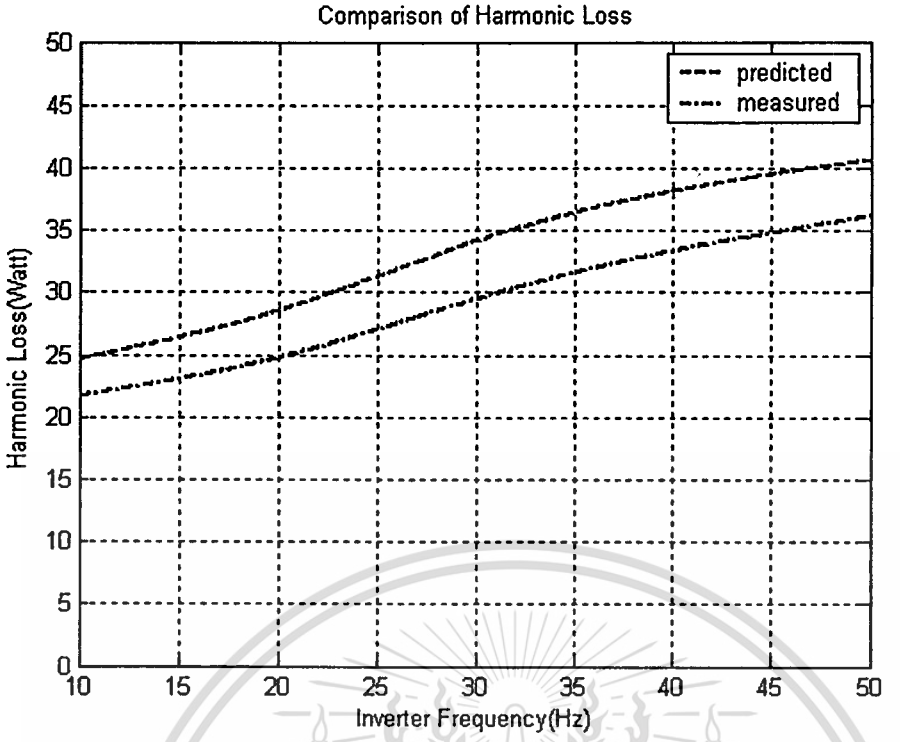


**Figure 5.2** Comparison between predicted and measured harmonic loss with variation of inverter frequency , 50% load torque and 1kHz switching frequency

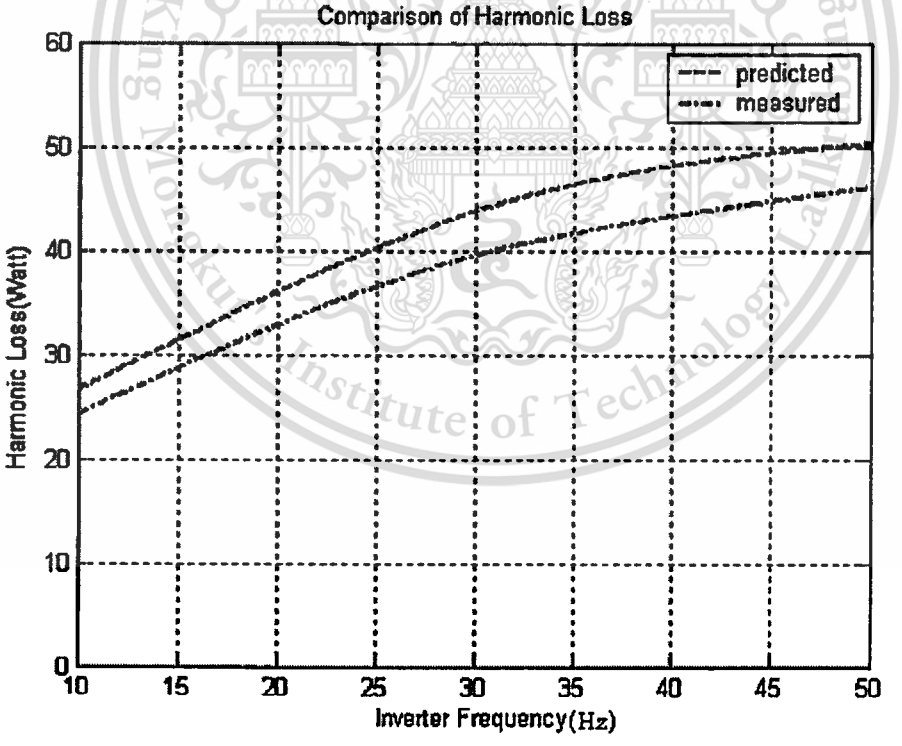


**Figure 5.3** Comparison between predicted and measured harmonic loss with variation of inverter frequency , 90% load torque and 1kHz switching frequency

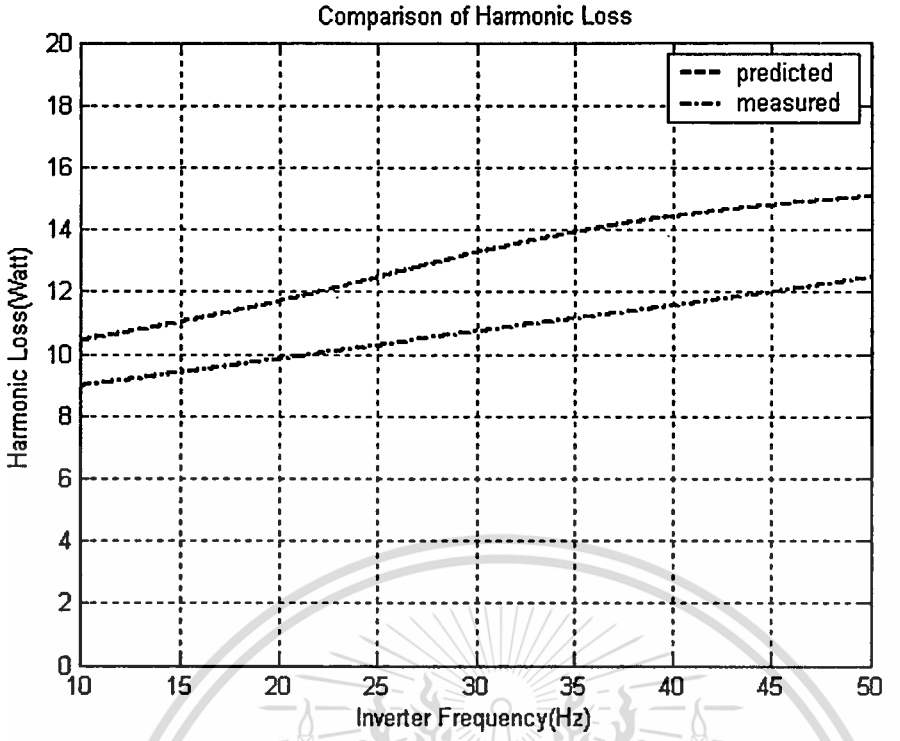


**Figure 5.4** Comparison between predicted and measured harmonic loss with variation of inverter frequency , 10% load torque and 3kHz switching frequency

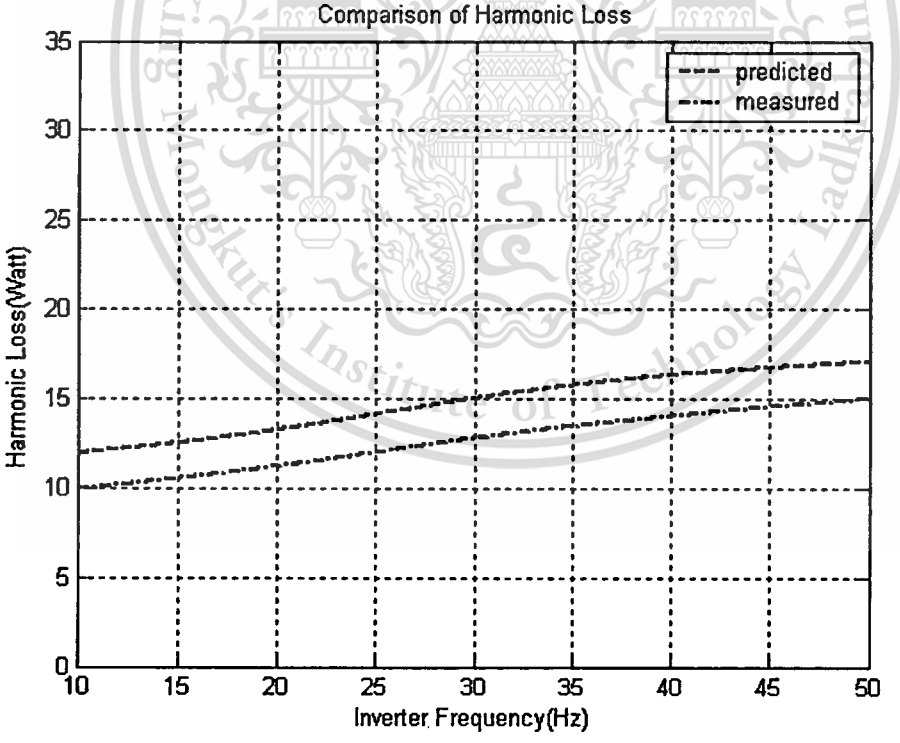


**Figure 5.5** Comparison between predicted and measured harmonic loss with variation of inverter frequency , 50% load torque and 3kHz switching frequency

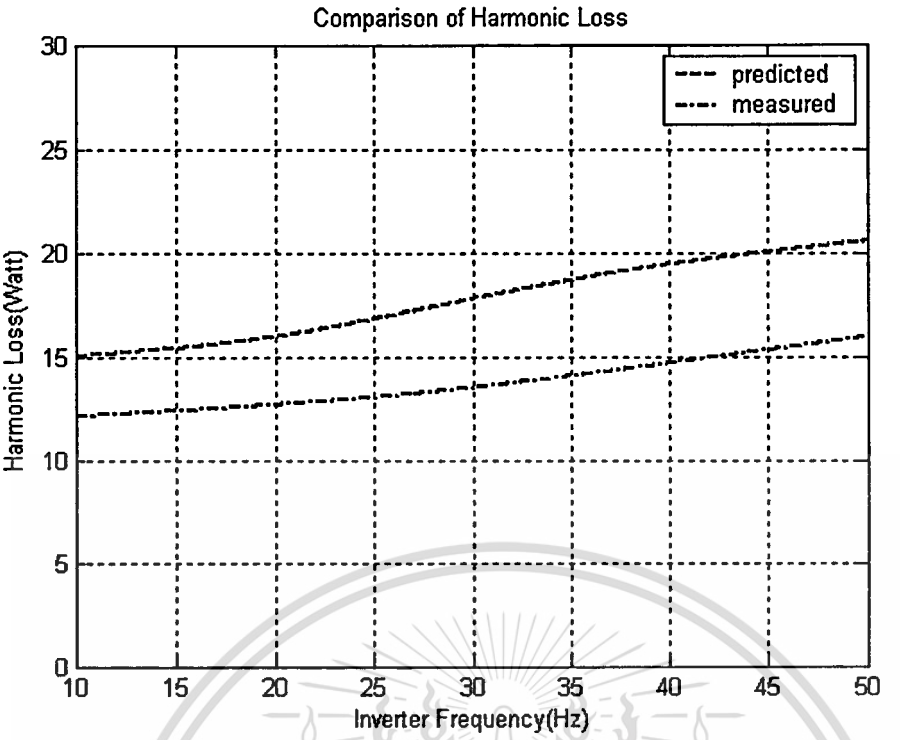


**Figure 5.6** Comparison between predicted and measured harmonic loss with variation of inverter frequency , 90% load torque and 3kHz switching frequency

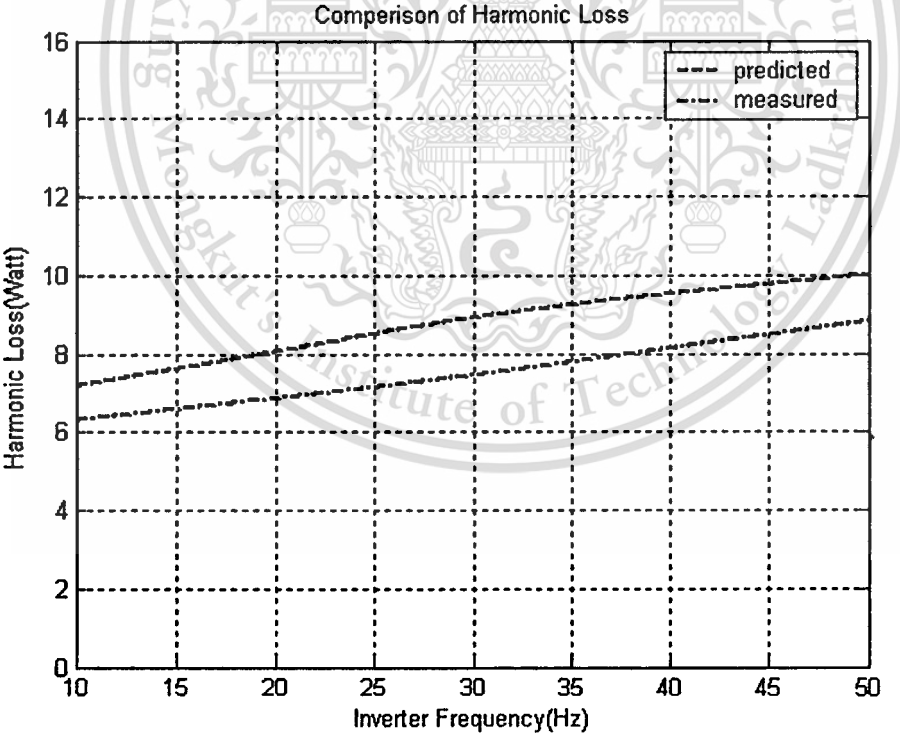


**Figure 5.7** Comparison between predicted and measured harmonic loss with variation of inverter frequency , 10% load torque and 6kHz switching frequency

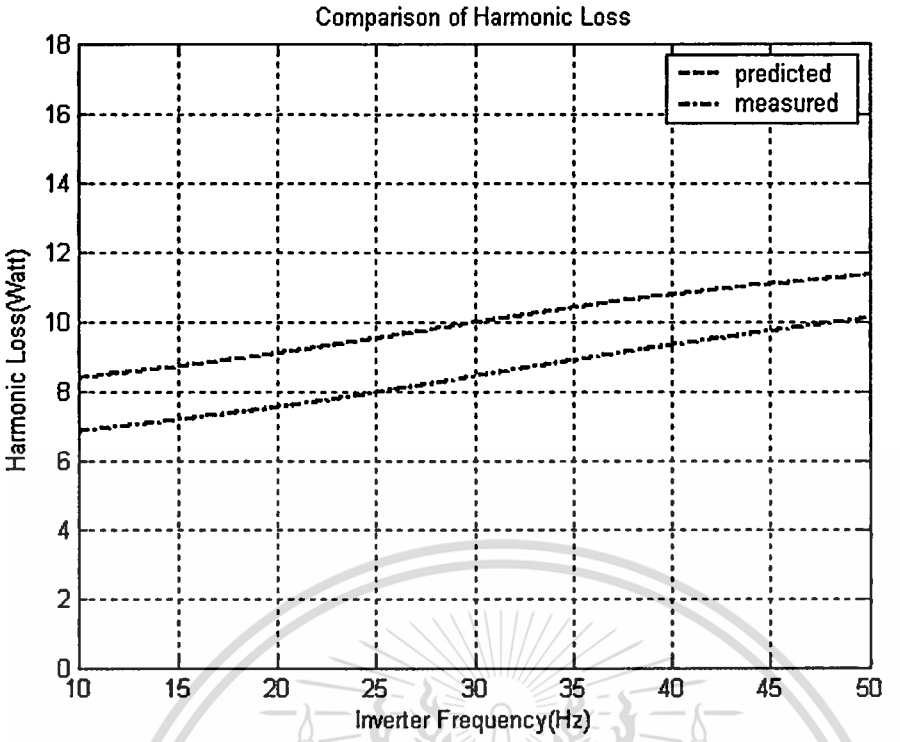


**Figure 5.8** Comparison between predicted and measured harmonic loss with variation of inverter frequency , 50% load torque and 6kHz switching frequency

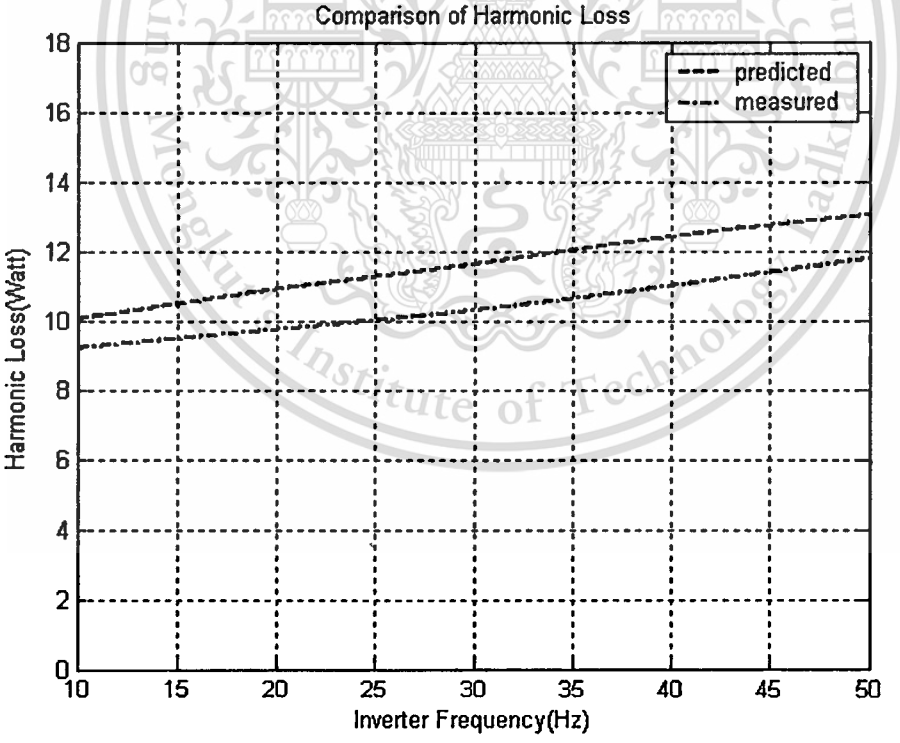


**Figure 5.9** Comparison between predicted and measured harmonic loss with variation of inverter frequency, 90% load torque and 6kHz switching frequency

Figure 5.1 to 5.9 show the comparison between of predicted and measured harmonic losses with variation of inverter frequency and load conditions. For this results implemented with switching frequency 1 kHz, 3 kHz and 6 kHz and for a range of load conditions. It is very clearly, that PWM switching frequency increases for both the total harmonic loss decreases.

## 5.3 Comparison of predicted and measured fundamental Voltage under variation of modulation index(ma)

Figure 5.10 show the comparison of fundamental voltage between predicted and measured results under variation of modulation index. It is very clear, when modulation index increases, the fundamental voltage increases too (V/f is constant) and usually the fundamental voltage of induction motor should be 220 Volt by measurement, but the result is less then 220 Volt. This error is depended by data reading or error of Power Analyzer (PZ 4000).

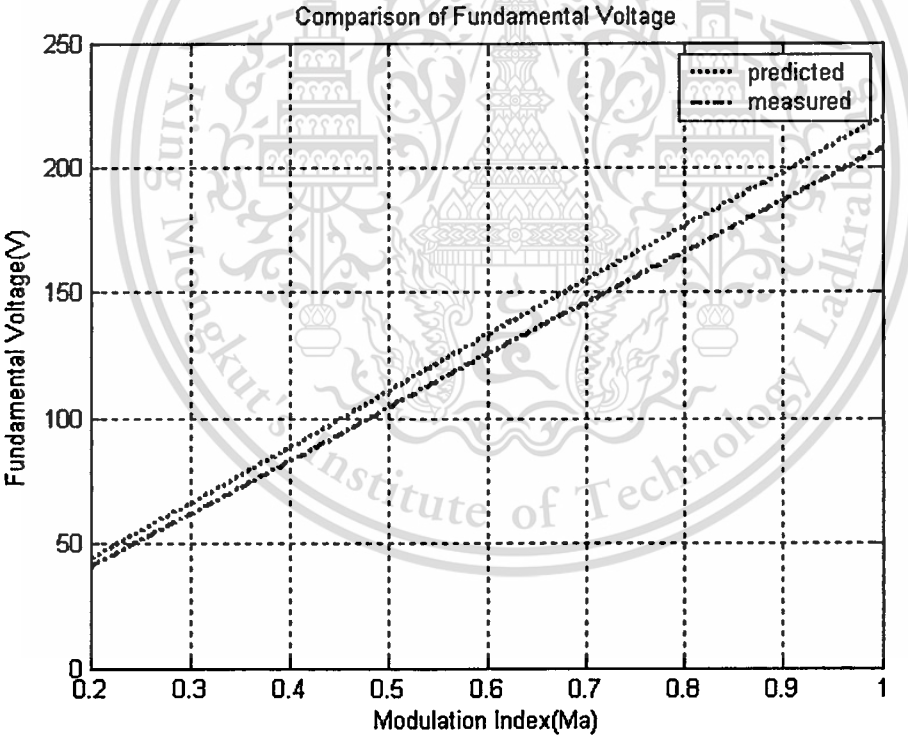


**Figure 5.10** Comparison between predicted and measured fundamental voltage with variation of modulation Index (ma).

## 5.4 Efficiency ($\eta$) of Induction Motor

The efficiency ($\eta$) of induction motor can be computed by:

$$\eta = \frac{P_{out}}{P_{in}} \leq 1 \qquad or \quad \eta_{(\%)} = \frac{P_{out}}{P_{in}} \times 100 \leq 100\% \tag{5.1}$$

with

$$P_{out} = \omega T = \frac{2\pi n}{60} T \tag{5.2}$$

and

- Input power derived from experiment.

where

$P_{in}$ is input power

$P_{out}$ is output power

T is torque

n is speed

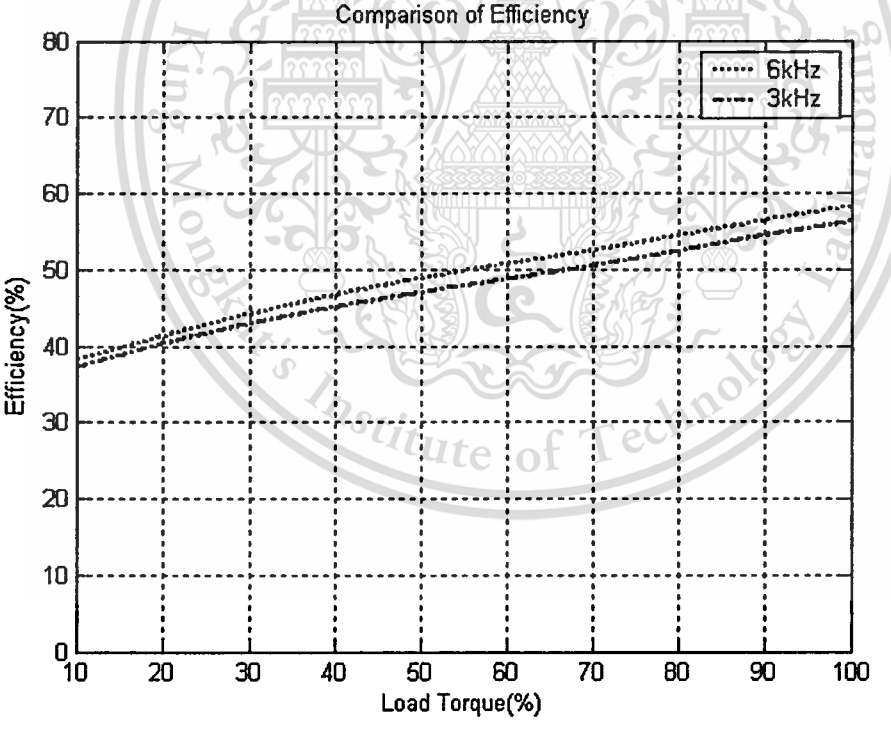


**Figure 5.11** Comparison of efficiency between switching frequency of 3 kHz and 6 kHz by 10Hz inverter frequency

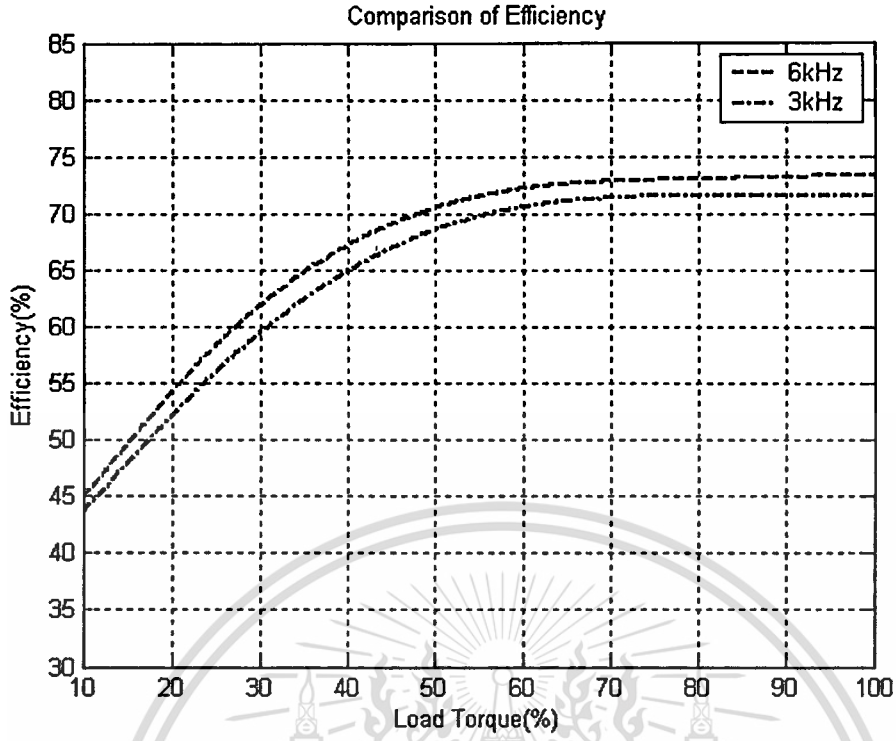


**Figure 5.12** Comparison of efficiency between switching frequency of 3kHzand 6 kHz by 20Hz inverter frequency

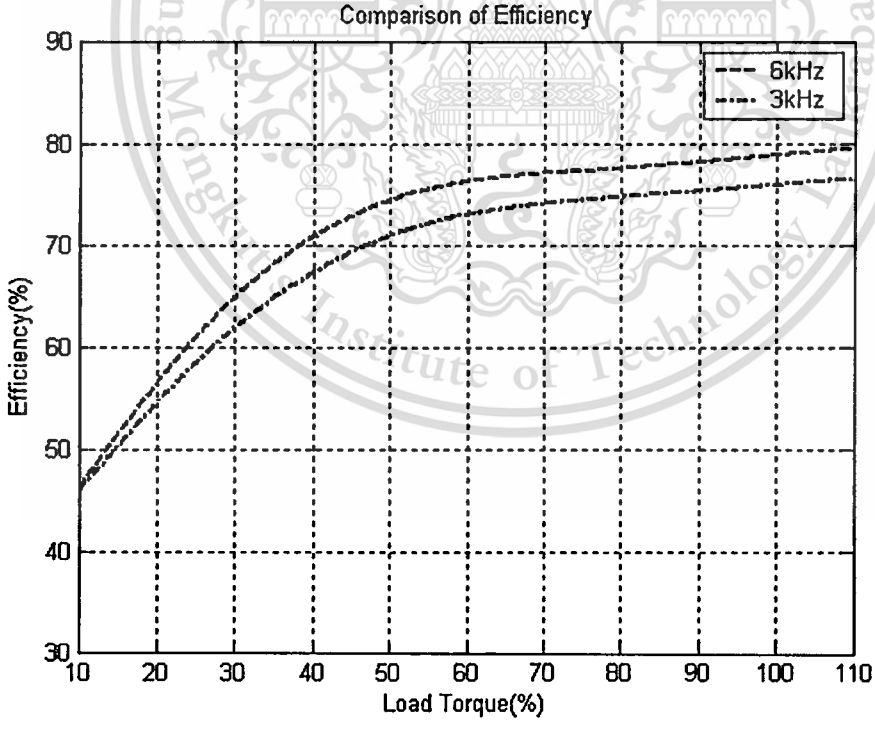


**Figure 5.13** Comparison of efficiency between switching frequency of 3 kHz and 6 kHz by 30Hz

inverter frequency

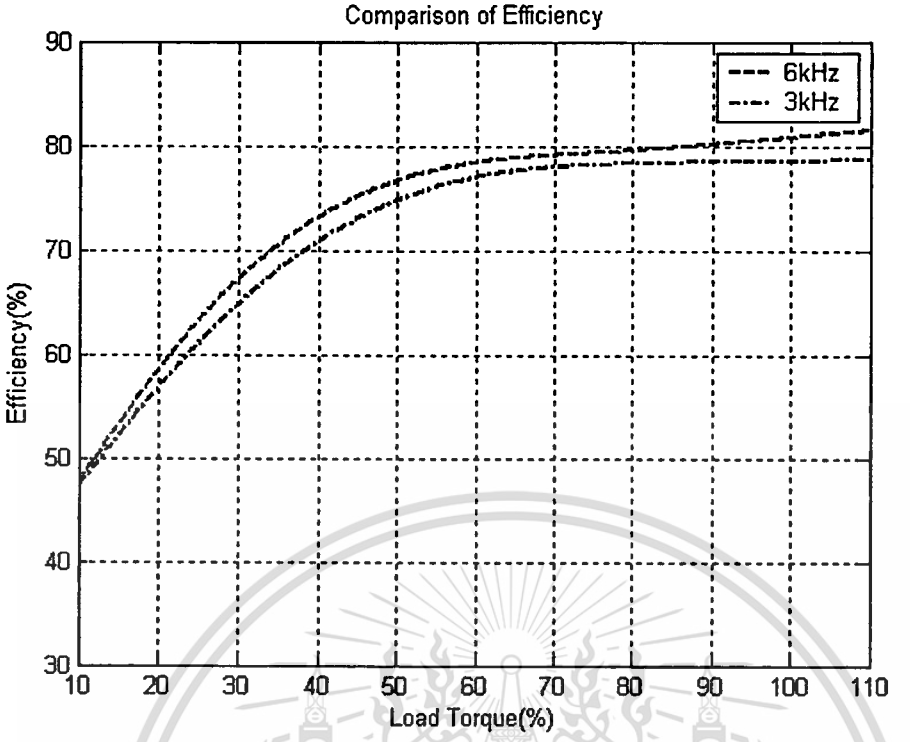


**Figure 5.14** Comparison of efficiency between switching frequency of 3 kHz and 6 kHz by 40Hz inverter frequency

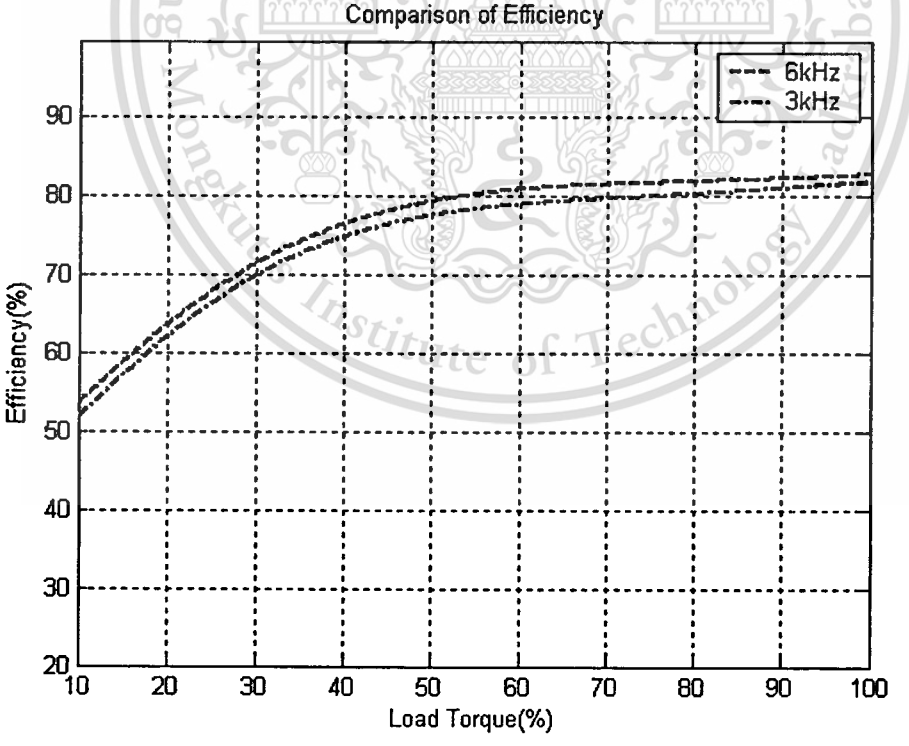


**Figure 5.15** Comparison of efficiency between switching frequency of 3 kHz and 6 kHz by 50Hz

inverter frequency

Figure 5.11 to 5.15 show the comparison of efficiency of induction motor. It is clear, that higher switching frequency the efficiency is higher than lower frequency and by full load and higher inverter frequency ,it means inverter frequency is maximum 50Hz ,then the efficiency became maximum (see Figure 5.15).

## 5.5 Conclusion

Predictions and Tests have been limited to 6 kHz by the hardware and software used. This frequency needs to be extended to accurately determine the shape at higher frequencies. However, extrapolating the derived curve to 6 kHz gives good predictions for total harmonic losses for switching frequencies up to 1 kHz since the bulk of the loss occurs in or near the frequency range of the measurements. It has been suggested in some publications that at very high frequencies the loss factor might increase although as yet there are no experimental results to support this.

The prediction of total harmonic losses using the predicted loss factor model is in good agreement with loss measurements. The proposed model allows a clear visualisation of individual harmonic losses and accurate loss prediction with SVPWM supply with known harmonic voltages.

With the aid of the loss factor model it is possible to deduce how the conventional equivalent circuit model should be extended to give improved harmonic loss prediction.. This gives better insight into the distribution of losses and shows that the harmonic stray load loss associated with the high frequency effects of the leakage flux is extremely important. This result is in good agreement with the proposed model. The efficiency of both methods is almost the same results. Figure 5.11 to 5.15 show the comparison of efficiency between predicted results and measured results. The output power derived from the prediction in Equation (5.2). In fact the efficiency of induction motor is around 85%, but for these results is maximum 83% less than origin 2%. This error is from the test implementation and the different of capacities of induction motor under test and DC motor as a load.

# CHAPTER 6

# CONCLUSION AND FUTURE WORK

## 6.1 Conclusion

The thesis has predicted total harmonic loss of induction motor using loss factor characteristics and has examined harmonic loss through the comparison of predicted results using loss factor curve and measured results using measurement system test rig. The prediction of harmonic losses were made using loss factor curve and variation of PWM parameters such as modulation index, inverter frequency and switching frequency. This loss factor curve is derived from a standard equivalent circuit of induction motors for a given different load at each frequency normalized to the square of the harmonic voltage amplitude. The predicted harmonic loss factor curve enables harmonic loss calculation on PWM supply with known the spectral characteristics to be predicted directly and also provides a good way of assessing the accuracy and shortcomings of loss model. A comprehensive predicted investigation into harmonic loss mechanisms and the influence of the effects such as motor load torque, inverter frequency and switching frequency. The measurement of harmonic loss were set up the measurement system test rig. This detail can be found in APPENDIX A.

The main findings of this work are as follows:

- The total harmonic loss variation with frequency due to the inherent harmonic copper, core and stray loss component has been predicted and measured.
- At low harmonic frequency, the predominant harmonic copper loss decreases rapidly as harmonic frequency increases, while at high harmonic frequency, the predominant harmonic core loss decreases gradually for more detail can be found with A. Boglietti's work [16].
- The change of modulation depth on core loss is in significant. It is higher modulation depth should be made for drive control.
- Higher PWM switching frequency results in a slow decrease in core losses. Consequence, the effect of PWM scheme is significant on core losses. Note that higher switching frequency insignificant reduces core loss compared to lower switching frequency. However, higher switching frequency results increases inverter losses.

- The predicted results have confirmed that the modulation depth plays an important role on core losses in the magnetic drives fed by PWM inverter[1]
- The prediction of total harmonic losses using the loss factor curve is good agreement with measured losses.
- Finally, these predicted results can be guidelines for selection of PWM parameters suitable for drive applications such as switching frequency and can suggest useful advices to the motor designers and users, when induction motors fed by PWM inverters have to be designed or utilized.

## 6.2 Future Work

- In order to develop more accurate loss models and to improve understanding of loss mechanisms higher frequency measurements are required. The technique developed in this work should be extended to higher frequencies through the use of an improved hardware/software implementation.
- The technique developed in this work should be extended to higher frequency through the use of an improved hardware and software implementation.

Further experimental work on machines with various rotor slot shapes would be beneficial to confirm the influence of rotor leakage inductance and to determine more efficient designs.

- Further predicted and experimental work on machines should have various motor rating configurations.

# LITERATURE CITED

[1] T.M. Underland & N. Mohan, "Over modulation and Loss Considerations in High-Frequency Modulated Transistorized Induction Motor Drives", in Conf. Rec. 1988 IEEE Transaction on Power Electronics, vol. 3. No.4, October 1988

[2] Aldo Boglietti,Poalo Ferraris, Mario Lazzari, and Michele Pastorelli " Influence of the Inverter Characteristics on the Iron Losses in PWM Inverter-Fed Induction Motors" , IEEE, Trans. On Ind,Applications, vol. 32, No 5 , September/October 1996, pp. 1190-1194.

[3] S.Khomfoi, V.Kinnares and P. Viriya. " Investigation in to Core Losses due to Harmonic Voltages in PWM fed Induction Motors", in Conf. Rec.July 1999 PEDS'99 IEEE, pp.104-109.

[4] S.Khomfoi, V.Kinnares and P.Viriya. "Influence of PWM Characteristics on the core losses due to Harmonic Voltages in PWM Fed Induction Motors", in Conf. Rec.Jan. 2000, pp. 365-369.

[5] V.Kinnares "Measurement, Analysis and prediction of Harmonic Power losses in PWM fed Induction Motors", Ph.D.Thesis, The University of Nottingham, UK,October 1997.pp.168, 169,170 and181

[6] D.W.Novotny et ai.,"Frequency dependence of time harmonic losses in induction machines", in Int. Conf. on Electric Machines, Cambridge, MA, August 1990, pp.233-238.

[7] K.Atallah, Z.Q.Zhu and D.Howe, "An Improved Method for Predicting Iron Losses In Brushless Permanent Magnet DC Drives", IEEE Trans. On Magnetics, Vol. 28, No.5, September 1992, pp. 2997 -2999.

[8] B.Bahola,"Accurate measurement and prediction of iron losses in three-phase cage induction motors" Ph.D. Thesis, 1997, University of Shelffield, England.

[9] R.Kaczmarek, M.Amar and F. Protat, "Iron loss Under PWM Voltage Supply on Epstein Frame and Induction Motor Core", IEEE Trans. On Magnetics, Vol.32, No.1, January 1996, pp.189-194.

[10] M.Amar and R.Kaczmarek, "A General Formular for prediction of Iron Losses Under Non-Sinusoidal Voltage Waveform", IEEE Trans. On Magnetics, Vol.31, No.5, September 1995, pp. 2504-2509.

[11] P.K.Budig and S.Bauer, "Iron loss in thin laminations of rotating electrical machines", Int Conf. on Electr. Mach.(ICEM), Pisa/Italy 1988, Proc. pp. 39-44.

[12] H.M.Metwally et al., "Core loss in switched Reluctance Motor Structure; Experimental Results" , Int. Conf. on Electri. Mach. (ICEM), Pisa/Italy, 1988, pp.31-34.

[13] K.Venkatesan and J.F.Lindsay." Comparative Study of the losses in Voltage and Current Source Inverter Fed Induction Motors",IEEE Trans. Ind.Appl., Vol. IA-18,No. 3, pp.241-245, May/June 1982.

[14] W.Prescott et al., "Computational Methods for the Steady-State performance prediction of cage induction machines fed non-sinusoidal supplies" Conf.Rec.IEE/EMAD, Sept. 1989, pp.271-274

[15] Van Der Brock et al., "Analysis and realization of pulsewidth based on voltage space vectors" IEEE Trans. On Industry Applications, Vol.24, No.1, Jan/Feb 1988 pp. 293-305.

[16] A Boglietti. "PWM Inverter fed Induction Motors losses Evaluation", Electric Machines and Power Systems, 22:439-449, 1994 Taylor &Francis.

[17] V.B.Honsinger, "Induction Motors Operating from Inverters", in conf.Rec 1980 Annu. Meeting IEEE Ind.Appl..Soc.,pp. 1276-1285.

[18] V.Kinnares, P.Jaruwanchai, D.Suksawat and S.Pothivejkul "Effect of Motor Parameter Changes on Harmonics Power Loss In PWM Fed Induction Machines"in Con.PEDS'99 July 1999, pp.1061-1066.

# APPENDICES

## Appendix A

### The Publication

P.Indarack , S. Douangsyla, C.Joochim , A.Kunakorn, M.Kando and V. kinnares
" A Harmonic Loss Calculation of PWM -Fed Induction Motors Using Loss Factor Characteristics," IEEE 2004 International Conference on Analog and Digital Techniques in Electrical Engineering, TENCON 2004, 21-24 November 2004, Chiang Mai, Thailand, pp 236-239.

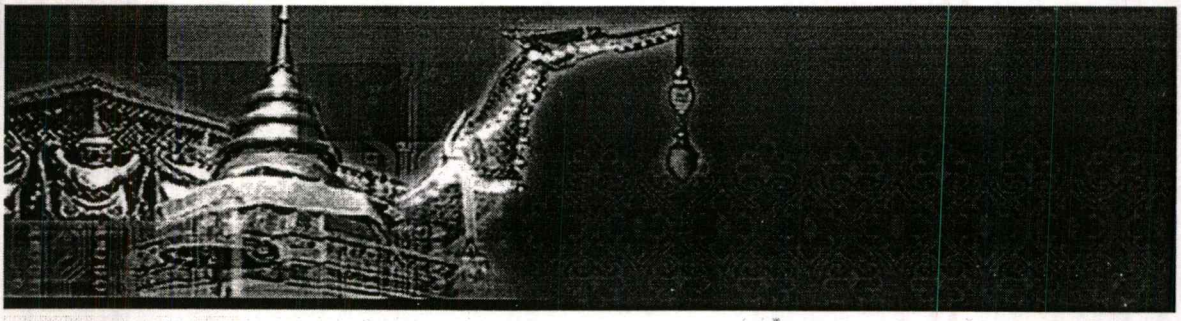

# TENCON 2004

## Conference Proceedings

*Analog and Digital Techniques in Electrical Engineering*

**21 – 24 November 2004, Chiang Mai, THAILAND**

**Organizer: IEEE Thailand Section**

***Sponsored by: IEEE Region 10***

**Venue: Lotus Hotel Pang Suan Kaew**

IEEE Catalog Number: 04CH37582C

ISBN: 0-7803-8561-6

# A Harmonic Loss Calculation of PWM-Fed Induction Motors Using Loss Factor Characteristics

*P.Indarack*, S. Douangsyla*, C.Joochim**, A..Kunakorn*, M.Kando***and V. kinnares**

*Dept. of Electrical Engineering, Faculty of Engineering, King Mongkut's Institute of Technology Ladkrabang, Bangkok 10520, Thailand Phone: (662) 737-3000 Ext. 3519
E-mail: phumy_i@hotmail.com
**College of Industrial Technology, King Mongkut's Institute of Technology North Bangkok, Bangkok 10800, Thailand Phone: (662) 585-8540 Ext. 6438 E-mail: cjch@kmitnb.ac.th
***Department of Electrical & Electronic Engineering Tokai University, Japan
Phone: (81) 463-58-1211 Ext. 4029 E-mail: mkkando@keyaki.cc.u-tokai.ac.jp

## ABSTRACT

This paper presents a harmonic loss calculation of PWM-Fed induction motor, based on harmonic loss factor curves under load conditions and various motor configurations. The individual harmonic losses can be calculated from loss factor characteristics and individual harmonic voltages squared. The calculation results can be guidelines for selection of PWM parameters suitable for drive applications such as switching frequency and can suggest useful advices to the motor designers and users, when induction motors fed by PWM inverters have to be designed or utilized.

## 1. INTRODUCTION

At the present time, the induction motors are widely supplied from PWM inverter and commonly used in industrial applications. Despite the very great number of PWM drives in operation, the harmonics loss mechanisms are still not well understood by motor design and drive communities, there is a lot of myths and misunderstanding. With modern higher carrier frequency PWM drives neither approach is in predicting harmonic loss for all modulation strategies and operating conditions. The high frequency effect on harmonic loss is difficult for modeling machine. The effects on the core losses due to the modulation depth in case of a PWM inverter supply have been test on wound core and on induction motors . The calculating results have confirmed that the modulation depth plays an important role on core losses in the magnetic devices fed by PWM inverter [1].

The main aim of this work is to profoundly investigate the effects of PWM harmonic voltages on mechanisms of harmonics core losses. This fact is important to estimate the impact of using of different magnetic material or the influence of different design criteria in order to improve the motor efficiency and the output performance.

## II. POWER LOSS OF INDUCTION MOTOR

The energetic balance of an induction motor can be computed by the relation.

$$P_{in} = P_{Fund} + P_h \quad (1)$$

and

$$P_h = P_{in} - P_{Fund} \quad (2)$$

Where,

$P_{in}$ : input power
$P_{Fund.}$ : fundamental power
$P_h$ : harmonic power loss

### A. Harmonic power loss excluding skin effect .

The total of harmonic power loss excluding skin effect of induction motors can be expressed by[2]:

$$P_{h(ex.)} = \sum_{n=1} I_n^2 R_n \quad (3)$$

With

$$I_n = \frac{V_n}{n f_1 X} \quad (4)$$

Hence

$$P_{h(ex.)} = \frac{1}{X^2} \sum_{n=1} \left(\frac{V_n}{n f_1}\right)^2 R_n \quad (5)$$

*where,*

$P_{h(ex.)}$ : harmonic power loss excluding skin effect
$I_n$ : $n^{th}$ harmonic current
$V_n$ : per unit (pu) $n^{th}$ harmonic voltage
$f_1$ : per unit (pu) fundamental frequency
$X$ : per unit (pu) leakage reactance at base freq.
$R_n$ : resistance of motor to the $n^{th}$ harmonic
( i.e. $R_n$ is constant for negligible skin effect )

### B. Harmonic power loss including skin effect.

0-7803-8560-8/04/$20.00©2004IEEE

The $n^{th}$ harmonic power loss including skin effect of induction motors can be expressed by[5]:

$$P_{h(loss)} \approx I_n^2 (R_s + R_r) \quad (6)$$

With,

$$I_n \approx \frac{V_n}{2\pi f_n L_\sigma} \quad (7)$$

Hence

$$P_{h(loss)} \approx \left(\frac{V_n}{2\pi f_n L_\sigma}\right)^2 (R_s + R_r) \quad (8)$$

Assuming that all of the stator resistance and rotor resistance have skin effect and that skin depth is relatively small compared to conductor size, then total resistance become:

$$R_s + R_r = k\sqrt{f_n} \quad (9)$$

Therefore,

$$P_{h(loss)} = \sum_{n=1} \frac{kV_n^2}{f_n^{1.5}} \quad (10)$$

Where,

$P_{h(loss)}$ : total harmonic power loss including skin effect

$L_\sigma$ : leakage inductance

$R_s$ : stator resistance

$R_r$ : rotor resistance

$f_n$ : per unit (pu) fundamental frequency

$k$ : constant

**C. Harmonic loss characteristic curves**

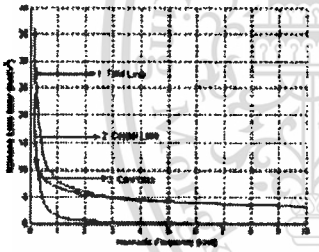

Fig.1 Harmonic loss factor curves for a given load [1,4,6]

Frequency dependent loss characteristics under various operating conditions are shown in Fig.1 . Total harmonic loss can be expressed as[3] :

$$P_h = \sum_{n=1} \left(\frac{A}{f_n^{\alpha}} + \frac{B}{f_n^{\beta}}\right) V_n^2 \quad (11)$$

where, $V_n$ is the $n^{th}$ harmonic voltage influenced by modulation depth., $f_n$ is harmonic frequency

A, B, $\alpha$, $\beta$, are constant values in loss characteristic curves. Basically, the exponent $\alpha$ is 1.5 and $\beta$ varies between 0.3-0.5. In this work, A=1.38, B=6.74, $\alpha$ = 1.5 and $\beta$=0.32 are used [3].

## III. HARMONIC VOLTAGE SPECTRA

Due to the frequency and voltage dependence of core losses, the PWM voltage spectra need to be determined at various modulation depth ($m_a$), $m_a$=0.4 and $m_a$=1 under various inverter frequency of 20Hz and 50 Hz, . Figures 2 and 3 shown the simulated results of PWM voltage spectra with a variation of modulation depth. This results shows that the SVM simulation program used in order to predict and accurate for good understood. When increasing modulation depth , the reduced dc link voltage is required for keeping constant flux level, thus decreasing harmonic voltage as shown in the Fig.2 and 3. This result can be referred to loss characteristic in curves Fig.1, it can be seen that in order to reduce core losses in the higher harmonic frequency region, the harmonics voltage should be minimized by keeping modulation depth( $m_a$) as high as possible. Therefore, in order to keep a constant flux operation, the dc link voltage must be reduced.

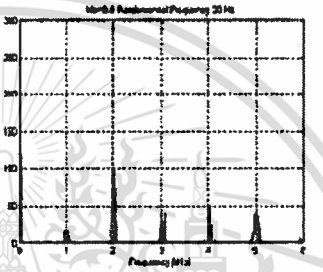

Fig. 2 Simulation results of voltage spectra with $m_a$ = 0.4, Fundamental Frequency 20 Hz and switching frequency of 1kHz.

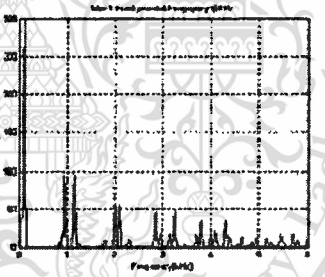

Fig. 3 Simulation results of voltage spectra with $m_a$ = 1, Fundamental Frequency 50 Hz and switching frequency of 1 kHz.

## IV. CALCULATED RESULTS AND DISCUSSION

The method presented in this section used MATLAB program. In industrial application, the asynchronous PWM technique nowadays is commonly used where the carrier frequency is fixed and stays constant as the modulating frequency is varied. The reason for its is because of the simplicity of control. Therefore, the fixed PWM switching frequency over wide range of inverter frequency is used here. In a comparison of total the harmonic

losses for various modulating waves, PWM switching frequency varies between 1-5 kHz and inverter frequency varies between 10-50 Hz. DC link voltage is approximately 600 V. The 50 Hz sinusoidal loss for 7.5 kw induction motor at full load is approximately 1.050 kw. In order to keep the ratio of the fundamental output voltage to inverter frequency ($V_1/f_1$) constant over a wide range of constant torque operation, the modulation index varies linearly with inverter frequency.

Figures 6 A-8B illustrate total harmonic losses of 7.5 kw induction motors( see appendix) under various operating conditions( PWM types, PWM switching frequency, and inverter frequency). For each motor at the same load conditions , the trend of total harmonic loss for over a range of inverter frequency are quite similar. As switching frequency increases, harmonic losses decreases . Quite clearly when increasing inverter frequency approximately up to 30 Hz the harmonic loss increases rapidly particularly for lower switching frequency ( 1 kHz ). However, for higher switching frequency, harmonic loss will increase quite slowly. This results from the sensitivity of copper loss to low PWM switching frequencies and the sensitivity of core loss to high PWM switching frequencies. Also this results from the distribution behavior of harmonic voltage spectra changing with the modulation index. Note that at higher inverter frequency operation ( more than 30 Hz ), total harmonic loss trend to decrease. As can be seen in figures 6A–8B, the difference of total loss for PWM switching frequencies of between 3-5kHz is considerably insignificant when comparing to the total harmonic loss at switching frequency of 1 kHz . The higher load will produce large harmonic loss at lower load.

For the comparative investigate on motor A and B were conducted for the same operating conditions. Figures 5 A and 5 B show the comparison of loss characteristic curves for motor A and motor B for various load conditions. Clearly for both light and heavy load condition at low harmonic frequencies, the large loss factor is with motor B than motor A. For higher harmonic frequencies, these loss curves tend to decrease slowly.

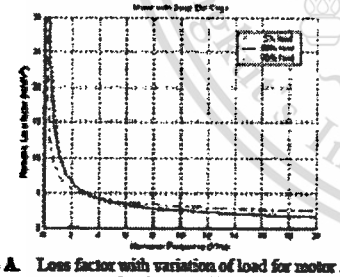

Fig. 5 A. Loss factor with variation of load for motor A with deepbar cage [3].

For this machine with a deep bar rotor, the functions at given load and rated flux are used the loss factor equations as follows[5] ($\beta$ varies between 0.3-0.55):

For loss of 5%, 50% and 90%

$$k_{h(5\%)} = \frac{1.38}{f_n^{1.5}} + \frac{6.47}{f_n^{0.32}} \quad \text{(12 A)}$$

$$k_{h(50\%)} = \frac{5.7}{f_n^{1.5}} + \frac{7.77}{f_n^{0.31}} \quad \text{(13 A)}$$

$$k_{h(90\%)} = \frac{7.64}{f_n^{1.5}} + \frac{5.06}{f_n^{0.36}} \quad \text{(14 A)}$$

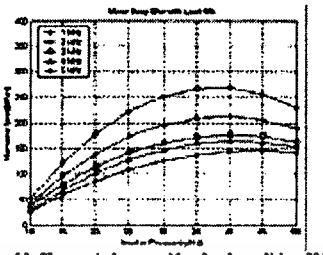

Fig. 6A. Harmonic loss with load condition 5%

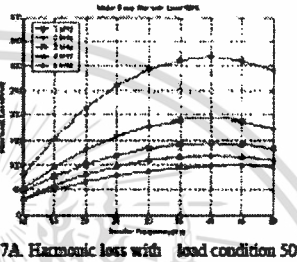

Fig.7A. Harmonic loss with load condition 50%

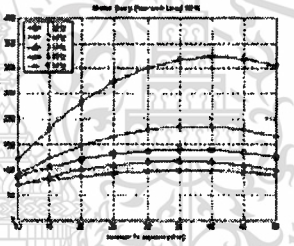

Fig. 8A. Harmonic loss with load condition 90%

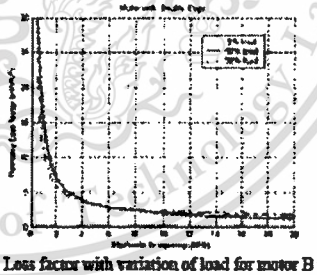

Fig. 5 B. Loss factor with variation of load for motor B with double cage [3].

For this machine with a double cage rotor, the functions at given load and rated flux are used the loss factor equations as follows [5] ($\beta$ varies between 0.3-0.6) :

For loss of 5%, 50% and 90%

$$k_{h(5\%)} = \frac{6.09}{f_n^{1.5}} + \frac{4.54}{f_n^{0.34}} \quad (12\ B)$$

$$K_{h(50\%)} = \frac{8.06}{f_n^{1.5}} + \frac{5.75}{f_n^{0.52}} \quad (13\ B)$$

$$k_{h(90\%)} = \frac{10.28}{f_n^{1.5}} + \frac{5.77}{f_n^{0.59}} \quad (14\ B)$$

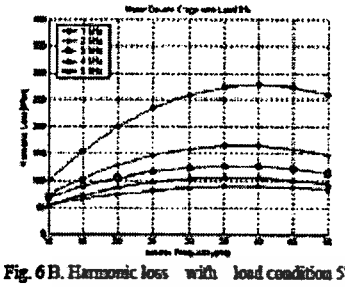

Fig. 6 B. Harmonic loss with load condition 5%

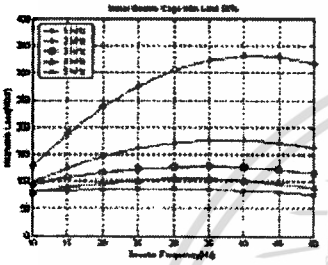

Fig. 7 B. Harmonic loss with load condition 50%

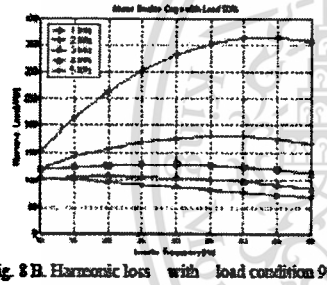

Fig. 8 B. Harmonic loss with load condition 90%

## V. CONCLUSIONS

This paper has deal with the investigation using the loss factor characteristics of PWM parameter such as modulation depth, switching frequency and PWM strategies on the induction motor losses. Main findings of this work can be summarized as follows: The change of modulation depth on core losses is significant. It is higher modulation depth should be made for drive control. As consequence dc link voltage level must be reduced Higher PWM switching frequency results in a slow decrease in core losses . Consequently, the effect of PWM scheme is significant on core losses. Note that higher switching frequency insignificant reduce core loss compared to lower switching frequency. However, higher switching frequency results increases inverter losses. At low harmonic frequencies, the predominant harmonic copper loss decreases rapidly as harmonic frequency increases, when at higher harmonic frequencies the predominant harmonic core loss (plus stray) loss decreases gradually.

## VI. APPENDIX

Motor A: 3-phase induction motor with a deep bar and skewed rotor cage, 7,5Kw : power rating, rated voltage : 415V-Delta rated current:14,58A,rated speed 1454 rpm, frequency : 50Hz, stator slots : 36 and rotor slots : 32.

Motor B: 3-phase induction motor with a double and skewed rotor cage, 7,5Kw : power rating, rated voltage : 400/440 V-Delta, rated current:14,5/13.2A, rated speed 1440/1740 rpm, frequency : 50/60Hz, stator slots : 54 and rotor slots : 48.

## VII. ACKNOWLEDGMENTS

The Authors would like to give a special recognition to AUN/SEED-Net, JICA for the contribution.

## VIII. REFERENCES

[1] TORE M. UNDERLAND, and NED MOHAN " Over modulation and Loss Considerations in High-Frequency Modulated Transistorized Induction Motor Drives ", in Conf. Rec. 1988 IEEE Transaction on Power Electronics, vol. 3. No.4 , October 1988

[2] J.M.D. Murphy and Egen, " A Comparison of PWM strategies for Inverter Fed Inverter Fed induction Motors " , IEEE, Trans. On Ind.April., vol. IA-19, No 3 , May , June 1983, pp. 363-368.

[3] S.Khomfoi, V.Kinnares and Viriya. " Investigation in to Core Losses due to Harmonic Voltages in PWM fed Induction Motors", in Conf. Rec.July 1999 PEDS'99 IEEE, pp.104-109.

[4] S.Khomfoi, V.Kinnares and Viriya. " Influence of PWM Characteristics on the core losses due to Harmonic Voltages in PWM Fed Induction Motors", in Conf. Rec.Jan. 2000, pp. 365-369.

[5] V.Kinnares, " Measurement, Analysis and prediction of Harmonic Power losses in PWM fed Induction Motors," Ph.D.Thesis, The University of Nottingham, UK,October 1997.pp.168, 169,170 and181

[6] V.Kinnares, P.Jaruwanchai, D.Suksawat and S.Pothivejkul "Effect of Motor Parameter Changes on Harmonics Power Loss In PWM Fed Induction Machines"in Con.PEDS'99 July 1999, pp.1061-1066

## Appendix B

### Research Laboratory

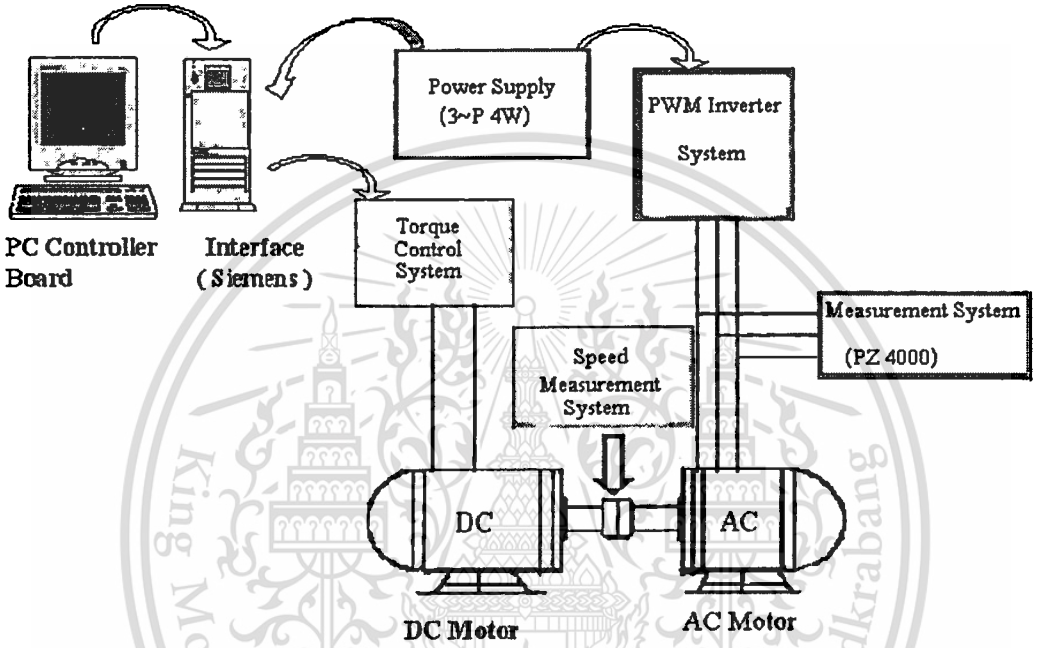


**Hardware Measurement Test Rig System**

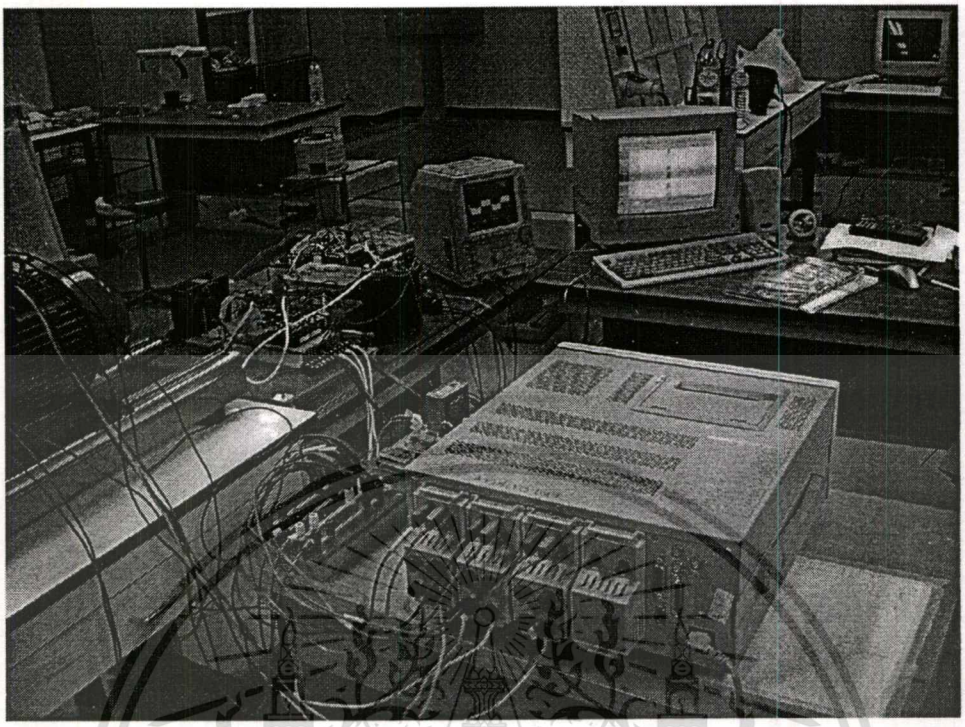

**Driver Test Rig**

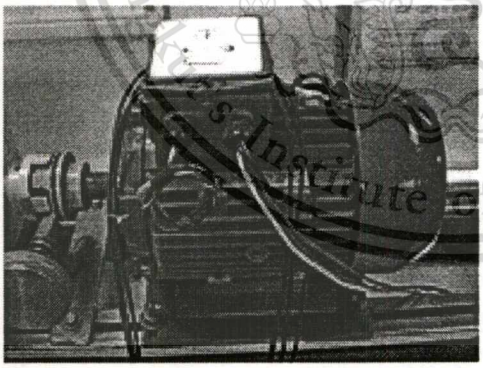

**Three-Phase Induction Motor220/380V(Y/Δ)**

**Dc Motor ( Load)**

Power rating: 2.2 kW (3HP), Rated Speed: 1420rpm

Rated Current: 5/8.7A, Cosφ=0.82

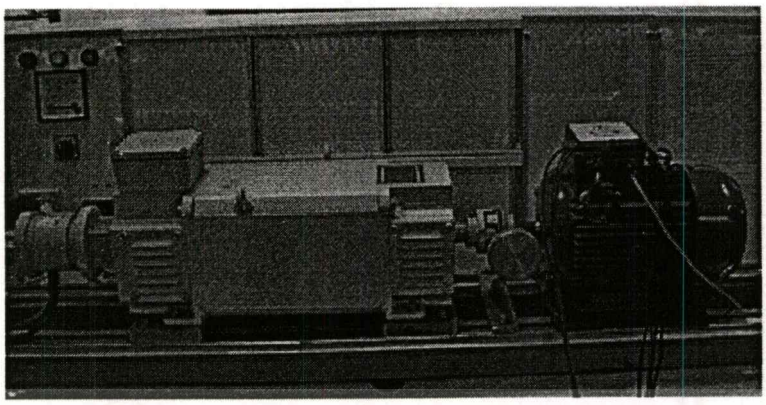

**The connection between AC Motor under Test and Dc Motor ( Load)**

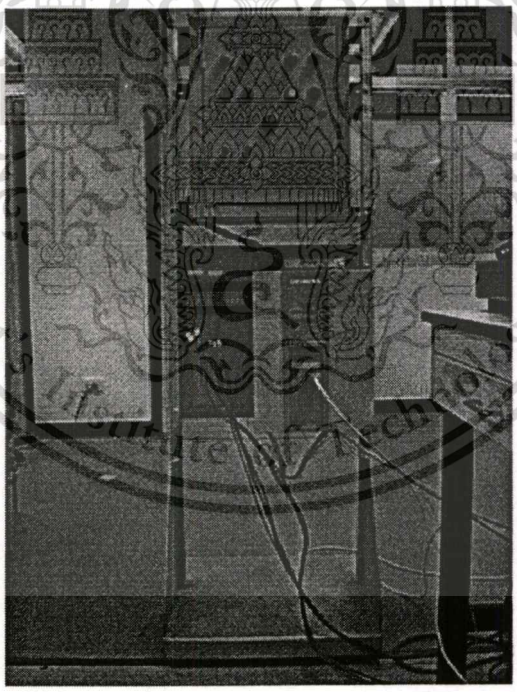

**Converter SIMOVIS DC drive with torque control**

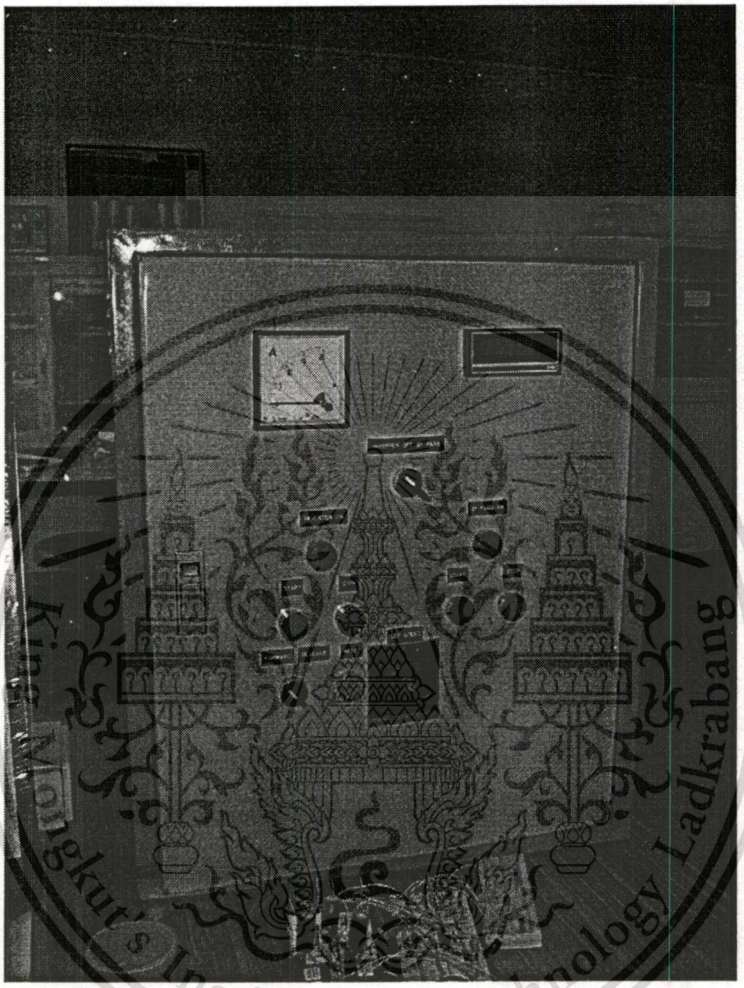

COMMANDER CD ( Variable Frequency Inverter )

TYPE CD 550 (Max. Motor Size 5.5 kW)

# APPENDIX C

**MATLAB Program for Harmonic Loss Prediction**

```
vd = 220*sqrt(2);
%for fs=10:5:50
 fs = 50;
%modIndex =(0.9*(fs)+10)/50; %v*2*sqrt(2)/vd;
modIndex =(220/218.6165)*(fs/50);
  fc = 1000;
  Th = 1/fs;
  dt = Th/fc;
  t = 0:dt:Th;

  g = 6;
  order0=(fc/fs)*g;
  CSignal = sin(2*pi*fs*t);
  refSignal = carrier(CSignal,fc,t);

  Va = modIndex*sin(2*pi*fs*t);
  Vb = modIndex*sin(2*pi*fs*t-120*pi/180);
  Vc = modIndex*sin(2*pi*fs*t+120*pi/180);

  pwmao = PWMk(Va,refSignal,vd);
  pwmbo = PWMk(Vb,refSignal,vd);
  pwmco = PWMk(Vc,refSignal,vd);
  pwman = (1/3)*(2*pwmao-pwmbo-pwmco);

   ffta=abs(fft(pwman)/fc);
  [ffta,frequency] = MyFFT(pwman,t);

  data=ffta(1:order0)/sqrt(2);
```

```
Xaxis=(1:order0)*(fs/1000);
figure(1)
plot(Xaxis,data);
title('Spectrum of Voltage');
xlabel('Frequency(kHz)');
ylabel('Fundamental Voltage(V)')


order=6000/fs;
for run=3:order;
A=0.55;
B=0.70;
alpha=1.5;
beta=0.51;
fn(run)=(run*fs)/fc;
vn(run)=ffta(run);
copper_loss_factor(run)=A/(fn(run).^alpha);
iron_loss_factor(run)=B/(fn(run).^beta);

loss_factor(run)=(((A/((fn(run)).^alpha))+(B/((fn(run)).^beta))))*0.001;
harmonic_loss(run)=loss_factor(run)*((vn(run).^2));

end
figure(2)
dataP=harmonic_loss(3:order0);
XaxisP=(3:order0)*(fs/1000);
plot(XaxisP,dataP);
title('Harmonic Loss(Watt) ');
xlabel('Frequency(kHz)');
ylabel('Harmonic Loss(W)')
```

```
figure(3)
plot(harmonic_loss);
title('Total harmonic loss spectra');
xlabel('Harmonic order');
ylabel('Harmonic Loss(Watt)')


figure(4)
dataZ=sum(dataP);
XaxisZ=(3:order0)*(fs/1000);
plot(XaxisZ,dataZ);
title('Total harmonic loss');
xlabel('Frequency(kHz)');
ylabel('Harmonic Loss(Watt)')
```

# BIOGRAPHY


| | |
|---|---|
| Name : | Mr. Phoumy Indarack |
| Date of Birth : | 30 July 1961 in Luangprabang Laos |
| Address : | Department of Electronic Engineering |
| | Faculty of Engineering, National University of Laos |
| | Sokpaluang Road P.O.Box 4242, Vientiane, Lao P.D.R |
| | Tel.office : (856-21)31 2423 |
| E-Mail : | phumy_i@hotmail.com |
| Education : | B.Eng.degree in Electrical Engineering from Institute of Engineer Pedagogy Gotha East Germany in 1983 |
| Experience : | Since 1987 up to present, lectured in Department of Electronic Engineering, Faculty of Engineering, National University of Laos. |